ACTIVITY-DEPENDENT LATERAL INHIBITION IN THE MOUSE OLFACTORY BULB

By

Armen C. Arevian

Bachelor of Arts, University of California, Berkeley, 2001

Submitted to the Graduate Faculty of

Arts and Sciences in partial fulfillment

of the requirements for the degree of Doctor of Philosophy

University of Pittsburgh

2008

UNIVERSITY OF PITTSBURGH

SCHOOL OF ARTS AND SCIENCES

This thesis was presented

by

Armen C. Arevian

It was defended on

April 16, 2008

and approved by

Justin Crowley, Ph.D.

G. Bard Ermentrout, Ph.D.

Jon Johnson, Ph.D.

Diego Restrepo, Ph.D.

Alan Sved, Ph.D.

Thesis Advisor: Nathaniel N. Urban, Ph.D.

ACTIVITY-DEPENDENT LATERAL INHIBITION IN THE MOUSE OLFACTORY BULB

Armen C. Arevian, Ph.D.

University of Pittsburgh, 2008

Lateral inhibition is a circuit motif found throughout the nervous system that often generates contrast enhancement and center-surround receptive fields. While widespread lateral inhibition of mitral cells (the principal output neurons of the bulb) is mediated by granule cells (inhibitory interneurons), due to the distributed representation of odorant-evoked activity it is currently unclear how this inhibition is specified or what functions it mediates.

Given the reciprocal nature of the connection between mitral and granule cells, mitral cells that are the targets of lateral inhibition (postsynaptic) are able to modulate the activity of the granule cells mediating this lateral inhibition. This led us to hypothesize that lateral inhibition could be modulated by the activity of both pre- as well as postsynaptic mitral cells. I first characterize the lateral interactions between mitral cells and show that the effectiveness of lateral inhibition between them is dependent on the activity of the postsynaptic neuron such that lateral inhibition is only able to reduce the firing rate within a specific range of postsynaptic firing rates. I call this activity-dependent lateral inhibition. I then investigated this novel form of inhibition further and provide evidence indicating that it results from cooperative activation of the inhibitory granule cells.

I investigated the mechanism and functional implications of these physiological results further using computational techniques. First, I show that integration of activity between pre- and postsynaptic mitral cells within a granule cell is sufficient to result in activity-dependent inhibition. I then used this model to show that activity-dependent inhibition is able to enhance the contrast and decorrelate initially similar input patterns to the network in a spatially independent manner. These results provide evidence for a novel form of neuronal interaction dependent on the activity of neurons within the network which could have important functional implications in olfaction as well as other brain areas.

PREFACE

The work presented in this dissertation is based on two manuscripts.

Chapter 2 is based on:

Arevian, A.C., Kapoor, V., Urban, N.N. (2008) Activity-dependent gating of lateral inhibition in the mouse olfactory bulb. *Nature Neuroscience* 11(1):80-7.

Chapter 3 is based on:

Arevian, A.C., Ermentrout, G.B., Urban, N.N. Dynamic connectivity and its functional implications in olfaction. (*in preparation*)

TABLE OF CONTENTS

LIST OF FIGURES

1.0 INTRODUCTION

We perceive the invisible world of odors through a complex interaction of neurons located in the nose, olfactory bulb and in higher locations in the brain. From the initial entry point in the nasal epithelium, odors activate millions of odorant receptors and the activation of these receptors and subsequent processing in the olfactory system allows humans to distinguish up to hundreds of thousands of different volatile compounds.

Work presented in this dissertation addresses one of the fundamental questions in olfaction: how lateral interactions between neurons in the olfactory bulb are mediated and what are the functional implications of these interactions. Specifically, we focus on lateral inhibition, an interaction known to enhance contrast, facilitate discrimination of similar stimuli and mediate competitive interactions between active neurons (Hirsch and Gilbert, 1991;Urban, 2002). These properties are due to reductions in the degree to which input-driven activity is correlated across neurons responding to stimuli (Friedrich and Laurent, 2001).

Despite the importance of lateral inhibition it is still unclear what functional role it has in the olfactory bulb. Given the distributed representation of odorants throughout the olfactory bulb, olfaction differs from other sensory systems in that there does not appear to be a fine-grained arrangement of neurons based on their response profiles which underlies the pattern of lateral inhibitory connectivity (Katoh et al., 1993;Johnson and Leon, 2000a;Uchida et al., 2000;Wachowiak and Cohen, 2001;Mori et al., 2005). In this dissertation, I explore a novel method for determining the effectiveness of lateral inhibition based on the activity of individual neurons. In this way, lateral inhibition is specified dynamically, based on the activity of neurons in the network, largely independent of their physical location.

Several aspects of the olfactory bulb yield itself to mediating this kind of dynamic connectivity. In the rest of this introduction I review the primary anatomical and physiological properties that serve as the substrates for dynamic connectivity. I then discuss how odorants are represented in the olfactory bulb. Finally, I explore what is known about how the anatomical and physiological properties of the bulb come together to modulate odorant representation to help form our perception of the olfactory world.

1.1 THE ANATOMY OF SMELL

1.1.1 Olfactory Receptor Neurons

Sensory perception of odors begins in the nose when volatile molecules enter the nasal cavity and activate the bipolar olfactory receptor neurons (ORNs) located in the nasal epithelium. ORNs have a single dendrite projecting into the mucous covering the nasal epithelium and project 20-30 cilia. Volatile odorants enter the nasal cavity and absorb differentially in the complex nasal mucosa (Mozell, 1964;Hornung and Mozell, 1977;Hornung et al., 1987;Hornung et al., 1987). In fact, olfactory binding proteins have been characterized that facilitate the transfer of some compounds through the mucosa (Pelosi, 1996). Odorant molecules then bind to and activate odorant receptors located on the cilia of olfactory receptor neurons (Buck and Axel, 1991;Axel, 1995;Buck, 1996). There are over 1000 different genes in mice (Zhang and Firestein, 2002) and about 350 in humans (Glusman et al., 2001;Zozulya et al., 2001;Malnic et al., 2004), each encoding a different odorant receptor. Odorant receptors are the largest group in the G-protein coupled receptor (GPCR) family and each ORN expresses only one type of odorant receptor (Buck, 1996). Like other GPCRs, odorant receptors are comprised of seven alpha-helical transmembrane domains. When a ligand binds to the receptor, a signal transduction cascade results in activation of the ORN. This cascade starts with the activation of

the G-olf protein which activates adenylyl cyclase (ACIII). This results in an increase in cAMP concentrations which then activate cyclic nucleotide gated (CNG) channels in the receptor (Ronnett et al., 1993). When open, the CNG channels allow Na^{+} and Ca^{++} ions to flow inside the cell, thus depolarizing it (Zufall et al., 2000). Sufficient depolarization initiated in the cilia results in action potentials generated at the soma which propagate down the axon and into the glomerular layer of the olfactory bulb. Much of the actual depolarization is thought to be due to a calcium-activated chloride channel (Lowe and Gold, 1993).

Expression of particular ORN types occurs within one of several zones in the epithelium. In the mouse, four such zones are arranged from dorsomedial to ventrolateral (Ressler et al., 1993;Vassar et al., 1993;Miyamichi et al., 2005). ORNs of a particular type are widely distributed among other receptor types within an individual zone. This zonal organization has also been shown to be reproduced in the olfactory bulb (Fujita et al., 1985;Schwob and Gottlieb, 1988). Some studies also suggest that odorant receptors with highly homologous amino acid sequences are located in the same zones (Malnic et al., 1999).

1.1.2 ORN Input to the Olfactory Bulb

ORNs located in the olfactory epithelium send their axons through the cribriform plate to enter the central nervous system where they synapse in the olfactory bulb. The olfactory bulb is the initial processing point for odor information in the brain (Shepherd and Greer, 2004). In mice, the olfactory bulb is separated into two main divisions, the main olfactory bulb (MOB) and the accessory olfactory bulb (AOB). While the functional role of these two regions is a subject of some debate, it is generally considered that the MOB is primarily involved in processing volatile molecules while the AOB processes mostly nonvolatile compounds, many of which are pheromones important in mediating specific behaviors (Dulac and Torello, 2003). Therefore, the AOB is thought to have a larger role in behavioral responses while the MOB is thought to primarily contribute to perception of volatile odorants (Restrepo et al., 2004), although

a)

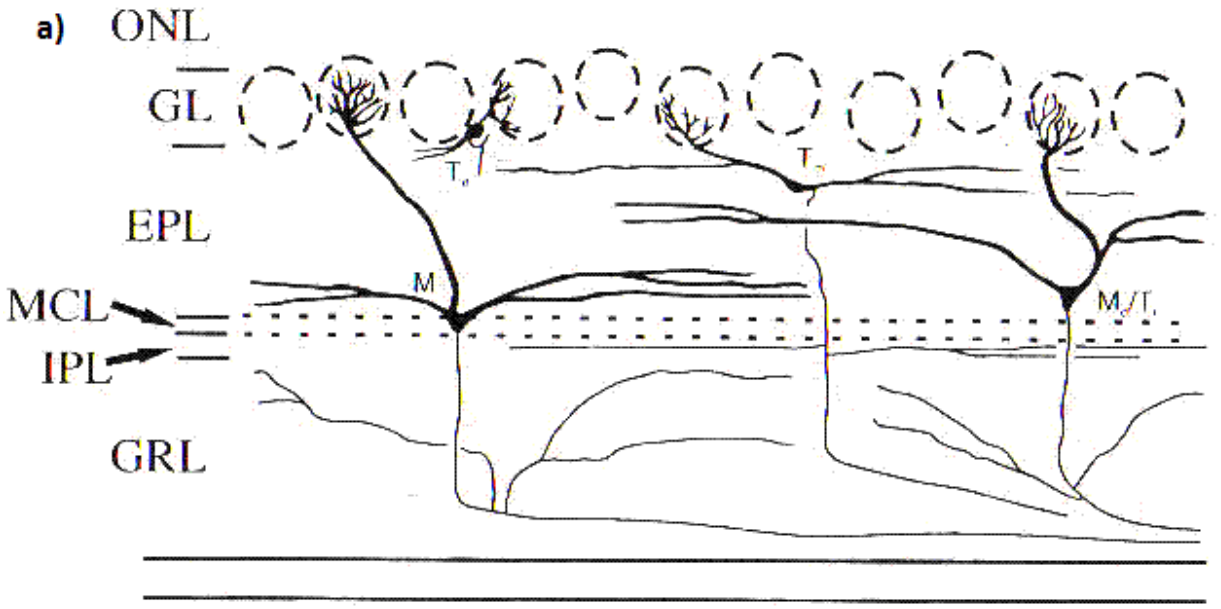
ONL
GL
EPL
MCL
IPL
GRL
M
M/T

b)

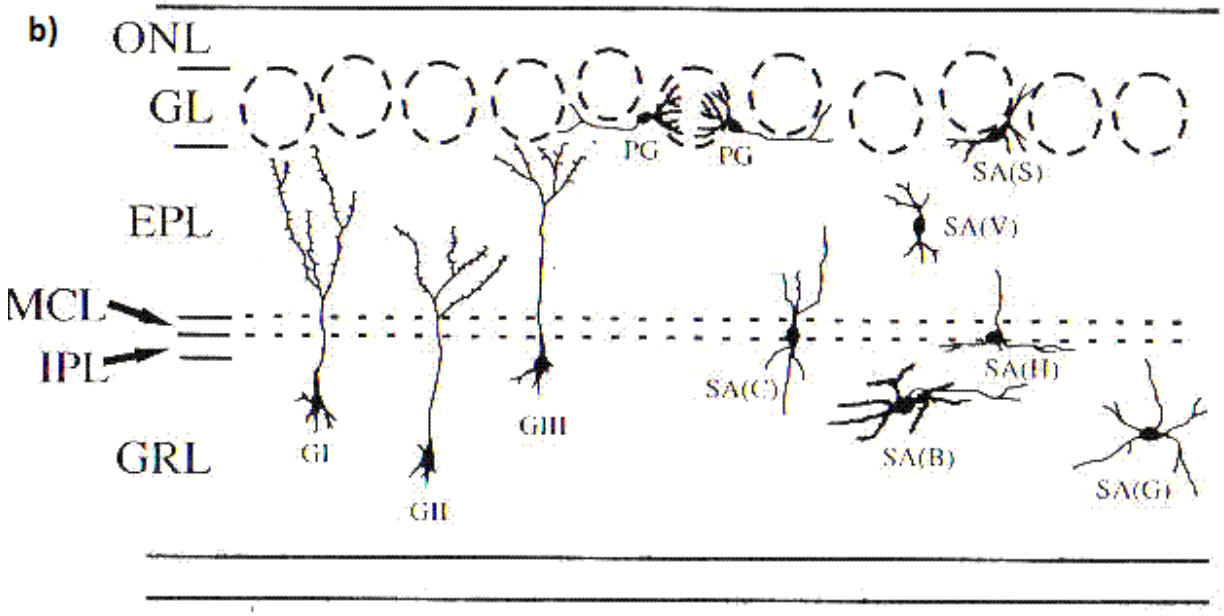
ONL
GL
EPL
MCL
IPL
GRL
PG
PG
SA(S)
SA(V)
SA(H)
SA(C)
SA(B)
SA(G)
GI
GII
GIII

Figure 1.1. Laminar organization of the olfactory bulb. From superficial (top of figure) to deep: olfactory nerve layer (ONL), glomerular layer (GL), external plexiform layer (EPL), mitral cell layer (MCL), internal plexiform layer (IPL), granule cell layer (GRL). In **a)** the principal output neurons of the olfactory bulb are depicted including mitral (M) as well as tufted (T) cells. In **b)** granule cells are separated into three classifications (GI-III) based on their dendritic distribution. Also, perigrlomerular (PG) and short axon (SA) cells mediate additional intrabulbar interactions. Modified from (Shepherd and Greer, 2004).

recent work highlight exceptions to this general categorization (Sam et al., 2001).

1.1.3 Glomerular Organization of Odorants

The olfactory bulb is comprised of five layers. They are (from most superficial to deep) the glomerular layer, external plexiform layer, mitral cell layer, internal plexiform layer and granule cell layer (**Fig. 1.1**).

The glomerular layer contains large spherical structures (30-50 microns in diameter in mice) called glomeruli. The number of glomeruli varies between species but there are about 1800 in mice (Shepherd and Greer, 2004). They contain axon terminals from ORNs, apical dendrites of mitral and tufted cells (the primary output neurons of the olfactory bulb) and are surrounded by various local interneurons, the main type of which are periglomerular (PG) cells (Pinching and Powell, 1971a;Pinching and Powell, 1971b;Pinching and Powell, 1971c). PG cells typically are thought to release GABA or dopamine and mediate local inhibitory interactions via their dendritic arborizations within the glomerulus (Halasz et al., 1982;Gall et al., 1987;Kosaka et al., 1988;Maher and Westbrook, 2008). Another cell type, the short axon (SA) cell, is glutamatergic and has recently been implicated in mediating inhibition by contacting PG cells between glomeruli separated by distances up to 2mm (Aungst et al., 2003).

1.1.4 Connectivity within the Olfactory Bulb

A key feature of the organization of olfactory information in the olfactory bulb is that each glomerulus receives input from ORNs expressing a single odorant receptor type (Mombaerts et al., 1996;Treloar et al., 2002). This results in ORN input to the bulb arranged in functional units based on glomerular connectivity (**Fig 1.2A**).

a.

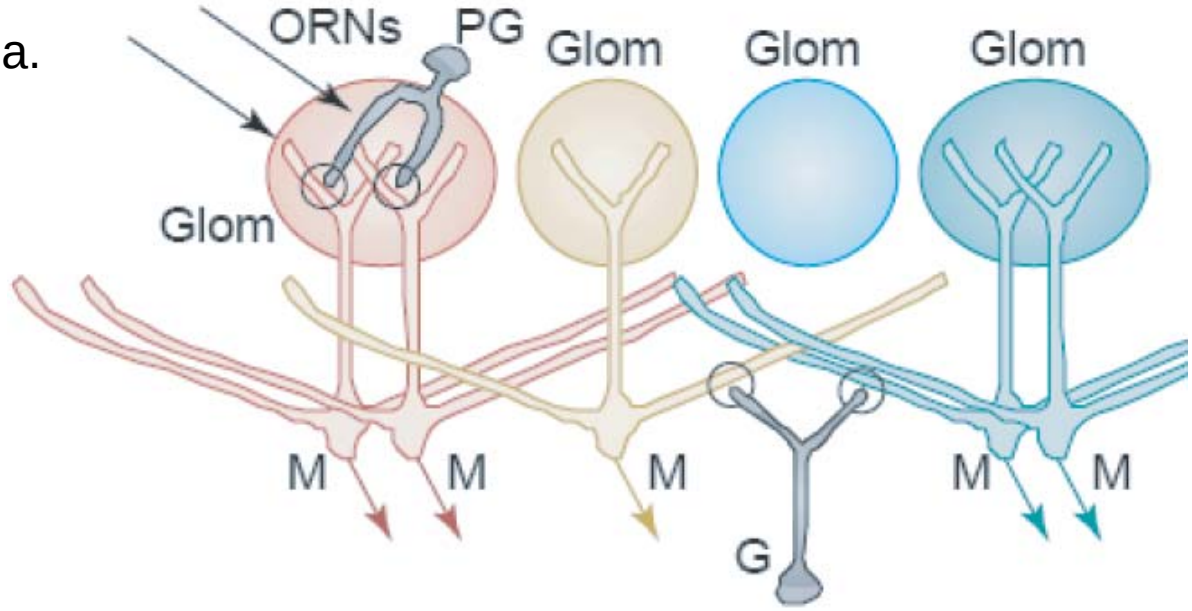

b.

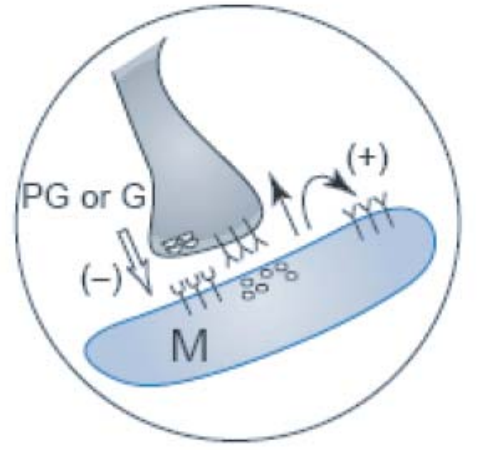

Glutamate receptors
GABA receptors

Figure 1.2. Connectivity within the olfactory bulb. a) Convergence of ORNs expressing a single odorant receptor onto a given glomerulus (Glom) and associated mitral cells (M). Recurrent as well as lateral inhibition mediated by granule cells (G) making dendrodendrtic connections with mitral cells across different glomeruli. Arrows indicate axons. In **b)**, schematic representation of the dendrodendritic synapse between mitral and granule/PG cell dendrites. Modified from (Schoppa and Urban, 2003).

Mitral cells are excitatory neurons that serve as the primary output of the olfactory bulb. Their cell bodies are located in the mitral cell layer, approximately 250-400 microns from the glomerular layer. Their primary or apical dendrite extends superficially through the external plexiform layer to the glomerular layer where they branch repeatedly to form a tuft-like structure that often fills the glomerulus (Shepherd and Greer, 2004). In addition to their primary apical dendrite, mitral cells extend lateral secondary dendrites within the external plexiform layer. These dendrites are aspiny, 1-6 microns thick and can extend for over 1 mm giving mitral cells dendritic coverage of up to half to two-thirds of the olfactory bulb (Mori et al., 1981). Tufted cells are the other primary output cells of the olfactory bulb and are located mainly in more superficial regions of the EPL (Cajal, 1995). They have similarly been categorized into subtypes based primarily on location within the EPL (Shepherd and Greer, 2004).

Deep to the mitral cell layer is the internal plexiform layer that contains axons of mitral cells as well as dendrites of granule cells. Granule cells lack an axon and instead their dendrites act as pre- and postsynaptic structures (Rall and Shepherd, 1968). They are GABAergice and the primary inhibitory interneurons of the olfactory bulb. Their small cell bodies have a diameter of 6-8 microns and are located in the granule cell layer. They extend a primary, spiny dendrite superficially to synapse with mitral cell lateral dendrites in the external plexiform layer. They also have basal dendrites that branch within the granule cell layer. While it has been proposed in some models that granule cells make GABAergic synapses with one another (Freeman, 1979;Linster and Gervais, 1996), no direct evidence for such connectivity has been found. However, there is some evidence that granule cells make electrical synapses with one another (Reyher et al., 1991).

Some studies have separated mitral and granule cells into subtypes based on the pattern of projections of their dendrites in the bulb. Type I mitral cells are those sending their secondary dendrites to the deepest parts of the external plexiform layer while type II cells send their dendrites to the middle region of the external plexiform layer (Macrides and Schneider, 1982;Mori et al., 1983;Orona et al., 1984). Similarly, superficial granule cells (type III) have dendrites that ramify in superficial layers of the EPL and deep granule cells (type I) have

dendrites that are mainly localized to the deep EPL. Furthermore, there is a third type of granule cell (Kato et al., 1999) that has dendrites that arborize throughout the EPL. It is hypothesized that these different types of mitral and granule cells could form synaptic microcircuits within the olfactory bulb (Shepherd and Greer, 2004).

1.1.5 Olfactory Cortex

The olfactory system is unique in that it bypasses the relay through the thalamus that is common in other mammalian sensory systems (Shepherd and Greer, 2004). The olfactory cortex is broadly defined as all the areas that receive monosynaptic projections from the olfactory bulb (Price, 1973). These are the piriform cortex, olfactory tubercle, entorhinal cortex, agranular insula, cortical areas of the amygdala, as well as cortical areas in the olfactory peduncle. Most of these areas are classified as paleocortex, which is commonly described as having three layers as opposed to the six layers of neocortex. This area is also phylogenetically older than the more abundant neocortex. The piriform cortex has three primary layers. Layer I is most superficial and contains inhibitory large horizontal cells. It is subdivided into layer Ia which is superifical to layer Ib. Layer Ia receives input from the olfactory bulb via the lateral olfactory tract while layer Ib receives input from other olfactory cortical areas. Layer II contains a dense set of inhibitory cell bodies (Haberly and Price, 1978). Layer III contains the cell bodies of pyramidal cells, the primary output of the piriform cortex. The density of these cells is greatest in the superficial portions of the layer. Large multipolar cells increase in density in deeper portions of the layer. Pyramidal neurons have a large apical dendrite and several basal dendrites. The apical dendrites extend superficially and arborize throughout layer I where they receive input from mitral cells in the olfactory bulb. The endopiriform nucleus is deep to layer III and spiny multipolar neurons are the primary cell type in this area (Tseng and Haberly, 1989).

One important consideration in the olfactory cortex is the spatial pattern of connectivity from the olfactory bulb. Do mitral cells from an individual glomerulus (and therefore encoding information from a single olfactory receptor type) connect to specific populations of pyramidal

cells or do they send connections broadly throughout the olfactory cortex? Recent studies show that mitral cells that project to the anterior piriform cortex make synaptic contacts in broad patches (Buonviso et al., 1991). Studies using *c-fos* as a measure of odor-evoked activity show that stimulation by odors results in broad activity in the piriform cortex suggesting a distributed representation of odors identity in the piriform cortex. Recently, multiunit recording of cortical neurons confirm this broad projection of olfactory information throughout the cortex, also showing that not only do nearby cortical neurons respond to different odorants but that there is a rich temporal structure to their response as well (Rennaker et al., 2007). There is also extensive intracortical connectivity such that an individual cortical pyramidal cell may contact several thousand other piriform cortical neurons (Johnson et al., 2000). This broad connectivity is also seen in insects where approximately 800 projection neurons (analogous to mitral cells) project to about 50,000 kenyon cells in the mushroom body (analogous to the vertebrate cortical neurons) (Perez-Orive et al., 2002).

1.2 PHYSIOLOGY OF SMELL

1.2.1 Synaptic Connectivity in the Glomerulus

Mitral cells receive excitatory input from ORN axons via their apical dendrite synapsing in the glomerulus. About 5000 ORN axons enter the glomerulus and ramify making numerous synaptic contacts. These axons release glutamate at axodendriditic synapses with about 50 mitral and tufted cells per glomerulus as well as with periglomerular cells (Pinching and Powell, 1971a;Pinching and Powell, 1971b;Shepherd and Greer, 2004;Kasowski et al., 1999). Transmission probability from ORNs to mitral cells is very reliable with a probability of release of approximately 1 (Murphy et al., 2004). These EPSPs have a fast component mediated by the AMPA receptor (subunits GluR 1, 2/3, 4) as well as slow component mediated by the NMDA

receptor (subunits NR1, NR2A, NR2C) (Ennis et al., 1996;Pimentel and Margrie, 2008;Ma and Lowe, 2007).

The mitral cell tufts not only function as postsynaptic targets for ORNs but also have presynaptic functions as well due to their capability of releasing glutamate. While there is no evidence for direct excitatory synaptic contacts between mitral cells (Pinching and Powell, 1971a) release of glutamate from tufts is thought to activate other mitral cells via spillover (Jahr and Nicoll, 1982;Isaacson, 1999;Schoppa and Westbrook, 2002;Urban and Sakmann, 2002). Mitral cells are also electrotonically coupled which contributes to lateral excitation within the glomerulus (Schoppa and Westbrook, 2002). Periglomerular cells primarily release GABA or dopamine and mediate intraglomerular inhibition onto mitral/tufted cells as well as inhibition directly onto presynaptic ORN axon terminals (Wachowiak and Cohen, 1999;Aroniadou-Anderjaska et al., 2000;Berkowicz and Trombley, 2000;Ennis et al., 2001).

1.2.2 Mitral to Granule Cell Dendrodendritic Synapses

Early studies in the anesthetized rabbit showed that activation of mitral cells resulted in long lasting inhibition (PHILLIPS et al., 1963). It was hypothesized that this inhibition was due to activation of granule cells by mitral cells and subsequent inhibition back onto mitral cells (Shepherd, 1963;Rall and Shepherd, 1968). Later, electron microscopy studies confirmed the unique dendrodendritic synapse that mediates interactions between these two cell types (Rall et al., 1966). This synapse is unique because the mitral and granule cell dendrites have both presynaptic as well as postsynaptic functions (**Fig 1.2B,C**). Mitral cell dendrites are aspiny and back propagating action potentials initiated at the axon travel through the lateral dendrites and depolarize them resulting in glutamate release at synaptic contacts with granule cell dendrites (Chen and Shepherd, 1997;Isaacson and Strowbridge, 1998). In addition to activating granule cells, glutamate release from mitral cell secondary dendrites also activates NMDA autoreceptors (Isaacson, 1999;Montague and Greer, 1999;Petralia et al., 1994;Schoppa and

Westbrook, 2002). It has been proposed that these autoreceptors could be important in the temporal patterning of mitral cell spikes (Friedman and Strowbridge, 2000).

Granule cells make synaptic contacts with mitral cells via their spiny dendritic trees (Rall et al., 1966;Woolf et al., 1991b). Glutamate activates both ionototropic (NR1, 2A, 2B and GluR 2/3, 4) as well as metabotropic glutamate receptors (mGluR2, mGluR5) (Shepherd and Greer, 2004). Dendrodendritic synapses between mitral and granule cells result in excitation of granule cells via glutamate receptors and subsequent inhibition of mitral cells via the release of GABA from granule cells (Schoppa et al., 1998;Isaacson and Strowbridge, 1998;Nowycky et al., 1981;Jahr and Nicoll, 1982;Didier et al., 2001). This synaptic release has also been shown to be dependent on the NMDAR located on granule cells with their contacts with both mitral (Schoppa et al., 1998) as well as tufted (Christie et al., 2001) cells. However, under conditions that increase granule cell excitability or slow AMPAR kinetics, activation of the AMPAR is sufficient to result in GABA release (Isaacson, 2001). GABA activates $GABA_A$ receptors (composed of subunits alpha1, beta1,2,3, gamma2) on mitral cells (Barnard et al., 1998;Nusser et al., 2001). High voltage activated (HVA) Ca^{++} Channels such as P/Q type channels are important in release in both mitral (Isaacson and Strowbridge, 1998) as well as granule (Isaacson, 2001) cells. Furthermore, Ca^{++} entry via NMDAR has also been shown to be important in GABA release (Halabisky et al., 2000;Chen et al., 2000).

This reciprocal dendrodendritic synapse forms a microcircuit between mitral and granule cells where neurotransmitter release from mitral cells results in local release of GABA from granule cells without requiring somatic spiking (Shepherd and Greer, 2004). In fact, granule cell-mediated inhibition persists in the presence of TTX (Jahr and Nicoll, 1982;Isaacson and Strowbridge, 1998;Schoppa et al., 1998) as well as when GC somatic action potentials were blocked by dissecting the mitral cell layer from the granule cell layer thus isolating the dendrodendritic synapses (Lagier et al., 2004). This suggests that individual granule cells can mediate inhibition among different subsets of mitral cells dynamically, based on their level of excitation.

1.2.3 Dendritic Excitability of Mitral and Granule Cells

Action potential generation not only results in depolarization along the axon but also in backpropagating action potentials (BPAPs) that depolarizes the lateral dendrites of mitral cells. Given that the depolarization of lateral dendrites results in activation of granule cells, it is interesting to ask what conditions influence this propogation and therefore possibly influence the subsets of granule cells activated by mitral cell activity. Early studies provided evidence that action potential propagation was decremental as distance increases from the soma (Margrie et al., 2001;Lowe, 2002;Christie and Westbrook, 2003) suggesting a possible mechanism for mediating contrast enhancement as seen in other systems (see below). However, later studies showed preserved propagation of BPAPs in distal dendrites (Xiong and Chen, 2002). Furthermore, they showed that granule cell mediated inhibition elicited at a particular location along the lateral dendrite was sufficient to impede BPAPs. This suggests that the subset of granule cells activated by mitral cell activity could depend on the pattern of inhibition received along the secondary dendrites, possibly mediating interesting computational functions (Shepherd et al., 2007). Therefore, the extent of BPAP invasion in mitral cell dendrites and subsequent interaction with granule cells appears to be dependent on the dynamics of the network activity. Mitral cell dendrites also have several channels that modulate their excitability, including A-type K^+ and delayed rectifier K^+ channels (Wang and Buzsaki, 1996), channels resulting in attenuation of voltage in distal lateral dendrites (Wang and Buzsaki, 1996;Christie and Westbrook, 2003;Davison et al., 2004). Mitral cell lateral dendrites also contain small conductance calcium-activated potassium (SK) channels which have been shown to modulate mitral cell firing rate as well as dendrodendritic inhibition (Maher and Westbrook, 2005).

Due to their lack of an axon, granule cell's dendrites play a crucial role in synaptic transmission. Unlike neurons in many other systems including CA1 pyramidal neurons (Spruston et al., 1995), layer 2/3 neocortical pyramidal neurons (Svoboda et al., 1999) and layer

2/3 internerouns (Kaiser et al., 2001), action potentials initiated at the soma of granule cells result in robust Ca^{++} transients in even the most distal segments of the dendritic tree (Egger et al., 2003). These Ca^{++} transients have also been shown to be dependent on the T-type voltage gated Ca^{++} channel. GC's also have A-type potassium current (Schoppa and Westbrook, 1999) and BK channels that can be activated by NMDA autoreceptors (Isaacson and Murphy, 2001) located in abundance at GC soma (Knaus et al., 1996). This modulation of excitability mediated by A-type potassium and BK channels could have an important role in determining the temporal pattern of transmitter release suggesting that real-time network dynamics play a critical role in determining neuronal interactions in the olfactory bulb.

1.3 ODOR CODING AND REPRESENTATION

1.3.1 Sensory Maps

Knudsen et al. defined a sensory map as having two traits: 1) a spatial clustering of responses to a particular stimulus, and 2) a systematic relationship between the spatial position of a neuron and its response profile (Knudsen et al., 1987). This arrangement has been illustrated clearly in the somatosensory system for example, where receptors in the skin map to specific locations in the somatosensory cortex, satisfying Kneudsen's first requirment. Furthermore, receptors corresponding to nearby locations on the body map to nearby locations in the brain and thus satisfy Kneudsen's second requirement for a sensory map (Kandel et al., 2000). Sensory maps such as in the somatosensory system that are arranged in a similar manner as the physical arrangement of receptors have been termed feedforward maps (Wilson and Mainen, 2006).

Another type of mapping, called computational mapping (Knudsen et al., 1987;Wilson and Mainen, 2006), is achieved when specific aspects of the sensory stimulus that arise after

some level of processing are mapped to a network of neurons. The classic example of a computational map comes from the pioneering work of Hubel and Wiesel where by recording from neurons in the cat primary visual cortex, they found that cortical neurons responded to specific orientations of a bar in the visual scene (Hubel and Wiesel, 1963). The auditory system also exhibits several computational maps including those for interaural delay, interaural intensity difference, and sound source location in the brainstem (Knudsen and Konishi, 1978;Knudsen, 1982;King and Palmer, 1983;Wenstrup et al., 1986).

What might be the usefulness of such mapping? First, the use of sensory maps could be a result of developmental and physiological constraints considering that mapping neurons near one another reduces the amount of projections required to mediate interactions which would preserve space and energy (Cajal, 1995;Laurent, 1997). Sensory maps also facilitate interactions between sensory modalities as in the overlap between visual and auditory maps in the superior colliculus (Kadunce et al., 1997). Other than these practical considerations, sensory maps could also intrinsically encode some aspect of the sensory stimulus, as seen with sound localization in the auditory system (Carr and Konishi, 1988;Carr and Konishi, 1990).

The idea of sensory maps presents a particularly interesting problem in the olfactory system. If a classic sensory map as described by Knudsen et al. exists in the olfactory system, there must be some way of continuously mapping olfactory space onto the two dimensional olfactory bulb. To understand better how this might be achieved in olfaction, I review below odorant encoding by ORNs and the recent work regarding different mapping strategies that could possibly be implemented in olfaction.

1.3.2 Encoding Odorant Features by Olfactory Receptor Neurons

The first step in forming our perception of the world outside our body is the activation of sensory receptors. In general, the specific part of the sensory world that a neuron responds to is defined as its receptive field (Hartline, 1938;Mountcastle, 1957). In olfaction, our

perception of odor begins when volatile molecules bind olfactory receptors located in the nasal epithelium. The set of molecules that activate an odorant receptor is termed its molecular receptive range (MRR).

Some odorant receptors, called specialist channels, have very narrow MRRs and respond to only one or a few known molecules. For example, the necklace glomeruli are thought to be associated with suckling behavior (Teicher et al., 1980;Shinoda et al., 1989;Ring et al., 1997). Recently, this specialization has also been described in mice that have an odorant receptor that responds to a specific compound found in male mouse urine, methylthio-methanethiol. Not only was this odorant receptor specialized, but when activated resulted in increased investigation by female mice, indicating a social function (Lin et al., 2005). These specialist channels have been well defined in insects as well. Mosquitoes, for example, have an odorant receptor type that is narrowly tuned to a molecule contained in human sweat (Hallem et al., 2004).

However, other than a limited number of specialist channels, it appears that most receptors respond to a wide range of molecules and it is not clear if there are any common molecular features among them (Katoh et al., 1993;Mori et al., 2005;Malnic et al., 1999;Araneda et al., 2000;Johnson and Leon, 2000b). A recent study looking at the binding properties of receptors found that olfactory receptors recognize odors primarily as a result of van der Waals forces rather than hydrogen and ionic interactions as seen in other GPCRs (Katada et al., 2005) thus resulting in broader tuning of these receptors and could also explain the very transient dwell time of molecules in receptors of < 1ms (Bhandawat et al., 2005).

1.3.3 Spatial Representation of Odors

The idea that odor quality could be related to spatial location of neurons in the brain dates back to the early studies using evoked potentials conducted by Adrian (1950) where he observed that different odorants activated different areas of the olfactory bulb. Since these early studies

of odorant evoked responses, several studies using various techniques show that there is a stereotyped map of glomerular activity for different odors.

Some of the initial studies were done using [^{14}C] radiolabelled 2-deoxyglucose (2-DG) (Sharp et al., 1975;Stewart et al., 1979;Jourdan et al., 1980;Coopersmith and Leon, 1984;Royet et al., 1987). In this technique, rats were injected with 2-DG and then exposed to a particular odor. Areas showing increased odorant-evoked activity take up the 2-DG and show increased density in autoradiographs. These studies gave the first indications that exposure to odors resulted in the activation of a particular combination of glomeruli. Following initial studies using 2-DG, investigators used a marker for the immediate early gene *c-fos* as an indicator for neuronal activity (Guthrie et al., 1993). They found an increase in *c-fos* expression in recently active neurons as a result of odor exposure. Their results agreed with 2-DG studies, indicating focal activation of cells in the glomerular layer as well as a broader activation of cells in the underlying granule cell layer.

More recently, several optical imaging techniques have been employed to observe odorant-evoked responses *in vivo*. Intrinsic signal imaging is one of these techniques where intrinsic activity (a combination of presynaptic ORN activity as well as postsynaptic activity) is used to visualize the dorsal surface of the bulb *in vivo* (Rubin and Katz, 1999;Friedrich and Korsching, 1997). Other imaging techniques include voltage sensitive dyes (Spors and Grinvald, 2002), fMRI (Yang et al., 1998;Kida et al., 2002;Schafer et al., 2006) and 2-photon Ca^{++} imaging (Wachowiak et al., 2004) and have all supported the conclusion that odorants result in stereotyped patterns of activity in the olfactory bub. Furthermore, it has been shown that these patterns are bilaterally symmetric and similar between conspecifics (Belluscio and Katz, 2001), although some variation in glomerular patterning can occur (Strotmann et al., 2000)

Considering that ORNs of a particular type (and therefore having a distinct MRR) project to specific locations in the olfactory bulb, it is clear that the spatial map in the olfactory bulb satisfies Knudsen's first criterion (see above). However, a key remaining question is whether

Knudsen's second criterion is also satisfied. That is, is there a systematic progression in molecular features throughout the olfactory bulb?

Several studies have tried to answer this question. However, one of the challenges in addressing this question is finding a series of odorants that vary systematically with respect to one another. Probably the clearest results are from Meister and Bonhoeffer (2001) who presented molecules with increasing carbon chain lengths to mice and recorded glomerular activity using intrinsic signal imaging. Their results showed a relationship of preferred chain length and spatial position with glomerular activation shifting progressively with increasing carbon chain length similar to other studies (Belluscio and Katz, 2001;Uchida et al., 2000). However, this relationship was subtle and there was significant overlap in glomerular responses. Furthermore, a later study utilizing a marker of ORN vesicle release looking at the effect of carbon chain length presented conflicting results (Bozza et al., 2004). Nearby glomeruli have also been shown to have dramatically different odor tuning (Fantana et al., 2002). Similarly, mitral cells separated by only a few glomeruli can have very different odor tuning (Buonviso and Chaput, 1990;Motokizawa, 1996).

Given these results and the fact that it is difficult to find general molecular features that vary systematically other than certain features such as carbon chain length, what appears to be more likely is that the olfactory bulb exhibits broad grouping of odorant responses. In this manner, odors belonging to the same broad molecular class show glomerular responses that are grouped in the same broad region. For example, ketones, aliphatic alcohols and phenols cluster in lateral portions while hydrocarbons cluster in more ventral portions of the bulb (Rubin and Katz, 1999;Johnson and Leon, 2000a;Uchida et al., 2000;Wachowiak and Cohen, 2001). This has also been observed in zebrafish where amino acids tend to activate glomeruli in ventro-lateral positions, while bile acids and nucleotides activated other regions (Friedrich and Korsching, 1998). Taken together, these data suggest that odor identity is likely not represented in a fine chemotopic manner, but in a distributed, combinatorial manner. In a combinatorial coding scheme, it is only important which glomeruli are activated and not necessarily their spatial relationship to one another. In fact, broad but specific response

profiles, as exhibited by most ORNs, is thought to be the hallmark of population coding in the cortex (Pouget et al., 2000).

Of course, whether chemotopic or combinatorial, a key question is whether information is actually encoded in the spatial pattern of activity. One way of determining whether odorant identity is encoded by the spatial pattern is to observe how the similarity of spatial patterns effects odor discrimination. Consistent with the hypothesis of spatial encoding of odorants, it was found that animals cross-habituate between odors with very similar glomerular maps (Linster et al., 2001). It has been found that animals show a significant correlation between discrimination accuracy and map similarity (Uchida and Mainen, 2003). Although with training, animals are able to distinguish between even very similar maps (Rubin and Katz, 2001;Linster et al., 2002) suggesting that there might be other factors involved in the ability to make fine odor discriminations.

1.3.4 Temporal Representation of Odors

An alternative (or supplement) to a spatial code for odorants is that of a temporal code. A temporal code could be generally described as any neural response where the timing of spikes carries information about a stimulus. However, a more specific and useful definition that has been proposed states that a temporal code is one where information about the stimulus is encoded by spike fluctuations that occur on timescales faster than the fastest fluctuations of the stimulus (Dayan and Abbott, 2001). For example, if the identity of an odor delivered for 500 ms was encoded by bursts of activity occurring at 10 hz, this could be described as a temporal code. This definition has also been extended to include fluctuations in spiking that occur at much longer intervals than the stimulus fluctuations (Wilson and Mainen, 2006). For example, if a 100 ms odor pulse results in several seconds of spiking activity, this could be used for a temporal code as well.

One of the main features of olfactory physiology that is investigated with respect to temporal coding is that of oscillations. Many brain areas show oscillations in recordings of their local field potentials (LFPs) and this technique has been used to show some of the first evidence of odorant evoked activity in the olfactory bulb (Adrian, 1942). An LFP represents an average of activity across many neurons. When it shows on oscillatory pattern, this implies that neurons are firing approximately synchronously in the interval of the oscillations. Neurons only have to fire roughly at the same time to show oscillations in the LFP and some describe this as synchronous activity (Lei et al., 2002). However, classically, neurons are said to fire synchronously when the difference in the timing of their spikes is substantially smaller than their interspike interval (Usrey and Reid, 1999).

There are different timescales to oscillations present in the olfactory system. The slowest timescale is in the theta frequency and corresponds to the breathing rate of the animal of about 4-8 Hz (Onoda and Mori, 1980). Mitral cell spikes tend to peak at a certain phase of the respiration cycle and the precise location of the peak in the phase (inhalation, exhalation, or intermediate) varies for different mitral cells (Buonviso et al., 1992) but is reproducible suggesting that the timing of firing relative to respiration phase could be important in representing odorant encoding. There is also a faster oscillation present in the gamma frequency band. These are frequencies around 40-80 Hz depending on the species (Adrian, 1942;Eeckman and Freeman, 1990;Laurent and Naraghi, 1994).

One of the prominent theories relating to the functional role of oscillation in olfaction is that it allows for the sparsening of the odor code (Perez-Orive et al., 2002;Wilson and Mainen, 2006). This idea has been addressed most thoroughly in insects. When presented with an odor, insect projection neurons (analogous to vertebrate mitral cells), located in the antennal lobe (analogous to the vertebrate olfactory bulb), exhibit responses that are long lasting and highly probable. However, the targets of projection neurons, the Kenyon cells (analogous to cortical neurons) located in the mushroom body (analogous to vertebrate olfactory cortex) have brief responses and a low probability of firing. In fact, Kenyon cells have a baseline firing rate of 0.005 – 0.025 Hz (Perez-Orive et al., 2002). There is also significant divergence from the

antennal lobe (830 projection neurons) to the mushroom body (50,000 Kenyon cells). Therefore, by responding selectively only to certain, synchronous sets of projection neurons, Kenyon cells are believed to encode specific combinations of active glomeruli (Perez-Orive et al., 2002).

It has also been theorized that oscillations could provide a time base for relative timing of mitral cell action potentials (Hopfield, 1995). In this way, odorant information is encoded not only in the combination of active mitral cells but also in their relative timing, sometimes referred to as latency coding. In the olfactory bulb, recent studies in zebrafish indicate that information about odor identity is encoded in the timing of mitral cell activity relative to oscillation phase (Friedrich et al., 2004). In locusts, while the firing phase of projection neurons does not seem to encode the identity of an odor (Laurent et al., 1996) other studies suggest that it could be used to encode the concentration of an odorant (Stopfer et al., 2003). These latency patterns appear to be introduced by ORN transduction where different ORN types show specific latencies for particular odors and concentrations (Spors et al., 2006). While latencies are shortened with increasing concentration of odorants, the relative timing of mitral cells is preserved (Cang and Isaacson, 2003). This supports the hypothesis that spike latencies could allow for a concentration invariant coding mechanism in olfaction (Hopfield, 1995). Further evidence suggesting a mechanism for latency coding has also been characterized in olfactory bulb granule cells. Extracellular stimulation of glomeruli *in vitro* resulted in different activation latencies for different granule cells. These latencies were consistent for a given granule cell and were also dependent on the individual glomerulus that was activated (Kapoor and Urban, 2006).

However, while neurons in the olfactory bulb appear to exhibit precise modulations of the temporal patterning of odorant-evoked activity, its importance in olfactory discrimination is not fully understood. Blocking synchronous oscillations reduces an animal's ability to perform fine but not coarse discriminations (Stopfer et al., 1997;Teyke and Gelperin, 1999). Also, in the immature olfactory bulb and antennal lobe gamma band oscillations are absent however odor discrimination is not significantly affected by the lack of these oscillations (Fletcher et al.,

2005;Wilson and Laurent, 2005). This suggests that temporal features such as oscillations could play an important role in only fine discriminations. It is possible that oscillations can perform other functions such as translating the intensity of inputs to spike timing information (Hopfield, 1995) which has been proposed to mediate a method of comparing odors at different concentrations (Brody and Hopfield, 2003). Evidence also suggests that slower theta and beta oscillations could play a role in coordinating sensory information with other sensory, cognitive, or motor processes (Uchida et al., 2006;Komisaruk, 1970;Kay, 2005;Martin et al., 2007).

1.4 MODULATION OF SENSORY REPRESENTATIONS

In the preceding section, I reviewed the primary theories of the method of representation of odors in the olfactory bulb. While representation of the stimulus is a critical first step in sensory systems, it is only the beginning in the flow of information that eventually leads to conscious perception. Once represented, sensory information in every modality undergoes a series of transformations mediating various functions important in forming the eventual perception of the sensory stimulus. These functions are carried out by the circuitry and physiology of the neuronal networks at each stage of processing. Below I review one of the classic forms of processing that could play a significant role in olfactory processing, that of lateral inhibition, as well as the main types of computations it is thought to mediate in olfaction.

1.4.1 Lateral Inhibition

One of the classic methods of mediating neuronal interactions is that of lateral inhibition. Generally, lateral inhibition refers to the inhibition of one neuron as a result of the activation of

another. The idea of antagonism in biology can even be traced back to Descarte's description of the movement of the eye in 1662. He observed that in order to move the eye in a certain direction, it required the contraction of the muscle on the side corresponding to the direction of movement in addition to relaxation (i.e. inhibition) of the opposing muscle. This concept of antagonism was applied to our understanding of neuronal interaction by studies of the spinal cord reflex pathway. Renshaw showed that antidromic activation of motoneurons resulted in inhibition of those cells (Renshaw B, 1946). This was later found to be achieved by activation of intermediate inhibitory neurons that when stimulated, would result in feedback inhibition as well as inhibition of the motoneurons innervating the counteracting muscle (Eccles et al., 1954). This is one of the classic examples of a circuit motif (in this case lateral inhibition) mediating a physiologic function (motor reflexes).

This concept of antagonism between neurons also plays a central role in processing of sensory information as well and inhibition between neurons is thought to underlie many important computations within the nervous system. Below I review the some of the main functions that could be applicable to olfactory processing.

1.4.2 Contrast Enhancement and Gain Control

One of the classic functions mediated by the nervous system is that of contrast enhancement. The first observation of this effect came from Ernst Mach in 1866. He observed that when a looking at an image containing a light and dark region separated by a gradient, there were accentuated bands adjacent to the border of the two regions. In this way, the difference between the light and dark sides was in some way amplified at the border of these two regions and therefore the contrast between the two regions was enhanced.

a.

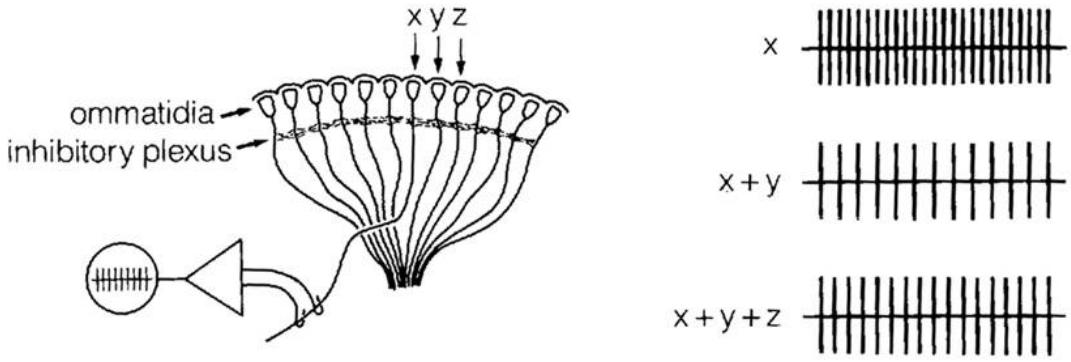
x y z
ommatidia
inhibitory plexus
x
x + y
x + y + z

b.

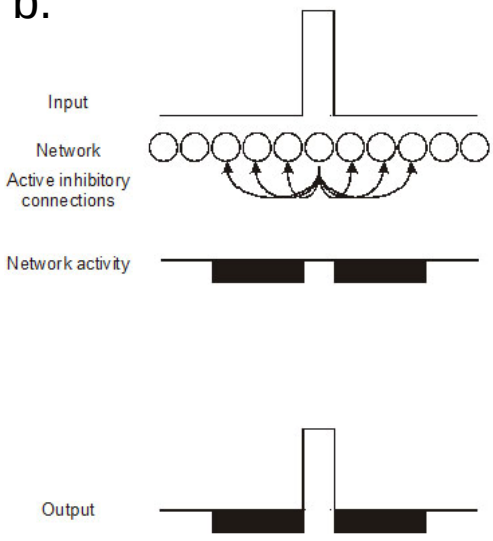
Input
Network
Active inhibitory connections
Network activity
Output

Figure 1.3. Lateral inhibition and contrast enhancement. Early studies of lateral inhibition in the eye of the *Limulus* depicted in **a)** where activation of multiple cells results in inhibition of nearby cells. **b)** Schematic of center-surround receptive fields generated from lateral inhibition. Upward stepped line represents excitatory input. Arrows indicate lateral connectivity between the cell receiving excitatory input and neighboring cells. Stimulation of the center cell results in inhibition of neighboring cells (represented by downward, solid bars) and a final network output showing center excitation and surround inhibition. Panel **a)** modified from Dowling's "The Retina".

The physiologic basis of this effect, now known as Mach bands, was later explored by Hartline (1938). In these pioneering experiments using the eye of the *Limulus*, he showed that activation of a particular region of the eye corresponding to the nerve fiber being recorded from resulted in an increase in firing rate. However, simultaneous stimulation of adjacent regions resulted in a reduction in this firing rate (**Fig. 1.3A**)(Hartline et al., 1956). It is now known that this effect is a result of lateral inhibition of photoreceptors such that activation of an individual receptor results in inhibition of nearby receptors (Werblin, 1972). In this way, lateral inhibition sharpens the tuning curves of individual neurons by enhancing the contrast between neurons activated by similar stimuli (**Fig. 1.3B**).

While the effect of lateral inhibition has been well characterized in the visual system, it is a general processing mechanism in other parts of the brain as well. The equivalent result of visual Mach bands was also found in the somatosensory system by stimulating nearby regions of the skin (Revesz, 1934). Subsequent studies showed that lateral inhibition also had a functional role in the somatosensory cortex where GABA-mediated inhibition plays a functional role in shaping receptive fields in the cat somatosensory cortex (Kaas et al., 1984) as well as rat barrel cortex (Kyriazi et al., 1996).

Could a similar mechanism be employed to process information in the olfactory system? The key requirement for contrast enhancement mediated by lateral inhibition as seen in other sensory systems is that neurons with similar receptive fields inhibit one another more than neurons with dissimilar receptive fields (**Fig 1.4**). Activation of a particular neuron then results in activation of inhibitory cells that in turn inhibit neurons that are located in nearby regions and therefore have similar receptive fields. Several studies have investigated the possible role of lateral inhibition in mediating this kind of center-surround inhibition. Notably, individual mitral cell responses to glomerular stimulation were also investigated in a study of rat mitral cells indicating that mitral cells located underneath a glomerulus that was stimulated were excited while nearby mitral cells were inhibited (Luo and Katz, 2001). Furthermore, aliphatic aldehydes of increasing carbon chain length were used in conjunction with single unit in vivo recordings in the cat (Yokoi et al., 1995). These experiments indicated that aldehydes with

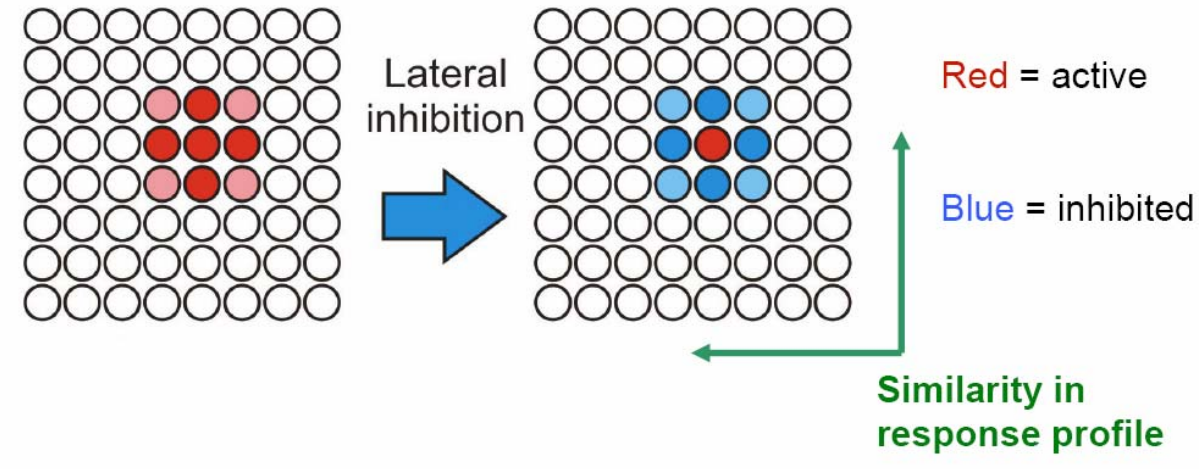
Lateral
inhibition
Red = active
Blue = inhibited
Similarity in
response profile

Figure 1.4. Specification of lateral connectivity. Lateral inhibition results in center-surround receptive fields. Activation of neurons within a network (red circles) results in activation of a subset of neurons (left panel). The addition of lateral inhibition (right panel) results in inhibition of nearby neurons (blue circles) resulting in contrast enhancement. However, lateral inhibition such as this that is based on the location of neurons within the network requires that neurons with similar response profiles are located near one another as well. This arrangement of neurons according to their similarity in response profile is depicted by the green arrows.

similar carbon chain lengths inhibited the response to aldehydes with similar chain lengths suggesting center-surround inhibition. However, it is unclear from these studies how much of this sharpening is due to inhibition simply reducing the activity and therefore sharpening the response of the neuron. Furthermore, it is unclear how this effect would generalize to molecules that do not have an obvious molecular feature that could be used to rank them according to similarity (like increasing carbon chain length).

As reviewed in the previous section, it is unlikely that a fine-grained chemotopic map exists in the olfactory bulb. Rather, it appears that odorants are represented by distributed activity throughout broad regions of the bulb (Rubin and Katz, 1999;Johnson and Leon, 2000a;Uchida et al., 2000;Wachowiak and Cohen, 2001;Friedrich and Korsching, 1997). This makes it difficult to reconcile how center-surround inhibition based on the physical location of neurons results in contrast enhancement in the olfactory bulb. Despite this difficulty, is it still possible that lateral inhibition could somehow enhance contrast in the bulb? Early studies blocking inhibition using the $GABA_AR$ antagonists picrotoxin and bicuculline showed that this resulted in broader odor-evoked activation of mitral cells (Duchamp-Viret et al., 1993). Similarly, a study performed in honeybees found that principal neurons were more broadly tuned when inhibition from local interneurons was removed (Sachse and Galizia, 2002). Furthermore, studies investigating the population responses of mitral cells in zebrafish using elecrophysiological (Friedrich and Laurent, 2001) as well as Ca^{++} imaging (Yaksi et al., 2007) techniques show that mitral cell responses are progressively decorrelated as a result of intrabulbar processing. Therefore, it appears that lateral inhibition could play an important role in mediating contrast enhancement and increasing the ability to discriminate between similar odors.

Gain control is another function hypothesized to be mediated by inhibition in the olfactory bulb. This is an important function in olfaction considering that exposure to odors can occur in a wide range of concentrations and that odor quality generally persists over a range of 100 factors (Lancet et al., 1988;Youngentob et al., 1990) although there are some examples of odor quality changing with increasing concentrations (Arctander, 1969;Gross-Isseroff and

Lancet, 1988). Indeed, feedback inhibition (Williamson et al., 1993) in the glomerular layer has been shown to suppress transmitter release (Wachowiak and Cohen, 1999). Additional studies indicate that this inhibition could be mediated via activation of $GABA_BRs$ (Aroniadou-Anderjaska et al., 2000) as well as dopamine receptors at presynaptic nerve terminals (Wachowiak et al., 2005). These physiological results agree with imaging studies showing concentration-invariant responses of ORN activity in the bulb (Xu et al., 2000;Johnson and Leon, 2000a;Schaefer et al., 2000;Wachowiak et al., 2002) as well as *in vivo* recordings from MCs that show relatively constant firing rates whether stimulated weakly or strongly (Margrie et al., 2003;Cang and Isaacson, 2003).

1.4.3 Dynamical Transformations

While spatial contrast enhancement and gain control as described above are some potential functional roles for inhibition in the bulb, others functional roles have been proposed that consider transformations of odor-evoked activity in time. Given the difficulty in determining how the multidimensional odor space could be mapped continuously in the two dimensional olfactory bulb, it would appear that mechanisms of processing that do not rely on this type of arrangement could be useful in olfactory processing. Modulation of temporal response patterns by inhibition has been shown to play an important role in many areas including cortical visual processing (Engel et al., 1992;Singer and Gray, 1995) and recent studies in auditory cortex have suggested that lateral inhibition functions mainly to alter the temporal responses of cortical neurons rather than sharpen their tuning curves (Wehr and Zador, 2003;Wehr and Zador, 2005).

Early studies have shown that inhibition in the olfactory bulb plays an essential role in developing the oscillations observed in response to odors (Bressler and Freeman, 1980;Mori et al., 1981;Segev, 1999). GABAergic inhibition has also been shown to result in tuning the precise rate of gamma oscillations in the bulb (Lagier et al., 2007). In this study, the investigators genetically deleted the alpha1 subunit of the $GABA_AR$ which is specifically expressed in MCs.

This resulted in MCs expressing the alpha3 subunit which has slower kinetics resulting in slower and smaller amplitude dendrodendritic inhibition and slower gamma oscillations. An interesting study by Galan et al. (Galan et al., 2006) also investigated the role of inhibition in generating oscillations in the olfactory bulb. By recording from mitral cells in the olfactory bulb, they found that synchronization was mediated by correlated input from common granule cells which agrees with previous theoretical studies (Teramae and Tanaka, 2004;Nakao et al., 2005).

While oscillations are present in the bulb, do they have a role in odor discrimination? Gamma oscillations have been shown to be enhanced in the olfactory bulb during discrimination tasks pointing to their potential physiological importance (Martin et al., 2007). The physiologic importance of oscillations was directly addressed in the locust where the addition of the $GABA_AR$ antagonist pricrotoxin resulted in an elimination of oscillations (Stopfer et al., 1997). Blocking oscillations in this way also resulted in impaired odor discrimination by locusts. This result potentially highlights the importance of inhibition-induced oscillations in odor discrimination. However, this result is only correlational since inhibition could be mediating functions important in discrimination other than oscillations. Interestingly, selective deletion of $GABA_ARs$ on GCs (while preserving $GABA_A$ receptors on MCs) in the mouse olfactory bulb resulted in an increased power of oscillations (Nusser et al., 2001). Behaviorally, this resulted in initially improved performance on odor discrimination tasks but performance after training was not as good as controls pointing to a potentially complex role for oscillations in discrimination and memory.

1.5 GOALS OF DISSERTATION RESEARCH AND SUMMARY OF FINDINGS

Lateral inhibition is a circuit motif that mediates important physiological interactions in many sensory systems such as contrast enhancement. While mitral cells receive significant lateral inhibition in the olfactory bulb, due to the distributed representation of odorant-evoked activity and the widespread connectivity throughout the bulb, it is unclear what functional role this inhibition has. Considering that mitral to granule cell connections are reciprocal and mediate both recurrent and lateral inhibition, we hypothesized that lateral inhibition could be modulated by pre- as well as postsynaptic neurons.

The research in **chapter 2** focuses on the physiological properties of lateral inhibition in the olfactory bulb. Specifically, we observed that the amount of lateral inhibition received by a given mitral cell (designated as the postsynaptic neuron) was dependent not only on the activity of the paired mitral cell (presynaptic neuron) but also on its own activity. In this way, the effectiveness of lateral inhibition is dependent on the activity of the neuron being inhibited. Furthermore, we found that the effectiveness of this activity-dependent inhibition was confined to a specific range of postsynaptic firing frequencies such that mitral cells firing at low rates as well as high rates were immune to the effect of lateral inhibition. The rest of the chapter presents results investigating the physiological properties of this novel form of lateral inhibition.

Considering the distributed representation of olfactory information and the widespread connectivity of mitral cells throughout the bulb, we hypothesized that this activity-dependent inhibition could allow for important functional interactions such as contrast enhancement. We investigated this possibility using computational techniques, the results of which are presented in **chapter 3**. First we investigated the mechanism underlying activity-dependent inhibition and show that integration of pre- and postsynaptic activity within a single granule cell is

sufficient to result in activity-dependent inhibition. Next, we investigated in detail the functional implications and found that not only was activity-dependent inhibition able to enhance contrast and decorrelate initially similar input patterns, but it was able to do so without requiring any spatial structure to the network or stimulus. Finally, we investigated the implications for parallel processing of odorant information by extending this computational technique to image processing and show that different features of an image can be extracted by neurons tuned to different frequencies of activity-dependent inhibition.

All of the experiments presented in this thesis were conducted by Armen C. Arevian except those presented in **Fig. 2.17** which were conducted by Vikrant Kapoor.

2.0 ACTIVITY-DEPENDENT GATING OF LATERAL INHIBITION

2.1 ABSTRACT

Lateral inhibition is a circuit motif found throughout the nervous system that often generates contrast enhancement and center-surround receptive fields. We have investigated the functional properties of the circuits mediating lateral inhibition between olfactory bulb principal neurons (mitral cells) *in vitro*. We find that the lateral inhibition received by mitral cells is gated by postsynaptic firing, such that a minimum threshold of postsynaptic activity is required before effective lateral inhibition is recruited. This dynamic regulation allows the strength of lateral inhibition to be enhanced between cells with correlated activity. These results show that this novel mechanism for specifying lateral inhibitory connections allows functional inhibitory connectivity to be dynamically remapped to relevant populations of neurons.

2.2 INTRODUCTION

Lateral inhibitory circuits are known to enhance contrast, facilitate discrimination of similar stimuli and mediate competitive interactions between active neurons (Hirsch and Gilbert, 1991;Urban, 2002). These properties are due to reductions in the degree to which input-driven activity is correlated across neurons responding to stimuli (Friedrich and Laurent, 2001).

However, for lateral inhibition to function effectively in this manner, inhibition must be stronger between cells that are activated by similar stimuli, i.e. between cells having correlated activity (Linster et al., 2005). When information is represented topographically, similar stimuli activate nearby neurons, so local inhibitory interactions are an effective means for contrast enhancement. This arrangement ensures that cells with correlated activity have strong inhibitory connectivity (Kuffler, 1953). However, there are alternative strategies of specifying effective lateral inhibitory connectivity. For example, neurons with similar receptive fields can be connected specifically, independent of their proximity (Bosking et al., 1997). In this study, we investigate a third possibility, in which the strength of lateral inhibition is dynamically enhanced between neurons with correlated activity

Based on the known properties of olfactory bulb circuits we hypothesized that such a dynamic specification of inhibitory connectivity may be possible and functionally useful in the olfactory bulb (Jahr and Nicoll, 1982). At the level of olfactory receptor neuron input to the olfactory bulb, stimuli are thought to be represented combinatorially with discontinuous topography (Uchida et al., 2000;Uchida et al., 2000;Friedrich and Korsching, 1997). Connectivity between mitral cells lacks obvious patterning (Egger and Urban, 2006;Willhite et al., 2006). Single molecule odorants activate many glomeruli distributed widely across the surface of the bulb. Unrelated odors can activate glomeruli in nearby areas and structural similarity of odorant molecules is often only weakly correlated with the relative position of the activated glomeruli (Uchida et al., 2000;Friedrich and Korsching, 1997;Rubin and Katz, 1999;Meister and Bonhoeffer, 2001).

Lateral inhibition in the olfactory bulb is mediated largely by reciprocal dendrodendritic synaptic connections between mitral cell lateral dendrites and the dendrites of inhibitory granule cells (Shepherd and Greer, 2004;Schoppa and Urban, 2003). Mitral cell dendritic trees are radially symmetric, spanning an area up to 2mm in diameter, connecting (disynaptically via the granule cells) a single mitral cell with as many as half of all the other mitral cells in the bulb (Orona et al., 1984;Mori et al., 1983). These lateral dendrites release glutamate which depolarizes granule cell dendrites which in turn release GABA back onto the presynaptic mitral

cell (recurrent inhibition) as well as other mitral cells (lateral inhibition) (Schoppa and Urban, 2003). The same population of granule to mitral cell synapses mediate both recurrent and lateral inhibition (Price and Powell, 1970). This suggests that when multiple mitral cells are active, recurrent and lateral inhibition will interact because multiple mitral cells will excite overlapping populations of granule cells (see **Figs. 2.9** and **2.18**). Such an arrangement may allow mitral cells to regulate (via their own activity and the input they provide to granule cells) the effectiveness of the lateral inhibition that they receive. Specifically, we predicted that the output of weakly activated granule cells would be facilitated by the activity of a given mitral cell, enhancing the lateral inhibition that this cell receives, similar to what has been reported recently in cortical circuits (Kapfer et al., 2007). In contrast, when granule cells are strongly active, additional input to these cells will not generate additional output.

The functional properties of inhibitory circuitry in the olfactory bulb are not well understood and the role of this circuitry in stimulus coding is controversial (Laurent, 1999). Here we show that the efficacy of lateral inhibition from an active mitral cell is enhanced when the postsynaptic mitral cell is also firing, i.e. when the mitral cells show correlated activity.

2.3 MATERIALS AND METHODS

2.3.1 Slice Preparation

Sagital slices of mouse olfactory bulb were prepared according to procedures described previously (Urban and Sakmann, 2002;Margrie et al., 2001). Briefly, 2-3 week old mice (strain C57/B6) were anaesthetized deeply with a mixture of Ketamine 0.1% and Xylazine 0.1%, decapitated and their brains quickly removed and placed in ice-cold Ringer's solution (containing (in mM): NaCl 125, KCl 2.5, NaHCO3 25, NaH2PO4 1.25, MgCl2 1, glucose 25, CaCl2 2.5). The olfactory bulbs were removed and glued, medial side down, to the stage of a vibratome where they were sliced in 300 micrometer sections. Following cutting, the slices

were incubated in the above solution for about one hour at 37°C after which they were allowed to equilibrate to room temperature.

2.3.2 Electrophysiological recordings

Whole-cell recordings (current clamp) from mitral cells were obtained using Multiclamp 700A/B amplifiers (Axon instruments, Foster City, CA), and ITC-18 data acquisition hardware. Cell morphology was visualized using differential interference contrast (DIC) optics (Zeiss Axioscope 2FS, 60x 0.9NA objective) and video microscopy (Photometrics CoolSNAP ES). Prior to recording, slices were placed in a submersion chamber and perfused at 1-2 ml/min) with oxygenated Ringer's solution maintained at 33°-35°C. Whole cell pipettes (3-7 MOhm) were pulled from borosilicate glass and filled with solutions containing (in mM): Potassium gluconate 130, HEPES 10, MgCl2 2, MgATP 2, Na2ATP 2, GTP 0.3, NaCl4, biocytin 0.5-1%, and Alexa 594 hydrazide 0.01 at pH 7.3. Theta glass pipettes and ISO-flex stimulus isolator (A.M.P.I., Jerusalem, Israel) were used to deliver current pulses for extracellular stimulation. Paired t-test used for all p-value calculations except **Fig. 2.13** where a Wilcoxon rank-sum test was used.

2.3.3 Calcium imaging

Loading and imaging of fura-2 was performed as described previously (Kapoor and Urban, 2006). Briefly, olfactory bulb slices were incubated in chamber containing 500ul of ringer's solution to which was added 3 µl of 0.01% Pluronic (Molecular Probes) and 5 µl of a 1 mM solution of fura-2 acetoxymethyl ester (AM) (Molecular Probes) in 100% DMSO solution. Slices were incubated in this solution at 37° C for 60-90 minutes.

Slices were imaged under an upright microscope using either 20x, 40x or 60x water immersion objectives. Slices were visualized for successful loading using excitation wavelength of 360-400 nm and emission wavelength of 480-520 nm. Experiments were performed at 37° C and Ringer's solution had Mg^{++} reduced to 0.2 mM to facilitate activation of granule cells

(Kapoor and Urban, 2006). A cooled back-illuminated frame transfer CCD camera (Micromax 512 BFT, Princeton Instruments) was used to capture sequences of images (movies) with exposure times of 25–50 ms per frame at 3x3 binning (final image size =170x170 pixels). Images were acquired and stored using software written in Igor Pro (Wavemetrics) using drivers (SIDX) from Bruxton Scientific. Movies were analyzed by first calculating ΔF/F frame by frame for whole movies. Sets of ten movies were collected for each condition. To determine the population of active cells we took the minimum (because in our conditions fura decreases its fluorescence when binding calcium) pixel value from this set of 10 movies. By taking the minimum projection we may overestimate the number of active cells (if some cells are active spontaneously) in proportion to the number of trials being considered. However, in our conditions there is very little spontaneous activity of granule cells and so we consider this method to provide a good estimate of the number of active cells even when the probability of a cell being active is ~ 30% as previously reported for granule cells.

2.4 RESULTS

2.4.1 Activity-Dependent Gating of Lateral Inhibition between Mitral Cells

To investigate the regulation of lateral inhibition by the activity of postsynaptic mitral cells, we recorded from these cells in slices of mouse main olfactory bulb while evoking lateral IPSPs via extracellular stimulation of nearby mitral cells. Mitral cells were activated by stimulation in the glomerular layer (40 pulses at 100 Hz, approx. 200 µm from the recorded mitral cell, **Fig. 2.1A**). Care was taken not to stimulate the glomerulus of the recorded mitral cell, which invariably resulted in EPSPs. The IPSPs evoked had a maximum amplitude of <2 mV and typically showed synaptic depression, consistent with previous results (**Fig. 2.2B**) (Dietz and Murthy, 2005). By injecting current steps of various amplitudes (400 ms, 0-1200 pA) into the mitral cell, we were

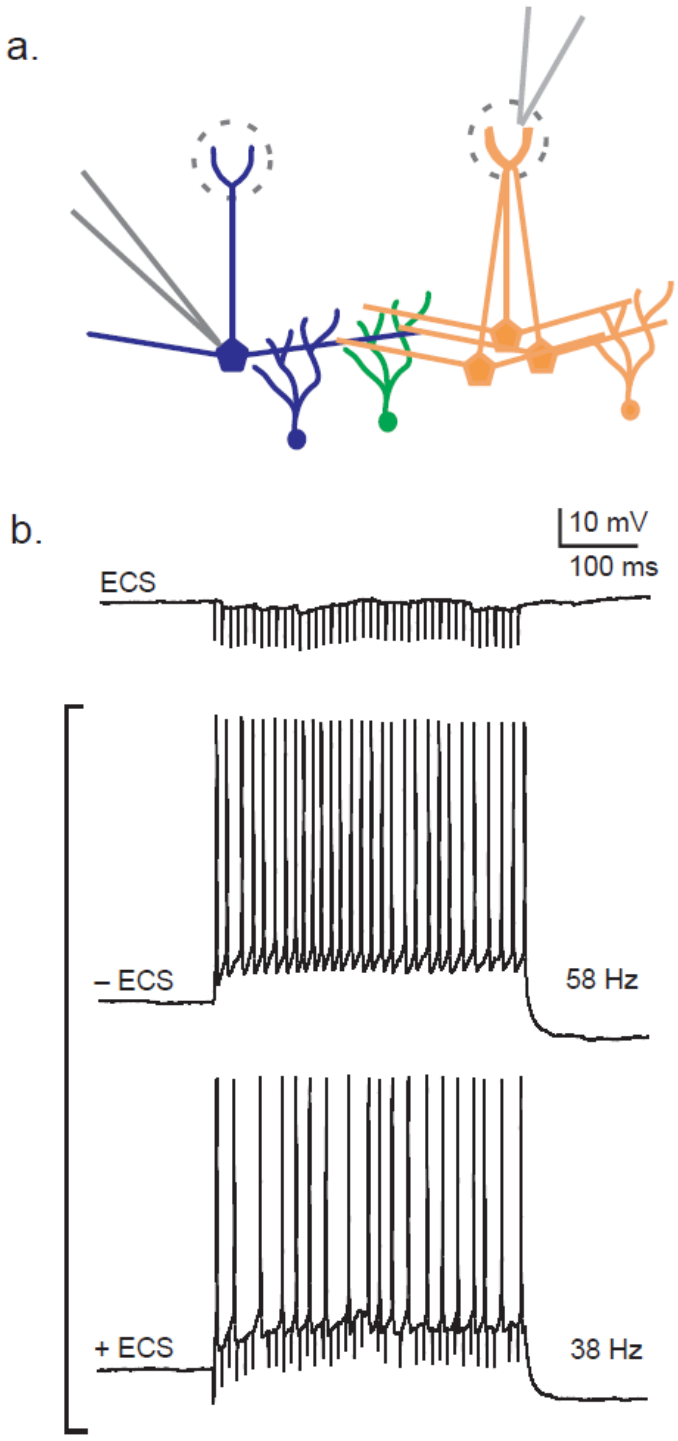
a.
b.
10 mV
100 ms
ECS
– ECS
58 Hz
+ ECS
38 Hz

Figure 2.1. Lateral inhibition evoked by glomerular stimulation. a) Schematic of experimental configuration. Whole-cell recording of a single mitral cell (blue cell, 'postsynaptic cell') during application of extraceullular stimulation (ECS) in the glomerular layer, activating a population of presynaptic mitral cells (orange cells). Mitral cells are disynaptically connected via the shared population of granule cells (green cells). Granule cells shown in blue and orange are connected to only the mitral cell of the same color. **b)** ECS (downward spikes shown are stimulus artifacts) evokes IPSPs in the recorded mitral cell and results in inhibition of firing rate for a given current step. The control firing rate (58 Hz) is reduced (to 38 Hz) by ECS.

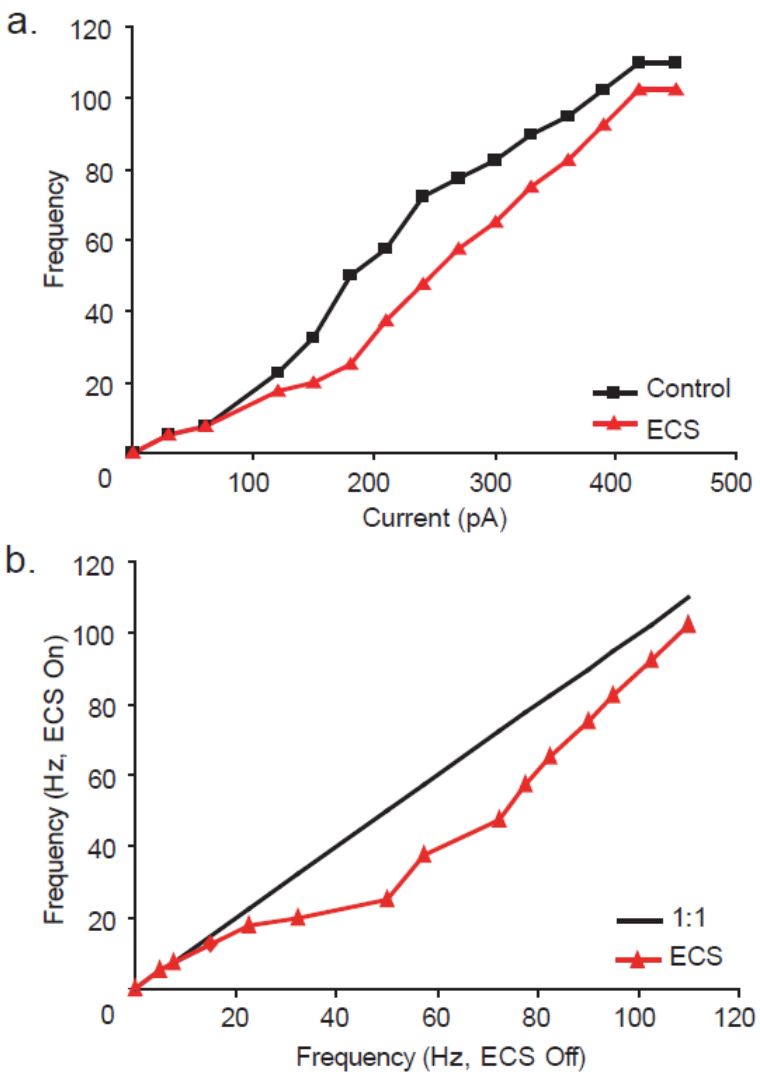

Figure 2.2. Activity-dependent gating of lateral inhibition. Effectiveness of ECS in reducing mitral cell firing rate is shown in a) by plotting F-I curves (red line with ECS and black line without ECS) and in b) by plotting frequency with and without ECS for the same current steps.

able to determine the relationship between injected current and firing frequency (F-I curve) of the postsynaptic mitral cell. F-I curves (**Fig. 2.2A, B**) obtained by current injection alone were compared to curves generated while eliciting IPSPs by extracellular stimulation. These data show that extracellular stimulation had no effect on mitral cell firing rate when the cells fired at low to moderate frequencies (0-25 Hz) or at very high frequencies (>65 Hz). Mitral cell firing was reduced by lateral inhibition specifically when cells were firing between 25 and 65 Hz (**Fig. 2.3**, 24 ± 4.1% (blue line) and 7 ± 1.25 Hz (red line) average peak reduction between 25 and 65 Hz, n=7, $p < 0.05$). Thus, we concluded that the efficacy of lateral inhibition is enhanced in a frequency-specific manner when mitral cells are firing at intermediate rates.

We next tested whether gating of inhibition by postsynaptic activity could be seen in the most basic unit of lateral inhibition: the circuit consisting of two mitral cells and their associated granule cells. To test this, we made simultaneous recordings from pairs of mitral cells (**Fig. 2.4**). A typical pair of mitral cells is depicted in **Fig. 2.4**, reconstructed from a biocytin filled tracing. Furthermore, it is possible to visualize the single apical dendrite and dendritic tuft branching in the glomerular layer of one of the mitral cells (closed arrow) while the second mitral cell's apical dendrite was cut due to the slicing procedure before reaching the glomerulus. We generated F-I curves in one mitral cell (chosen randomly, referred to as the postsynaptic cell) while stimulating the second mitral cell (referred to as the presynaptic cell) at a high, fixed rate (between 60 and 100 Hz) on alternate sweeps (**Fig. 2.5**). Similar to the experiment in **Fig. 2.1** above, activity of a single presynaptic mitral cell reduced the firing rate of the postsynaptic mitral cell, but only when that cell was firing in a particular range of frequencies (**Fig. 2.6A, B**). We observed a reduction in postsynaptic firing rate in 15 out of the 29 pairs tested and in all cases in which inhibition was observed its effectiveness was reduced or absent at very low and very high firing rates. Mitral cells were significantly inhibited when their postsynaptic firing rates were between 35 and 110 Hz (n=15 pairs, $p<0.05$, 18 ± 2.7% (blue line) and 8.7 ± 1.4 Hz (red line) average peak reduction in firing rate, **Fig. 2.7**). The magnitude of inhibition was largest at 81 Hz when averaged across all the mitral cell pairs (**Fig. 2.7**, red line). The range of firing rates over which inhibition was observed for the population of 15

mitral cell pairs exhibiting a reduction in postsynaptic firing rate are summarized in **Fig. 2.8**. On average, mitral cells were inhibited over a 32 ± 7 Hz range of postsynaptic firing rates. Interestingly, this inhibition occurred in many cases despite not observing any obvious IPSPs resulting from presynaptic activity alone (e.g. **Fig. 2.5**, top panel). This suggests the cooperative activation of the inhibitory granule cells by multiple mitral cells is critical to this phenomenon (see discussion). We confirmed that the inhibition we observed was at least in part due to granule cells because mitral cells that had their apical dendrites cut proximal to the tuft (as in **Fig. 2.4**) still exhibited activity-dependent gating of lateral inhibition, even though these cells would receive no inhibition from periglomerular cells. The remaining pairs did not exhibit any change in firing rate between the two conditions tested and may represent mitral cell pairs that form either no or only very week synapses with overlapping populations of granule cells (Egger and Urban, 2006).

2.4.2 Effect of Lateral Inhibition on Mitral Cell Spike Timing

We next wanted to determine how mitral cell spike timing was altered by lateral inhibition given results indicating the important role of spike timing and inhibition in olfactory processing within the bulb (Friedrich and Laurent, 2001;Abraham et al., 2004;Uchida and Mainen, 2003;Kapoor and Urban, 2006). To accomplish this we computed the difference in the time-dependent firing rate from our paired recordings between trials with vs. without activity of the presynaptic mitral cell. Spike trains from the postsynaptic cell were smoothed with a gaussian (standard deviation of 45 ms) and the smoothed firing rates for these two conditions were subtracted and these differences were averaged across all 15 pairs (**Fig. 2.9**). This analysis allowed us to determine when, during the 400 ms period of activity, lateral inhibition most effectively reduced firing. We found that at low postsynaptic firing rates, inhibition was weak and unreliable. At higher firing rates (Ravel et al., 2003) the largest reduction in firing rate was observed during the last 40 ms of the 400 ms firing period. Further increasing postsynaptic activity resulted in inhibition that began earlier and had a larger peak magnitude (-40 ± 5%

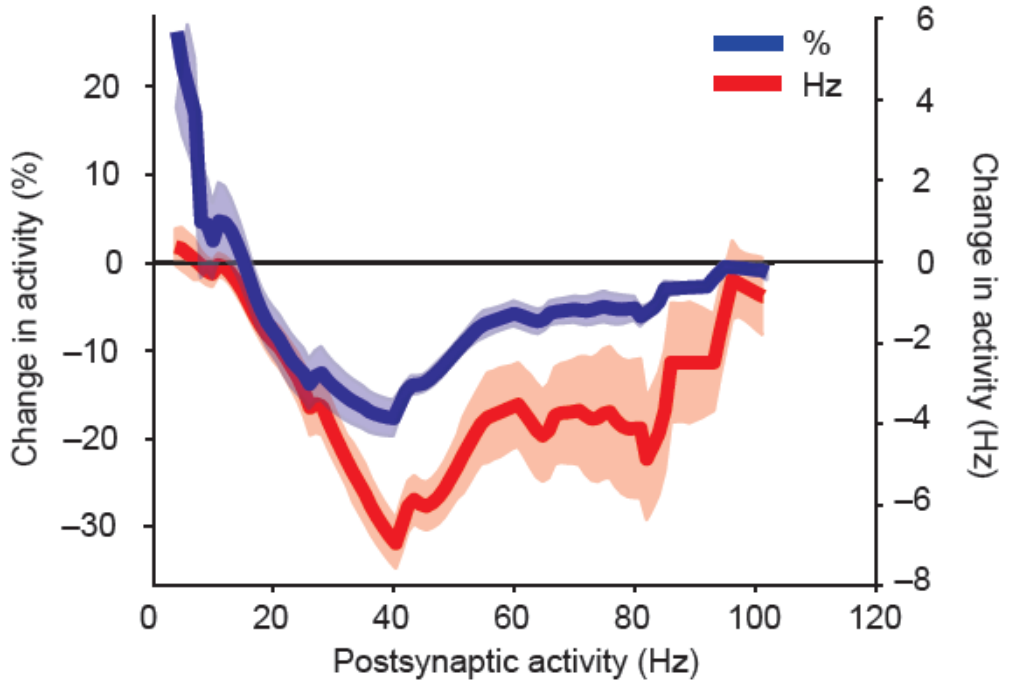

Figure 2.3. Aggregated absolute and % change in firing rate from glomerular stimulation. Percentage change (blue line) as well as absolute change in activity (red line) as a function of firing rate averaged across recordings. Shaded areas for this and subsequent figures indicate SEM.

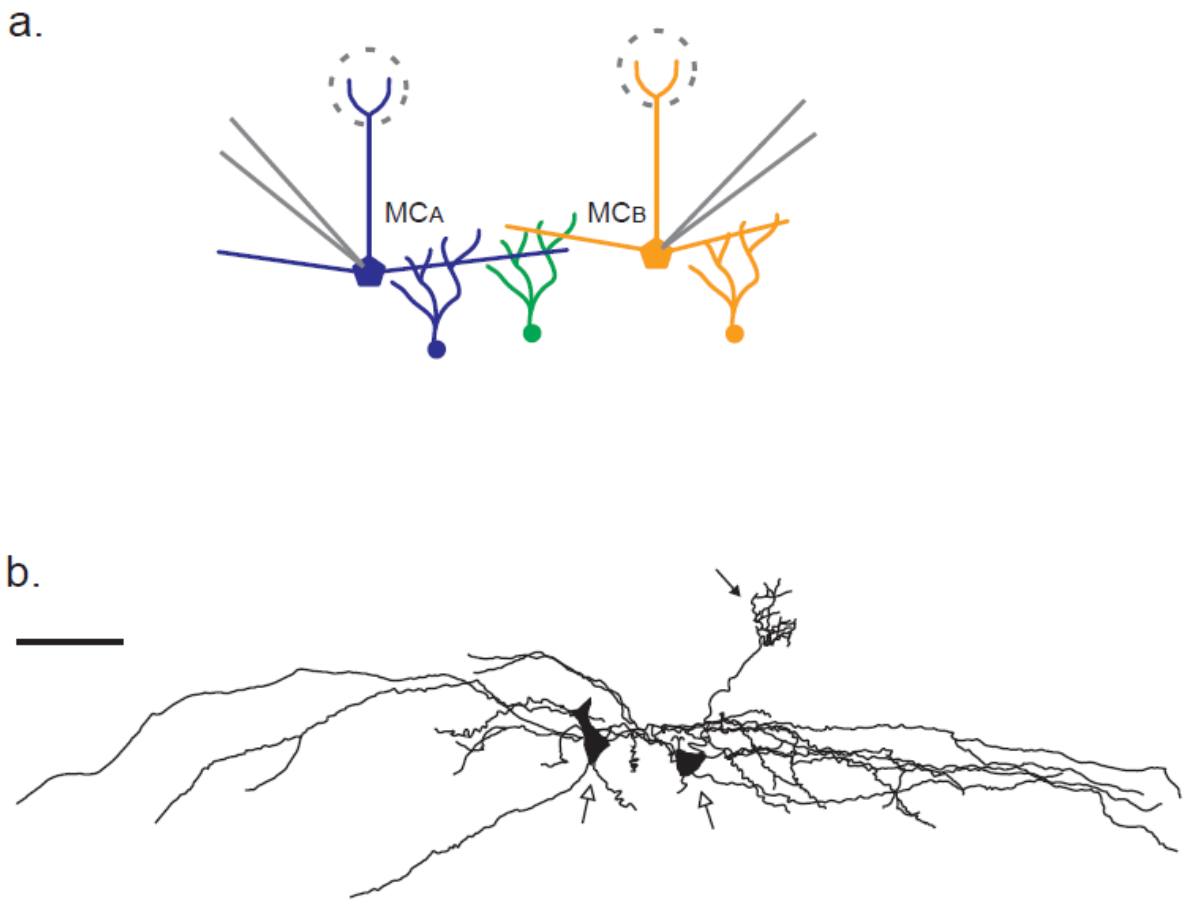

Figure 2.4. Recording from mitral cell pairs. a) Schematic of experiment, whole-cell recording from pairs of mitral cells disynaptically connected via the shared population of granule cells in green. **b)** Tracings from an example of a pair of mitral cells filled with biocytin (scale bar 75 microns). Open arrows indicate cell bodies, filled arrow indicates the tuft of one mitral cell while the other cell had a cut primary dendrite. .

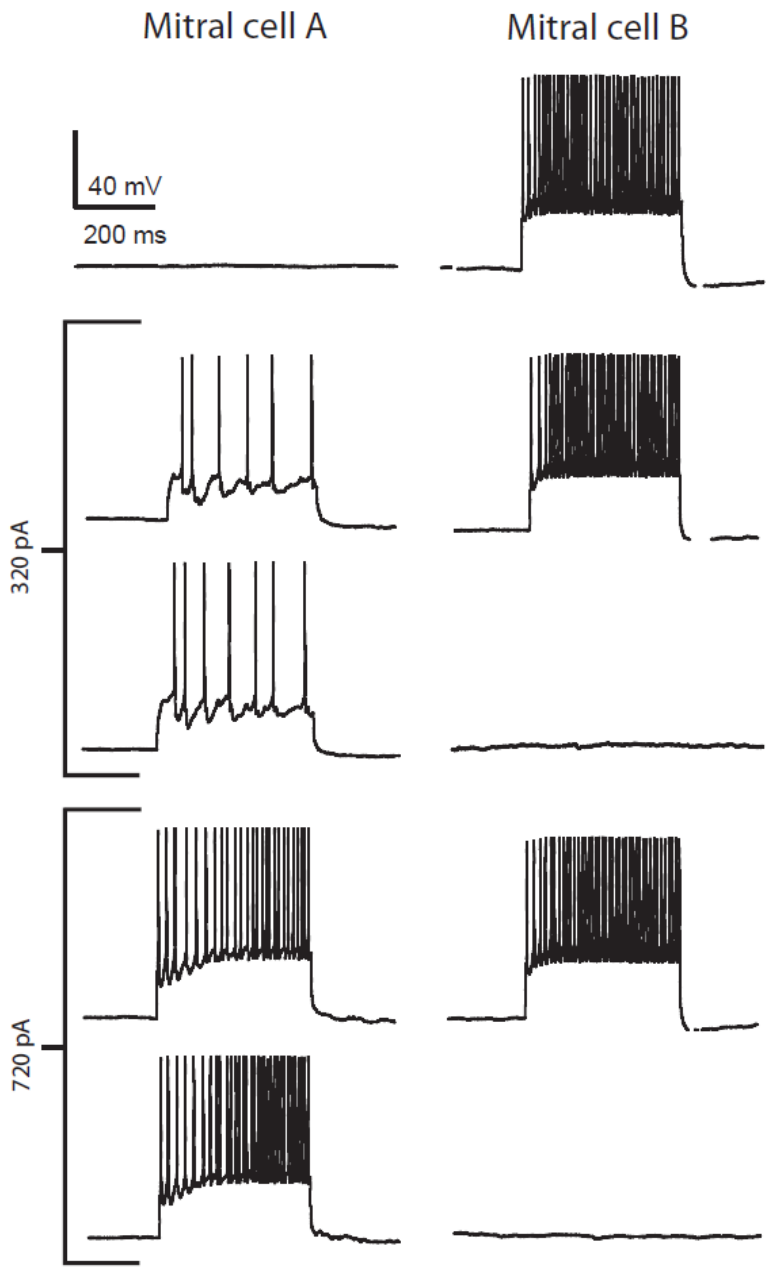

Figure 2.5. Lateral inhibition between mitral cell pairs. Activation of a single presynaptic mitral cell (Mitral cell B, MC_B) does not result in IPSPs in the postsynaptic cell (Mitral cell A, MC_A). Similarly, MC_B is ineffective at inhibiting MC_A when MC_A is firing at 32 Hz. However, at 85 Hz, MC_B is able to reduce the firing rate of MC_A to 65 Hz representing a 24% reduction.

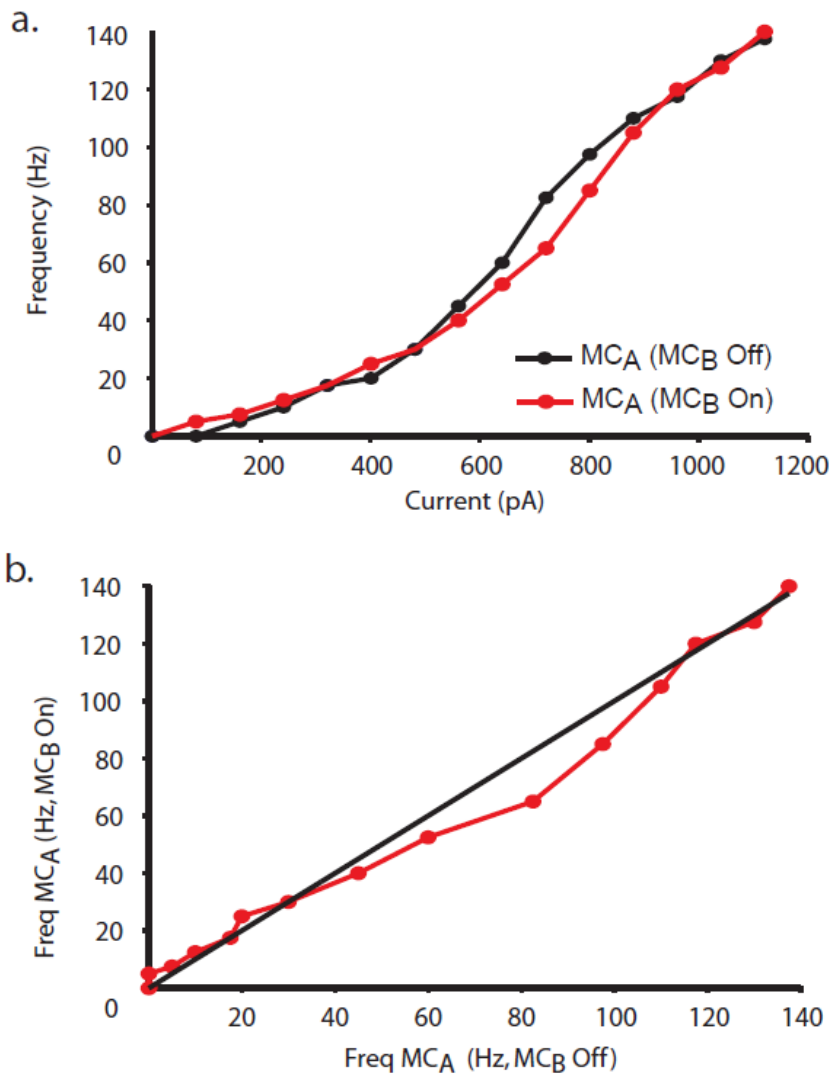

Figure 2.6. Activity-dependent inhibition between mitral cell pairs. Activity-dependent inhibition is illustrated in **a)** by comparing the F-I curves for the control condition (MC_B Off, red line) to the case when MC_B is activated (MC_B On, black line). **b)** Firing rate of MC_A plotted with respect to the two conditions tested showing a selective reduction in firing rate of MC_A only between 45 and 110 Hz.

instantaneous reduction of postsynaptic firing rate at 167 ± 32 ms after stimulus onset at 67 ± 9 Hz.) The large magnitude inhibition observed at high postsynaptic firing rates had a maximum duration of approximately 300ms. This is consistent with the observation that granule cell-mediated lateral inhibition undergoes synaptic depression during repetitive stimulation (Dietz and Murthy, 2005;Urban and Sakmann, 2002) and indicates that the strength of lateral inhibition between mitral cells not only depends on the instantaneous levels of pre- and postsynaptic activity but also on the recent history of activity.

2.4.3 Independent Measures of Activity Dependence

As an independent measure of lateral inhibition we also examined the magnitude of recurrent IPSPs recorded in the postsynaptic mitral cell with and without activity of the presynaptic cell. We quantified recurrent inhibition by measuring the hyperpolarization following a 400 ms train of action potentials of a given frequency (Margrie et al., 2001). This hyperpolarization was 31 ± 4.4% larger on trials in which the presynaptic mitral cell was firing, even when controlling for the firing rate of the postsynaptic cell (from -3.4 ± 0.7 to -4.6 ± 0.6 mV for 22 ± 3.4 Hz activity, $p<0.01$, **Fig. 2.10A**). These data demonstrate that stimulation of a single presynaptic mitral cell is sufficient to enhance recurrent inhibition. Since the hyperpolarization following trains of action potentials results from a combination of synaptic and intrinsic conductances (Margrie et al., 2001;Isaacson and Strowbridge, 1998) the increased hyperpolarization that we observe may underestimate the actual increase in synaptic inhibition (Isaacson and Strowbridge, 1998). We also examined whether granule cell-mediated inhibition was enhanced by temporal precision of mitral cell spiking (**Fig. 2.10B**). To test this we varied the timing of spiking in a single mitral cell to examine whether groups of action potentials at short intervals recruited additional inhibition. We found that changing the AP train from one with uniform intervals (8 spikes at 40 ms) to one in which spikes were clustered (4 pairs of spikes at 40 ms) had no effect on the magnitude of granule cell-mediated recurrent inhibition ($p>0.8$, $n=5$). The lack of sensitivity to temporal coincidence of input in granule cells is

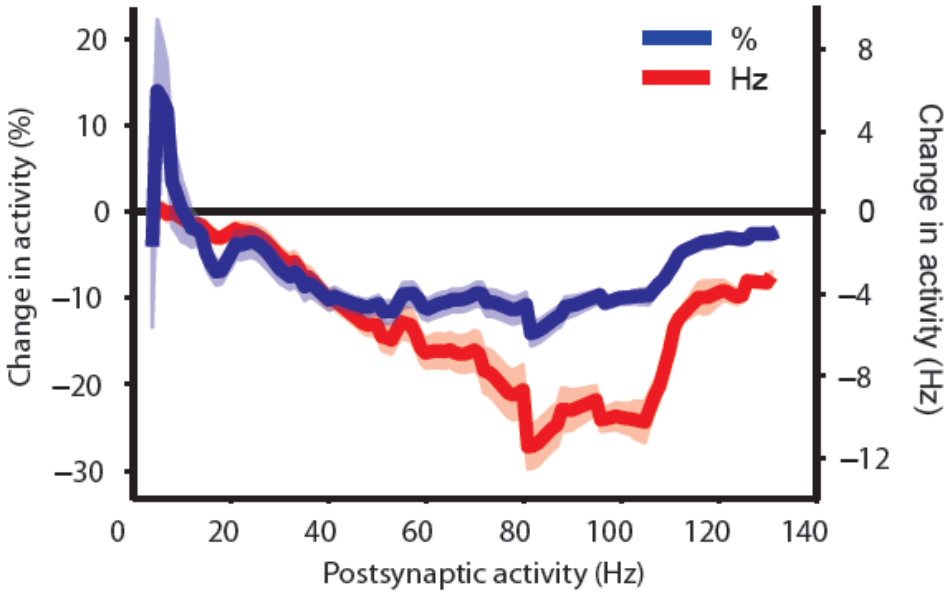

Figure 2.7. Aggregated absolute and % change in firing rate from paired recordings.

Percentage change (blue line) as well as absolute change in activity (red line) as a function of firing rate averaged across paired recordings.

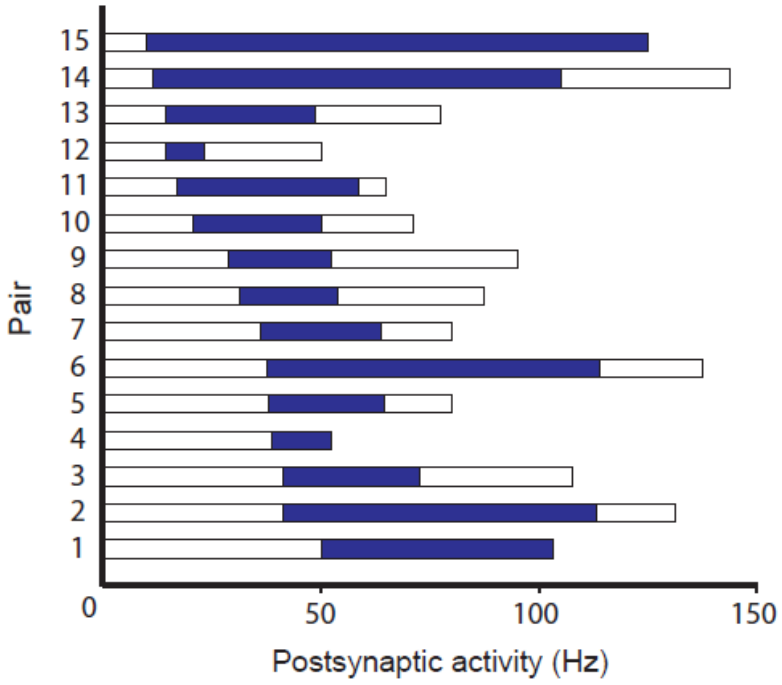

Figure 2.8. Distributed activity-dependent ranges of inhibition. Data from 15 mitral cell pairs exhibiting lateral inhibition. The range of inhibition is plotted with respect to postsynaptic activity. White bars indicate range of postsynaptic activity recorded while blue bars indicate frequencies of activity-dependent inhibition (defined as >=5% reduction in firing rate).

consistent with the observation that they respond at long latencies (Kapoor and Urban, 2006) and are best activated by prolonged inputs (Schoppa and Westbrook, 1999) (see discussion).

We hypothesized that the gating of lateral inhibition by coincident activity in mitral cell pairs is due to granule cells receiving common input from the mitral cells and that coincident activity of these mitral cells recruits additional granule cells which then contribute additional lateral inhibition (Jahr and Nicoll, 1982) (see **Figs. 2.11** and **2.18**). This hypothesis predicts that increasing the firing rate of the presynaptic mitral cell should decrease the requirement for high frequency firing in the second mitral cell and thus shift the range of postsynaptic firing rates over which activity-dependent gating of lateral inhibition occurs. To test this prediction, we generated F-I curves for a postsynaptic mitral cell while stimulating the presynaptic cell at 50 as well as 100 Hz, and compared this to the control condition of no presynaptic stimulation. As predicted, we observed that increasing the presynaptic firing rate from 50 to 100 Hz shifted the range of firing rates over which the postsynaptic mitral cell was inhibited to lower frequencies(**Figs. 2.12, 2.13A, B**, n=6, $p < 0.05$). Furthermore, there was a significant increase in the magnitude of lateral inhibition, measured as the fractional change in activity (**Fig. 2.13C**, n=6, $p < 0.05$), though the absolute change in firing rate was not significantly affected.

2.4.4 Effect of Integration of Activity within Granule Cells on Lateral Inhibition

Our proposed mechanism would predict that the direct activation of granule cells should generate lateral inhibition that depends less on simultaneous activation of postsynaptic mitral cells. Thus, we stimulated granule cells directly by placing extracellular stimulation electrodes in the granule cell layer while recording from a single mitral cell (**Fig. 2.14**). As predicted, direct activation of granule cells inhibited mitral cell firing throughout much of the mitral cell F-I curve (**Fig. 2.15**), with the inhibition saturating at very high firing rates (n=9, compare **Figs. 2.3** and **2.16**, blue lines). To investigate the role of the postsynaptic mitral cell, we blocked ionotropic glutamate receptors (with APV [50 μM] and CNQX [10 μM]) and therefore blocked the ability of the recorded mitral cell to contribute to the inhibition that it

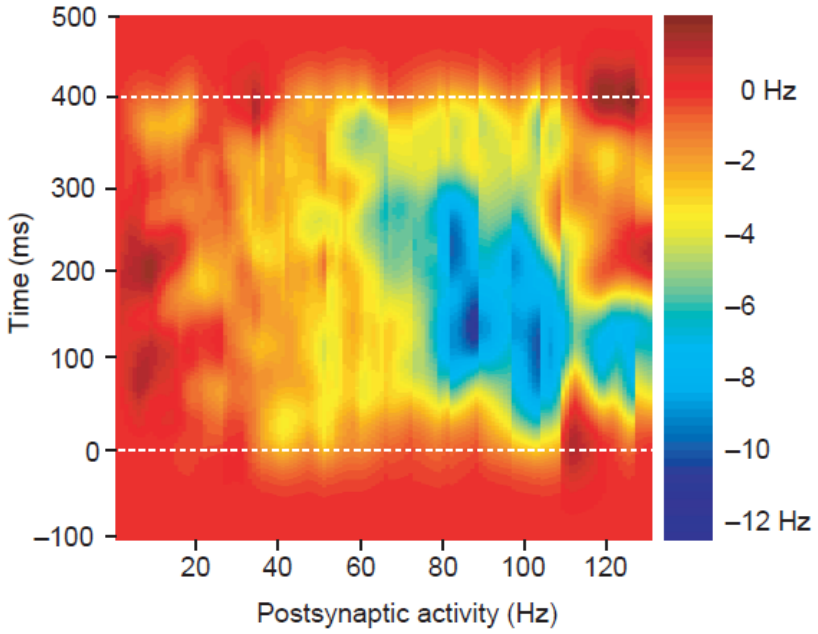

Figure 2.9. Lateral inhibition as a function of postsynaptic activity and time. Effectiveness of lateral inhibition with respect to both postsynaptic activity and time highlighted by taking the difference in spike density functions for paired recordings showing instantaneous inhibition with respect to postsynaptic activity as well as time.

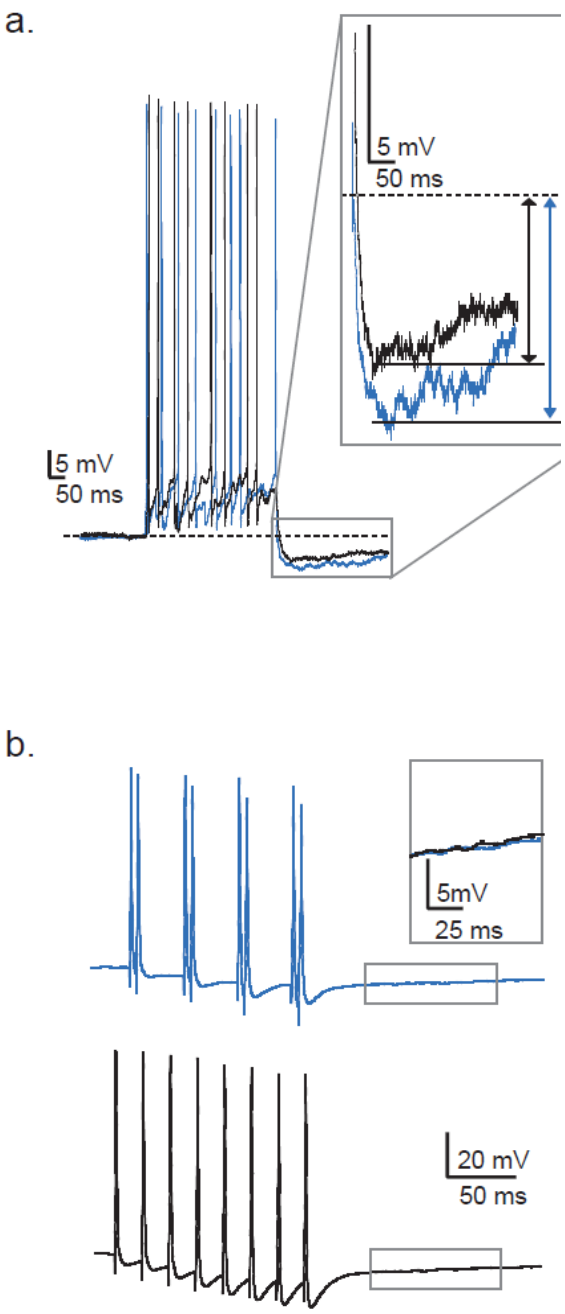

Figure 2.10. Recurrent inhibition and the effect of mitral cell spike timing. a) Example of increased recurrent inhibition during paired mitral cell stimulation. Black trace shows control recurrent IPSP and blue trace shows recurrent IPSP recorded during stimulation of presynaptic cell. **b)** Pairs of correlated spikes (blue trace) are not more effective at recruiting granule cell activity than distributed spikes (black trace)

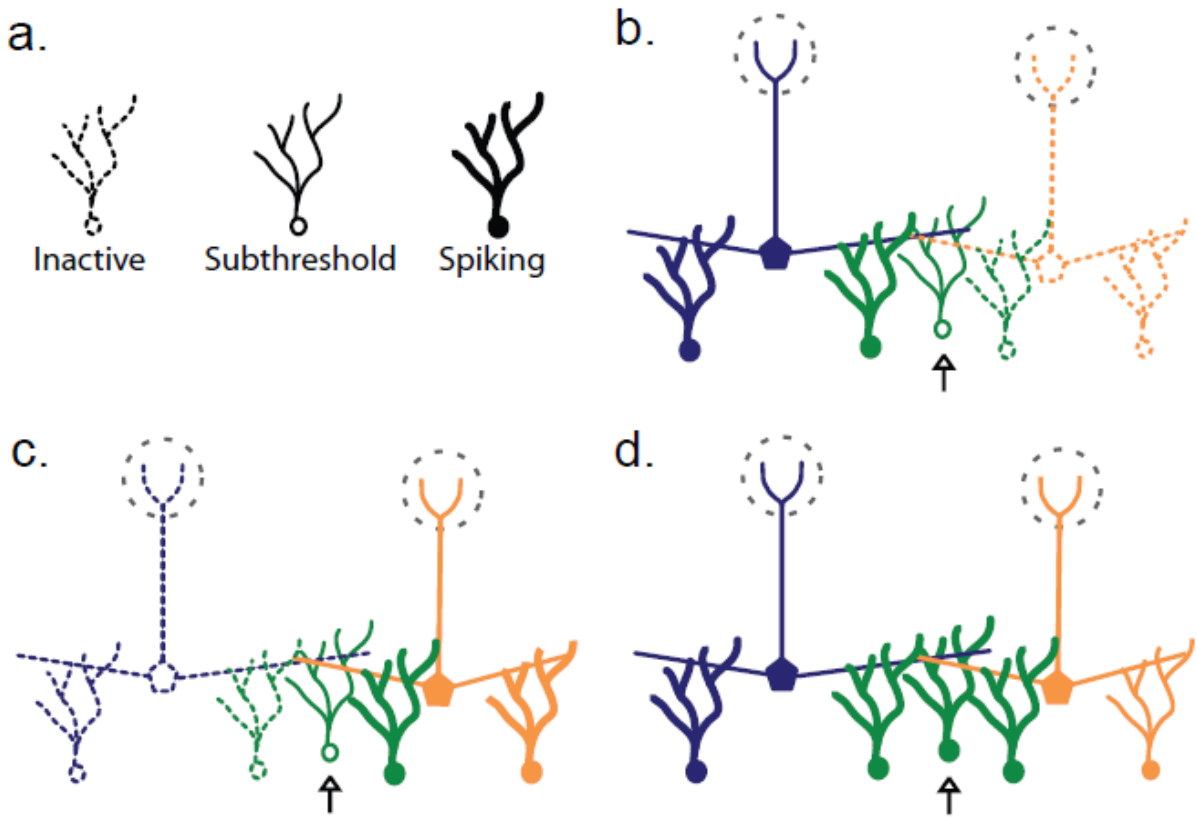

Figure 2.11. Proposed integration of activity within granule cells. Schematic of proposed integration within the granule cell population. **a)** Legend showing how granule cells with different activity levels are depicted. Stimulation of an individual glomerulus (**b** and **c)** is insufficient to activate all of the common granule cells between the glomeruli. **d)** Simultaneous stimulation of both glomeruli results in summation of subthreshold inputs and an increase in activated granule cells (open arrow indicates granule cell activated by only coincident stimulation of both glomeruli).

receives. This blockade had minimal effect on inhibition evoked by granule cell stimulation when mitral cells were firing at low and high firing rates, but substantially reduced the inhibition observed at intermediate mitral cell firing rates (firing rate in APV and CNQX during ECS was 59% higher at 25 Hz and significantly higher only from 12-44 Hz as compared to the condition without APV and CNQX, n=4, $p < 0.05$, **Fig. 2.16**, green line). This result indicates that release of glutamate from postsynaptic mitral cells causes enhanced granule cell-mediated lateral inhibition specifically in this intermediate range of firing rates, consistent with our prediction.

We examined the recruitment of granule cells by combined mitral cell inputs in more detail by imaging activity, in the form of calcium transients, in populations of granule cells following extracellular stimulation of single glomeruli. Previously, we have shown that granule cell calcium transients observed under these conditions are correlated with granule cell spiking (Kapoor and Urban, 2006). Extracellular stimulation of nearby glomeruli activated distinct populations of mitral cells and partially overlapping populations of granule cells, as reported previously (Kapoor and Urban, 2006) (about 29 ± 4% overlap, n=5 slices, 120 granule cells activated by stimulation of at least one of the two glomeruli, **Fig. 2.17**, top left panel). This shows that mitral cells in different glomeruli connect to common populations of granule cells. Simultaneous stimulation of the two glomeruli resulted in the recruitment of 50 ± 16% additional granule cells ($p<0.05$, n=5 slices) than the total that were activated by the stimulation of either of the two glomeruli singly (182 cells activated by simultaneous stimulation of two glomeruli, n=5 slices, **Fig. 2.17** bottom right panel and **Fig. 2.18**). These data show that when independent populations of mitral cells are stimulated, granule cells are activated in a cooperative fashion. This will allow the amplitude of lateral inhibition to increase non-linearly as more mitral cells are recruited (Kapfer et al., 2007).

2.5 DISCUSSION

We have explored the functional properties of the main circuit mediating lateral inhibition within the olfactory bulb. This circuit consists of pre- and postsynaptic mitral cells reciprocally connected via dendrodendritic synapses with inhibitory granule cells. We have shown that activity of a postsynaptic mitral cell influences the effectiveness of the lateral inhibition it receives and that this is due to the integration of activity from multiple mitral cells by those granule cells that provide lateral inhibitory input (**Figs. 2.11** and **2.18**).

The key requirement for this phenomenon is that the activity of the postsynaptic mitral cell is able to influence the output of the inhibitory granule cell from which it receives input. In the olfactory bulb circuit, mitral to granule cell connections are almost 100% reciprocal, favoring such interactions (Egger and Urban, 2006). The nature of this influence depends on the level of activity. At moderate levels of activity, correlated activity across mitral cells increases the strength of lateral inhibition due to cooperative activation of granule cells by the two mitral cells (**Fig. 2.18C, D**). That is, when mitral cells are firing at low-to moderate rates recurrent inhibition is weak. In this case, activity of and GABA release from granule cells is increased during coincident input from pre- and postsynaptic mitral cells. When the postsynaptic mitral cell is firing at very lower frequencies (less then about 30 Hz) we found that lateral inhibition is ineffective at reducing the level of activity in the postsynaptic cell. This could be due to several factors. First, if granule cells have a relatively high threshold for activation, the input from the presynaptic neuron alone will not be sufficient to stimulate granule cells above their threshold and result in the widespread neurotransmitter release required to elicit lateral inhibition. In fact, this hypothesis is supported by result from our paired mitral cell experiments where we rarely observed any IPSPs in the postsynaptic mitral cell resulting from activation of only the presynaptic cell (**Fig. 2.5**). In experiments where lateral inhibition was elicited via ECS in the glomerular layer, we did observe some IPSPs in the postsynaptic mitral cell as a result of ECS only. However, the activity of the postsynaptic mitral cell was still required for a reduction

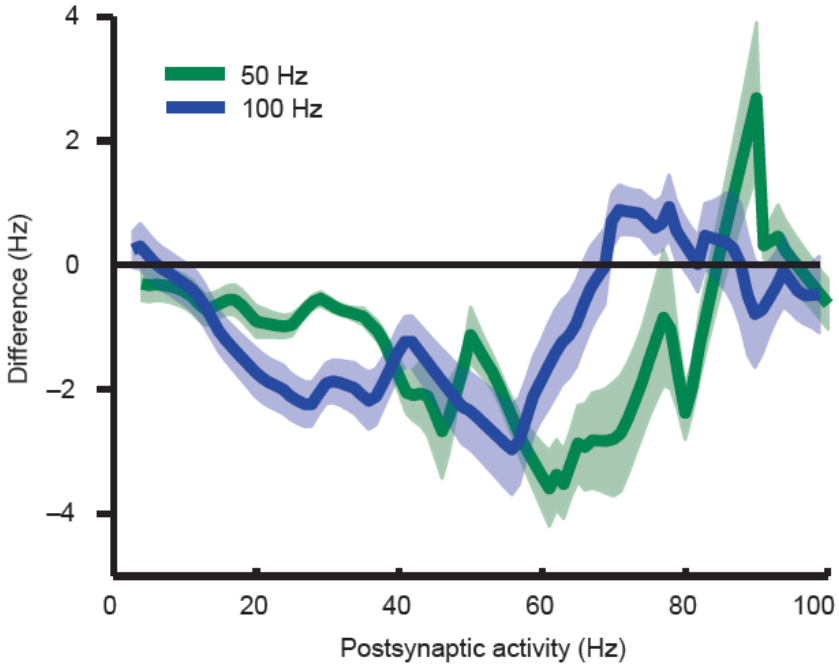

Figure 2.12. Modulation of activity-dependent range by presynaptic activity. Activity-dependent range of inhibition between pairs can be modulated by presynaptic firing rate (presynaptic firing rate of 50 Hz in green and 100 Hz in blue).

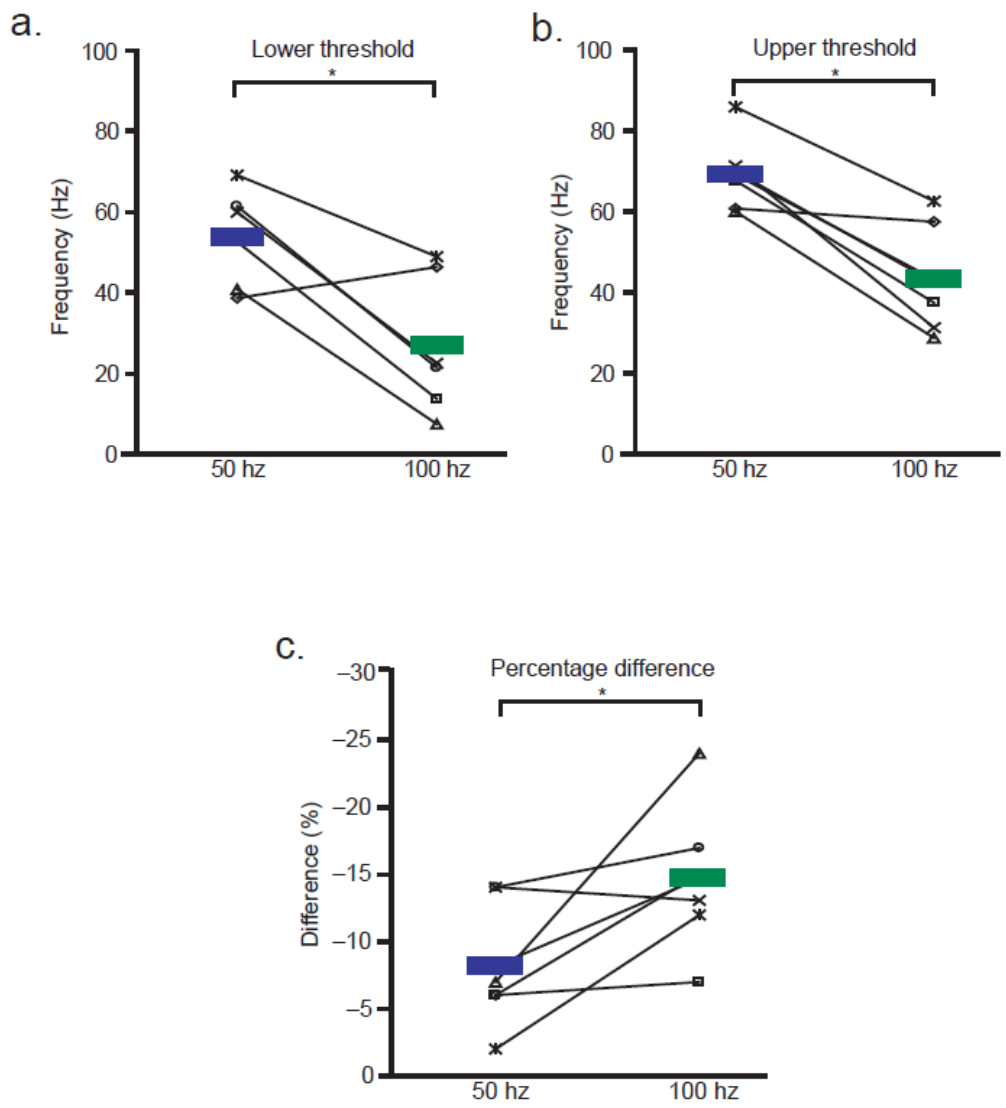

Figure 2.13. Aggregated change in activity-dependent thresholds and magnitude. Range of inhibition defined as >= 5% reduction in firing rate as a result of the activity of the presynaptic mitral cell. Lower and upper thresholds of this activity-dependent range of inhibition are reduced by increasing presynaptic mitral cell firing rate while the peak % change in activity is increased. In all panels, the firing rate of the presynaptic cell (either 50 or 100 Hz) is plotted on the x-axis. Each symbol within a figure represents a unique mitral cell.

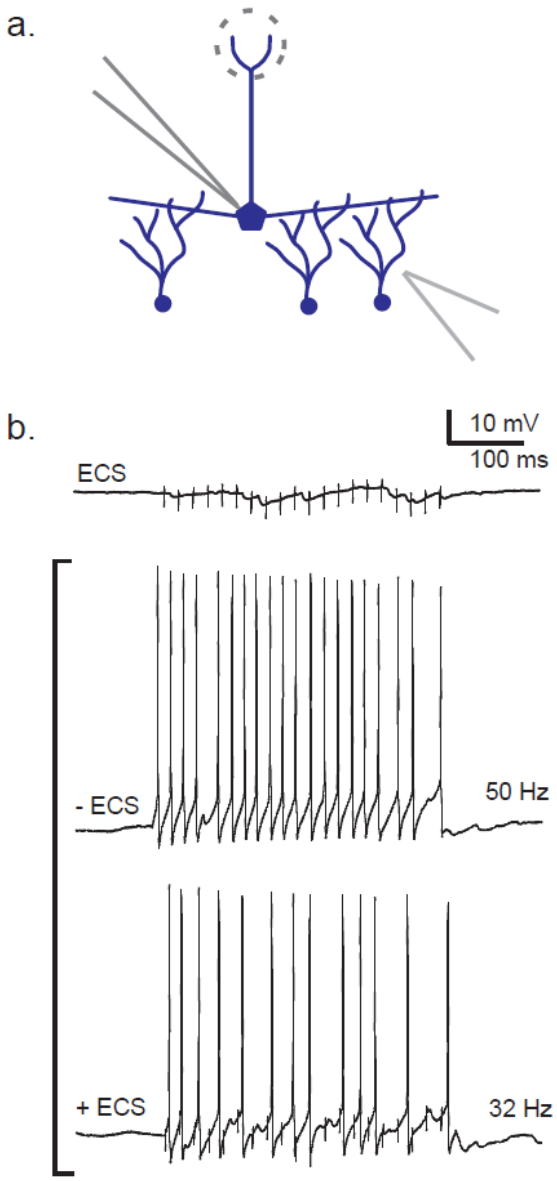

Figure 2.14. Inhibition evoked by direct granule cell stimulation. Inhibition evoked by direct stimulation of granule cells. **a)** Schematic of experimental configuration. A single mitral cell was recorded from while extracellular stimulation (ECS) was applied in the granule cell layer approx. 200-300 microns away. **b)** ECS results in IPSPs in the mitral cell and for a given current step ECS reduces mitral cell firing rate (50 Hz control firing rate reduced to 32 Hz when ECS applied).

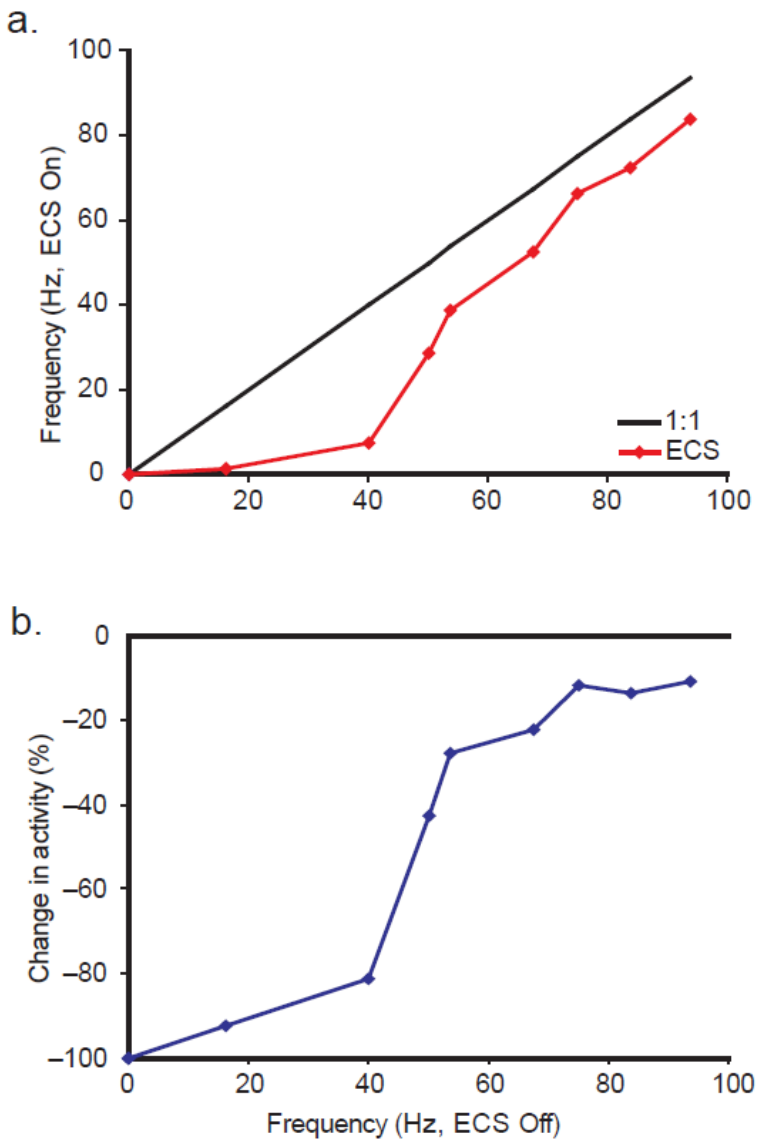

Figure 2.15. Granule cell stimulation results in subtractive inhibition. Example of frequency dependence of inhibition as a result of direct granule cell stimulation. Change in activity of recorded mitral cell plotted as absolute change in frequency in **a)** and as percent reduction in **b)**.

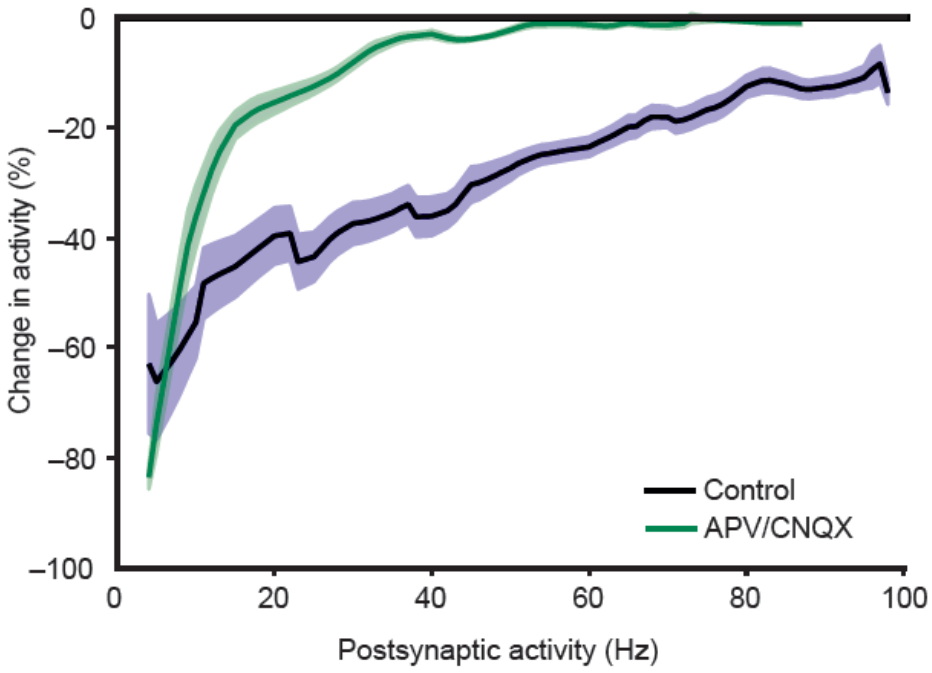

Figure 2.16. Contribution of postsynaptic mitral cell to recurrent inhibition. Aggregate results (n=9 for control in blue and n=4 for APV/CNQX in green) show that inhibition evoked via ECS in the granule cell layer exhibits saturation with increasing postsynaptic frequency but does not show activity-dependent gating at lower frequencies.

in firing rate (**Fig. 2.3**). In this case, the IPSPs resulting from ECS could be ineffective at reducing the postsynaptic firing rate for several reasons. First, it is likely that at least some of the synapses involved in producing these IPSPs would have been activated by postsynaptic activity alone (mediating recurrent inhibition) and therefore would not provide any additional inhibitory effect due to lateral mitral cell activity. Furthermore, it is possible that these IPSPs could affect spike timing without affecting average firing rate significantly. At high levels of postsynaptic activity, release from granule cells has been shown to saturate (Urban and Sakmann, 2002;Margrie et al., 2001). In this case, additional input to granule cells from the presynaptic mitral cell is relatively ineffective at evoking additional inhibitory input (**Fig. 2.18E,F**). This gating of lateral inhibition by postsynaptic activity thus depends critically on nonlinear integration of multiple mitral cell inputs by granule cells.

Granule cell activity is known to depend critically on several mechanisms that may mediate coincidence detection including molecular coincidence detectors such as the NMDA receptor and inactivating potassium channels (Isaacson and Strowbridge, 1998;Schoppa and Westbrook, 2002;Schoppa et al., 1998). Spatial integration of excitatory input within the granule cell dendritic tree also could play an important role (Egger et al., 2005). Furthermore, because granule cell mediated recurrent and lateral inhibition saturate at higher firing rates (Dietz and Murthy, 2005;Urban and Sakmann, 2002;Margrie et al., 2001), strongly active mitral cells "immunize" themselves against lateral inhibition by activating a large fraction of the granule cells that provide them with inhibition. The firing rates required for this suppression of lateral inhibition, while high, are observed *in vivo* in anaesthetized preparations (Margrie et al., 2001;Egana et al., 2005). This allows for information in cells firing at high rates to be preserved. These data demonstrate how strongly inhibition in the olfactory bulb is influenced by population activity, but also show that the firing of even a single mitral cell is sufficient to generate a significant reduction of firing rate in many other mitral cells. Increasing the number of active mitral cells increases both the range and efficacy of lateral inhibition, as it actives granule cells to both sub and superthreshold levels (Kapoor and Urban, 2006). Together these data provide a plausible implementation of the kind of connectivity that is required to achieve

a.

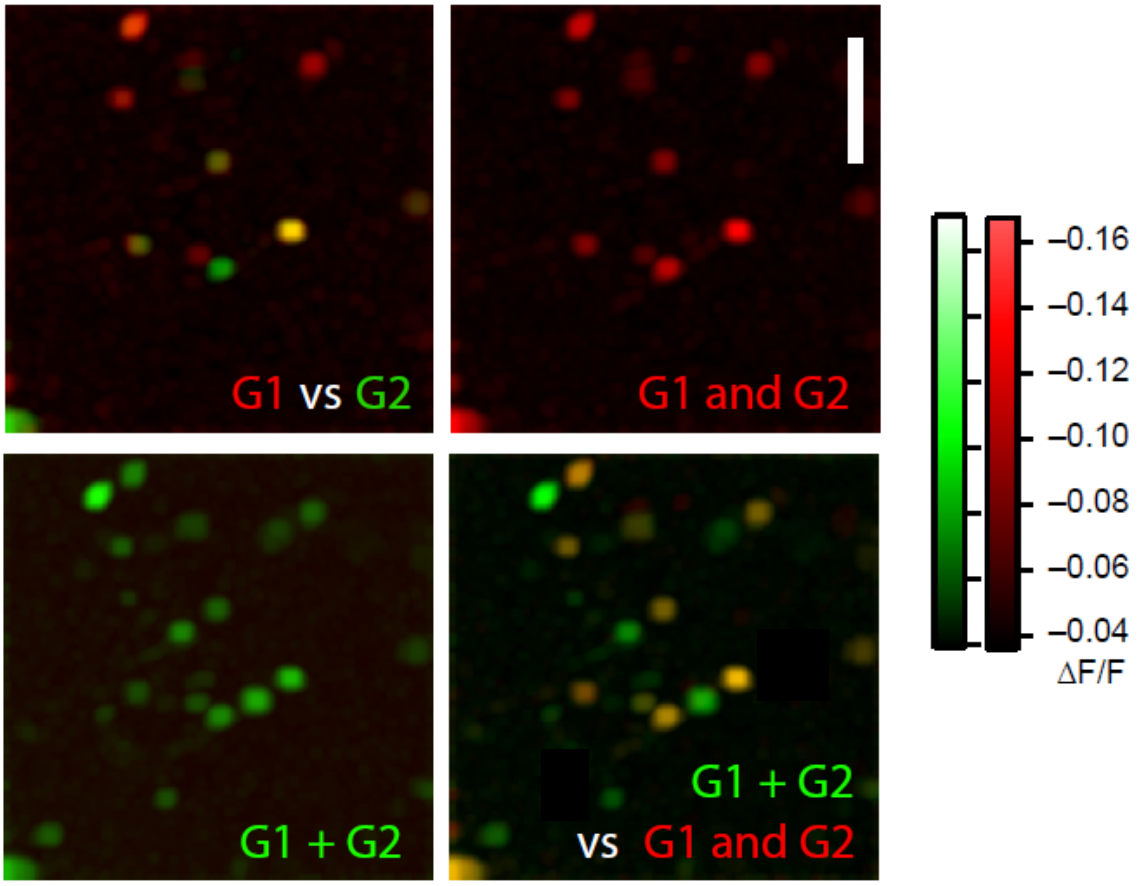
G1 vs G2
G1 and G2
G1 + G2
G1 + G2
vs G1 and G2
–0.16
–0.14
–0.12
–0.10
–0.08
–0.06
–0.04
ΔF/F

b.

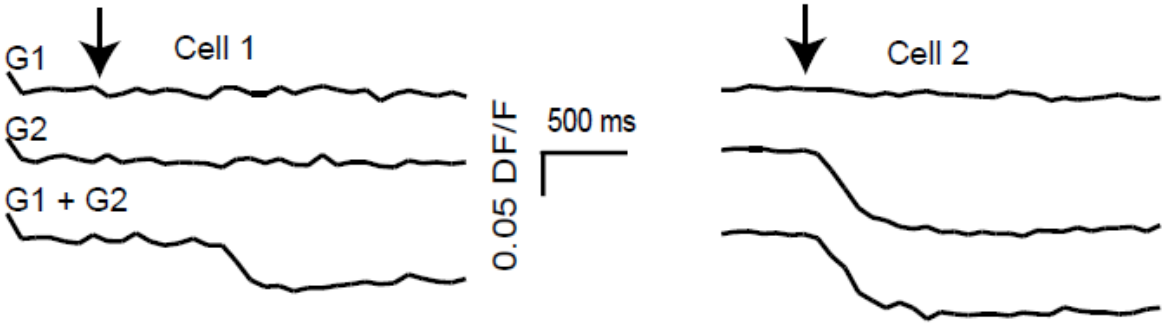
G1
Cell 1
G2
G1 + G2
0.05 DF/F
500 ms
Cell 2

Figure 2.17. Overlapping and cooperative activation of granule cells. a) Imaging of bulk-loaded calcium indicator (fura-2) from a population of granule cell layer neurons. Images show calcium-induced changes in fluorescence (ΔF/F) from populations of granule cells (images show minimum values for a given pixel across 10 trials). Top left image shows the population of granule cells activated by stimulation of one glomerulus (G1, red) and a second glomerulus (G2, green). Yellow cells were activated by stimulation of either glomerulus. Top right image shows a merge of the two color image in top left into the red channel (G1 and G2). Bottom left Image shows the population of granule cells evoked by simultaneous stimulation of both glomeruli (G1 $^{+}$ G2). Bottom right image shows the overlay of images from top right and bottom left. This overlay shows the population of granule cells that were activated only by simultaneous stimulation (in green). **b)** Calcium transients from two cells labeled 1 and 2 in the lower right panel of **a)**. Arrows indicate time of stimulation.

useful competitive interactions between active mitral cells. A similar sort of connectivity also was proposed as the most effective for explaining *in vivo* physiological data from honeybee olfactory system (Linster et al., 2005).

These results raise questions about how activity-dependent lateral inhibition differs from more usual center-surround mechanisms of lateral inhibition. This difference can be thought of by considering that activity-dependent lateral inhibition operates not on the spatial structure of the representation *per se* but rather on the distribution of activity (i.e. the histogram of firing rates). With long range inhibitory connectivity, as is seen between olfactory bulb mitral cells, activity-dependent lateral inhibition can be thought of as operating to change the distribution of activity across mitral cells. Mitral cells active at some intermediate range will have their activity reduced, with the amount of the reduction depending on the average activity level across the population of connected cells as well as on the initial activity level of the mitral cell. Functionally, this will increase the separation between those cells that are firing at highest rates and those firing at intermediate or lower rates. This will tend to produce a bimodal distribution of firing rates, resulting in a kind of contrast enhancement that does not depend on spatial features of the representation. That is, activity-dependent lateral inhibition will have little effect on activity of mitral cells most strongly and somewhat weakly activated by a particular odor stimulus, but will substantially reduce activity of mitral cells firing in an intermediate range. In this way, the degree of correlation between activity patterns evoked by similar odorants will be reduced, without substantially affecting the activity of strongly activated mitral cells. While this functionality is not dependent on the spatial representation of odorants, this does not rule out a role for the broad groupings of olfactory receptor types that has been reported (Mori et al., 2006;Johnson et al., 2004). This broad grouping could function to ensure that mitral cells responding to related odors are located in regions linked by their secondary dendrites and associated granule cells.

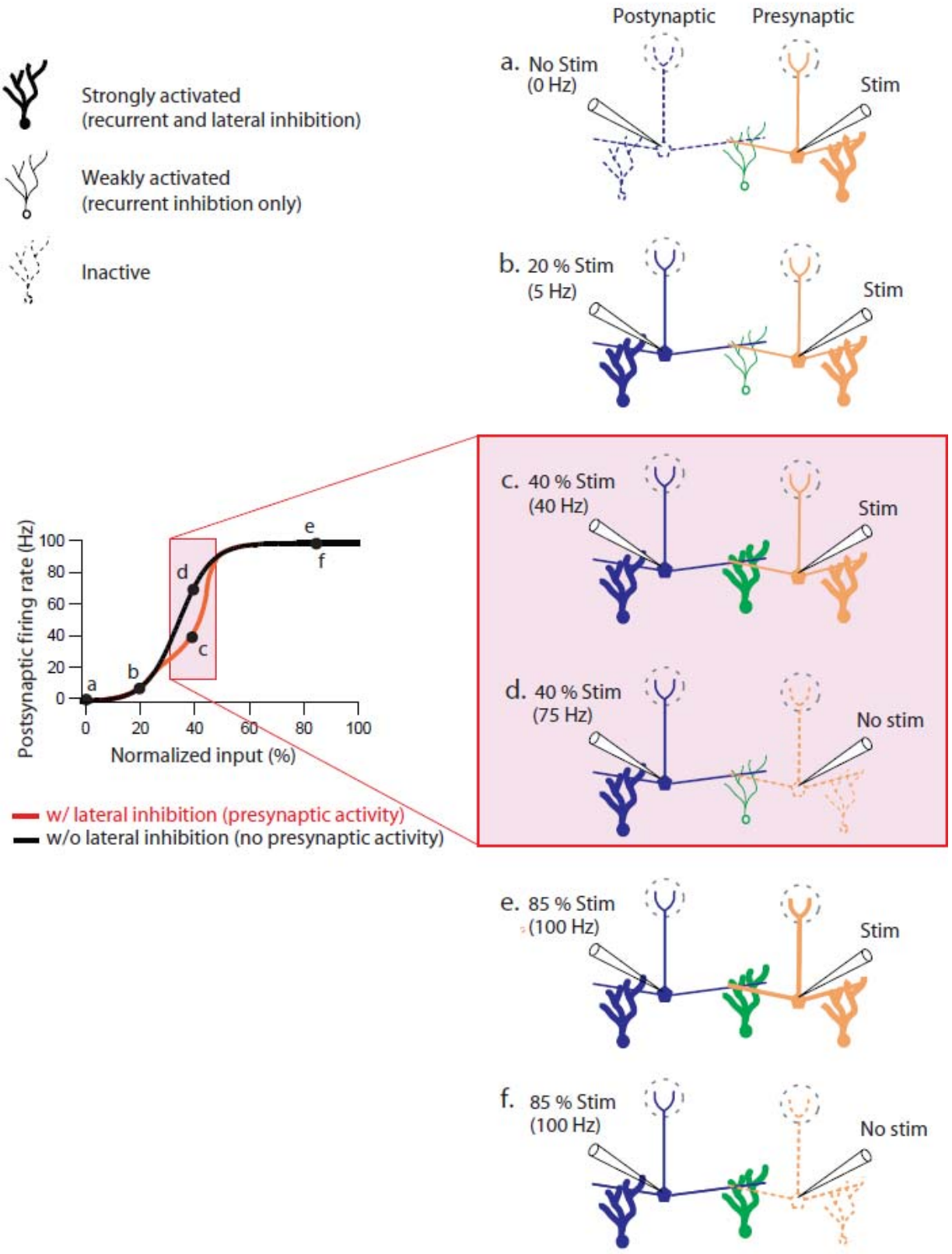
Strongly activated
(recurrent and lateral inhibition)
Weakly activated
(recurrent inhibtion only)
Inactive
Postynaptic
Presynaptic
a. No Stim
(0 Hz)
Stim
b. 20 % Stim
(5 Hz)
Stim
c. 40 % Stim
(40 Hz)
Stim
d. 40 % Stim
(75 Hz)
No stim
e. 85 % Stim
(100 Hz)
Stim
f. 85 % Stim
(100 Hz)
No stim
Postsynaptic firing rate (Hz)
Normalized input (%)
w/ lateral inhibition (presynaptic activity)
w/o lateral inhibition (no presynaptic activity)

Figure 2.18. Schematic of activity-dependent inhibition. Upper left: legend showing how granule cells with different activity levels are depicted. **a-f)** Schematics of olfactory bulb circuit showing pre- and postsynaptic mitral cells and associated granule cells. When the postsynaptic cell is unstimulated **(a)** or when this cell is firing at low rates **(b)**, no shared granule cells are activated sufficiently to generate lateral inhibition. **c)** When the rate of the postsynaptic mitral cell is increased above some threshold, some shared granule cells are activated sufficiently to generate lateral inhibition. This granule cell activity depends on coincident activation of pre- and postsynaptic mitral cells (compare **c** and **d**). At sufficiently high rates of postsynaptic activity, the firing of one cell alone is sufficient to cause activity of the shared granule cells, rendering lateral inhibition functionally silent (**e** and **f**). In all panels, '% Stim' indicates the intensity of stimulation given to a cell, where 100% represents the stimulation intensity resulting in that cell's maximum firing rate.

While our work has focused exclusively on the olfactory bulb, there are many brain areas (such as inferotemporal cortex and hippocampus) in which stimuli are not represented in obviously topographical ways (Leutgeb et al., 2005). Physiological data on the superlinear summation of inhibition in neocortical circuits (Kapfer et al., 2007) suggests that some features of activity-dependent lateral inhibition may be implemented in neocortical areas. Thus, this mechanism may provide a powerful computational algorithm for increasing discriminability between similar inputs that could be employed in other brain systems. Such a mechanism is especially well suited for brain areas in which stimulus representation is combinatorial and in which some connectivity is widespread. These findings represent a novel and general computational mechanism for increasing discriminability between similar inputs, based on the known physiology of inhibition within the bulb, where inhibitory output is dynamically gated in an activity-dependent manner.

3.0 FUNCTIONAL IMPLICATIONS OF ACTIVITY-DEPENDENT LATERAL INHIBITION

3.1 ABSTRACT

In **chapter 2** I presented results indicating a novel form of lateral inhibition between neurons based on the activity of both presynaptic as well as postsynaptic neurons. Given the multidimensional nature of olfactory space and broad connectivity within the olfactory bulb, I hypothesized that this activity-dependent lateral inhibition could allow for useful computations such as contrast enhancement in the absence of topographic arrangement of sensory input. I use simulations to demonstrate that this activity-dependent enhancement of inhibition allows functional properties of lateral inhibition to be implemented even when inputs are non-topographic and connectivity is spatially uniform. I also show that activity-dependent lateral inhibition can result from a simple network of integrative Wilson-Cowan style neurons.

3.2 INTRODUCTION

Odors present a unique challenge to encoding and processing of information in the olfactory system. The olfactory bulb is the initial processing point for olfactory information, where the principal neurons (mitral cells) receive input from olfactory receptor neurons in the nose (Shepherd and Greer, 2004). In mice there are about 1000 different olfactory receptor types, each having a unique set of odorants that it is responsive to (Zhang and Firestein, 2002). All ORNs of a given type send their axons to spherical structures in the olfactory bulb called

glomeruli where about 20-30 mitral cells send their apical dendrites (Mombaerts et al., 1996). In addition to serving as the primary output of the olfactory bulb, these mitral cells make reciprocal dendrodendritic synapses with inhibitory granule cells that mediate both reciprocal as well as lateral inhibition (Jahr and Nicoll, 1982). Therefore, like in other sensory systems, the olfactory bulb consists of a two-dimensional array of neurons that interact with local interneurons that modulate the sensory representation before sending their projections to higher processing centers (Shepherd and Greer, 2004). However, it is unclear how the multidimensional odor space maps onto this two dimensional set of neurons (**Fig 3.1**). Many groups have attempted to find and characterize one or a few dimensions that describe all odors and which odors could be arranged in a continuous topographic fashion (Meister and Bonhoeffer, 2001;Belluscio and Katz, 2001;Uchida et al., 2000). However, it appears that there is at most a broad grouping of related odors (Friedrich and Korsching, 1998;Rubin and Katz, 1999;Johnson and Leon, 2000a) which contrasts with the fine topographic organization found in the visual and auditory systems (Shepherd and Greer, 2004). Furthermore, lateral interactions are mediated via the long secondary dendrites of mitral cells which span up to 2mm in diameter. Considering that in other sensory systems, lateral interactions between neurons are determined primarily by their spatial location and connectivity, it is unclear what the functional role of these interactions in the bulb might be (Linster et al., 2005).

Our previous physiological investigation into the lateral interactions mediated by mitral cells in the olfactory bulb has provided some interesting insights into lateral inhibition in the bulb (see **chapter 2**). Through our direct electrophysiological recordings from mitral cells, we provide evidence for a novel form of lateral inhibition that we term activity-dependent lateral inhibition. We found that the effectiveness of lateral inhibition in reducing mitral cell firing rate was actually determined by the activity of the mitral cell being inhibited (postsynaptic mitral cell). Therefore, neurons needed to fire at an elevated rate (at least approximately 20-30 Hz) for them to be inhibited by other mitral cells. Furthermore, we found that when mitral cells were firing at very high rates (60-100 Hz) that they were immune to inhibition from lateral

mitral cells. This activity-dependence results in a dynamic remapping of effective inhibition to different subsets of mitral cells, based on the type of input to the network.

In the olfactory bulb, granule cells mediate recurrent and lateral inhibition of mitral cells (Jahr and Nicoll, 1982). They receive input from up to 50-100 mitral cells (Egger and Urban, 2006), and because these mitral cells receive input from different olfactory receptor neuron types (Mombaerts et al., 1996), are able to integrate activity between these glomeruli. We therefore hypothesized that the activity-dependence of the lateral inhibition that we observed physiologically could be achieved by integration of input from mitral cells within granule cells. To investigate this, we created a network model based on the integrative Wilson-Cowan neurons (Wilson and Cowan, 1972). We show that this simple network of integrative neurons is sufficient to reproduce the activity-dependent lateral inhibition observed in our experiments.

Given the dynamic nature of this form of inhibition, and the multidimensional nature of olfactory space (Godfrey et al., 2004), we hypothesized that activity-dependent inhibition could have interesting functional implications in the processing of olfactory information. Specifically, we hypothesized that activity-dependent lateral inhibition could mediate the same sort of contrast enhancement mediated by lateral inhibition in topographically arranged systems (Hartline et al., 1956;Shepherd and Greer, 2004), but without the requirement for spatial arrangement of sensory input. Furthermore, it has been shown that initially correlated patterns of activity in the olfactory bulb are decorrelated in time (Friedrich and Laurent, 2001;Yaksi et al., 2007). In the results below we show that activity-dependent lateral inhibition is able to mediate this decorrelation, without the requirement for any spatial structure to lateral connectivity.

These studies address a key aspect of sensory processing, how effective lateral interactions are able to occur in a network of neurons where sensory representations are not arranged in a fine topographic manner.

3.3 MATERIALS AND METHODS

3.3.1 Wilson-Cowan Computational Model

To explore how integration of activity within neurons potentially contributes to the formation of activity-dependent lateral inhibition, we created a computational model based on earlier work by Wilson and Cowan (Wilson and Cowan, 1972). This model consisted of two mitral cells (denoted as *E*) each making reciprocal connections with a single granule cell (denoted as *I*). The key feature of Wilson-Cowan neurons is that they exhibit a saturating, sigmoid activation function (see **Fig 3.2A** and **equation 1**). The activation of mitral cells was due to both excitatory input (simulated input different for each neuron) as well as inhibition from activation of the granule cell (Li and Rinzel, 1994). The magnitude of inhibition was determined by the activation of the granule cell, *I(t)*, as well as by a weight, β. In the equations below, τ represents the respective time constants for the different equations. Granule cell activation was a function of the summation of activity from the two mitral cells in the network (Li and Rinzel, 1994) as well as by a term representing the available reserve of inhibition, *W*. Granule cell output either exhibited unlimited reserve (i.e. activation of the granule cell resulted in inhibition for an infinite amount of time, **equation 4a**) or short-term depression (i.e. activation of granule cells resulted in a depletion of the available inhibitory reserve, **equation 4b**).

$$S(X) = \frac{1}{1+e^{-\alpha(X-\theta)}} \quad (1)$$

$$\tau_e \frac{dE_i}{dt} + E_i = S(input_i - \beta * I(t)) \quad (2)$$

$$\tau_{inh} \frac{dI_i}{dt} + I_i = S(\sum_{n=1}^{N} E_n(t)) * W \quad (3)$$

$$W = 1 \quad (4a)$$

$$\tau_w \frac{dWi}{dt} = w_{peak} - w_i - g_{STD} * I_i(t) \qquad (4b)$$

3.3.2 Network Computational Model

To investigate the functional properties of the physiologically observed activity-dependent gating of lateral inhibition in this study, we developed a continuous-firing rate network model created in Matlab (The Mathworks, Inc.). This model consisted of a 25x25 array of simulated neurons representing olfactory bulb mitral cells with their average firing rate represented by a continuous variable, *v* (Li and Rinzel, 1994). Each neuron received background noise calculated as the product of a random number (*rand*) and a gain term (g_n). Neurons also contained a leak current determined by a gain term (g_l) and the difference between the membrane potential and the leak reversal potential (E_l). Additionally, neurons received a time-dependent stimulus, *stim(t)*, representing input from olfactory receptor neurons. The stimulus value was calculated for each neuron by multiplying the conductance (g_s; 0 for *t*<*tstart*; 1 for *t*>=*tstart*) with a constant value E_s. The value for E_s was generated by randomly assigning activity values to 60 points in a 25x25 array and convolving the map with a circular Gaussian (standard deviation of 2 pixels). To remove any spatial patterning of the stimulus in the model, neurons exhibited all-to-all connectivity. Inhibition was determined using one of three methods depending on the condition being tested. Each method employed a gain term for the given inhibition type (g_{ia}, g_{is}, or g_{id}). For activity-dependent inhibition (equation 6a) it was calculated by the sum of network activity, *u(t)*, as well as an exponential function relying on the postsynaptic neuron's firing rate. This function approximated the activity-dependent gating of lateral inhibition observed in our results (compare **Figs. 2.6** and **3.5**) with the strength of inhibition maximal for the postsynaptic firing rate given by the term *peak.* For subtractive inhibition, the exponential function representing activity-dependence was removed (equation 6b). To simulate divisive inhibition, a fraction of the neurons own firing rate was used to calculate the amount of inhibition that it received (equation 6c). In order to approximate the delayed onset of

inhibition within the bulb, the inhibition in the model was multiplied by a delay function, *delay(t)*.

$$\tau \frac{dv}{dt} = noise + stim(t) - leak - inh(t) \quad (5)$$

$$noise = g_n * rand$$
$$stim(t) = g_s(t) * (E_s)$$
$$leak = g_l * (v(t) - E_l)$$

$$inh_a(t) = g_{ia} * u(t) * delay(t) * e^{\frac{-(v(t)-peak)^2}{\sigma}} \quad (6a)$$

$$inh_s(t) = g_{is} * u(t) * delay(t) \quad (6b)$$

$$inh_d(t) = g_{id} * v(t) * delay(t) \quad (6c)$$

$$u(t) = \sum_{n=1}^{N} v_n(t) \quad (7)$$

$$delay(t) = 1 + g_d * \tanh(t - t_{offset}) \quad (8)$$

To determine if activity-dependent lateral inhibition could decorrelate initially similar inputs we generated 16 different input maps with varying correlation (representing odors of varying similarity) for each 25x25 array of neurons. Digital image used in **Figs. 3.6** and **3.7** captured using Sony DSC-P72 digital camera. Image down-sampled to 300x427 pixels and imported to Matlab. This image was then used as the input map for the computational model.

3.4 RESULTS

3.4.1 Activity-Dependence as an Emergent Property of Integrative Neurons

Granule cells have a unique view of olfactory bulb activity. Not only do they mediate recurrent inhibition as a result of activity from a single mitral cell, but also mediate lateral inhibition due to lateral excitation from mitral cells connecting to different glomeruli (Jahr and Nicoll, 1982). Because of this unique position to integrate both pre- and postsynaptic activity, we hypothesized that the activity dependence of the lateral inhibition that we observed in the results presented in **chapter 2** could at least in part be due to integration of activity within granule cells. In fact, direct evidence of granule cells' ability to integrate activity across different glomeruli comes from the imaging results presented in **Fig. 2.17** showing that granule cells are recruited in a supralinear fashion as multiple glomeruli are activated.

To investigate if integration of activity within granule cells alone is sufficient to result in activity-dependent lateral inhibition, we created a simple model of mitral and granule cells (**Fig. 3.1A**). The neurons in this model were based on the original model by Wilson and Cowan (1972) and consisted of two excitatory mitral cells reciprocally connected to a single granule cell (**Fig 3.1A**). Activation of mitral cells resulted in activation of granule cells and subsequent inhibition back onto mitral cells based on the granule cell's activity (**Fig. 3.1A**). Each neuron integrates input using a sigmoidal transformation function (**equation 1** and **Fig 3.2B**). These neurons have a half-maximal activation expressed by θ and for large enough inputs their activity becomes saturated. Because of this activation function, an input to a neuron will result in the greatest change in activity when provided when the neuron is firing near the steepest part of its activation function (**Fig. 3.1B**).

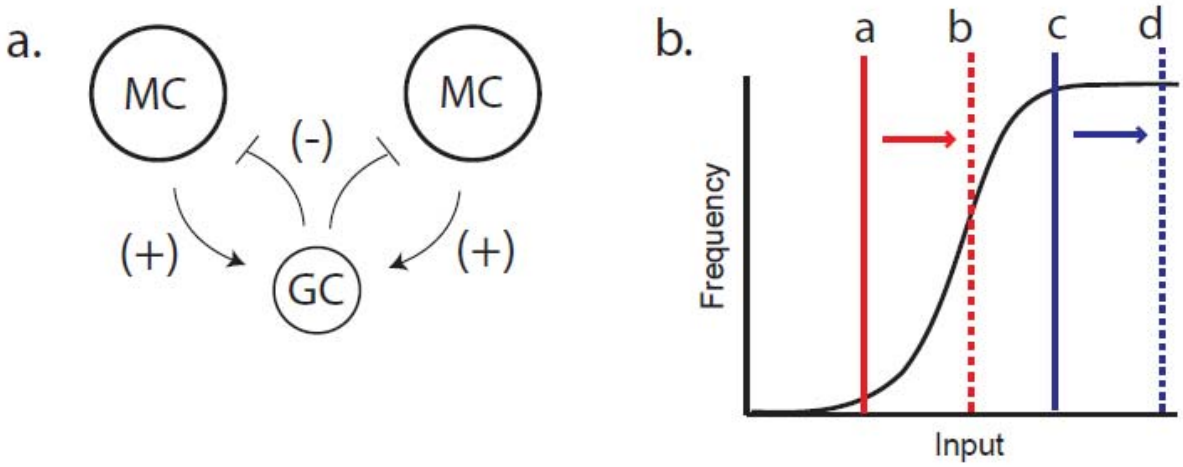

Figure 3.1. Wilson-Cowan implementation of mitral-granule cell inhibition. a) Schematic representation of the Wilson-Cowan network showing two mitral cells reciprocally connected to a common granule cell. **b)** Basic activation function of each Wilson-Cowan neuron showing sigmoidal response of output frequency as a result of increasing input. A given increase in input strength can result in a large change in activity if the intial activation level is low (a->b). However, if the neuron is already firing at elevated rates, an increase in input will have only a marginal effect on its firing rate (c->d).

To determine if activity-dependent inhibition could result from integration of activity within granule cells, we created a simple network of three neurons (one granule cell reciprocally connected to two mitral cells). Similar to our experimental paradigm of paired mitral cell recordings (see **section 2.4.1**), one mitral cell was given a range of input stimuli and the resulting activity of this mitral cell was compared under two conditions: one when it is given the input alone and the other when the second mitral cell is given a fixed amplitude stimulus. If the integrative nature of granule cells is sufficient to produce activity-dependent lateral inhibition then we should see a selective reduction in the first mitral cell's activity at a specific range of firing rates due to the stimulation of the second mitral cell. Consistent with our hypothesis, this simple network of integrative neurons was sufficient to reproduce the same kind of activity-dependent lateral inhibition observed in our previous results (compare **Fig. 2.6A** and **Fig. 3.2A**). As the activity of the postsynaptic mitral cell was increased, the amount of recurrent inhibition increased. However, after sufficient activation of the granule cell, the amount of lateral inhibition also increased due to input from the postsynaptic cell. In fact, the region of peak inhibition corresponded to the region of increasing activation of lateral input (**Fig. 3.2B**).

3.4.2 Integration of Activity and Time

An interesting continuation of the results of integration of activity within granule cells is the effect of the integration of activity and time. Our previous results show that inhibition occurs at earlier time points and saturates in shorter durations as activity of the postsynaptic cell increases (**Fig. 2.10**).

To reproduce these physiological results, we introduced a form of short term depression of granule cell output (**equation 4b**). Each granule cell had a fixed reserve of inhibition it was able to provide. Once depleted, the granule cell was ineffective at inhibition mitral cells similar

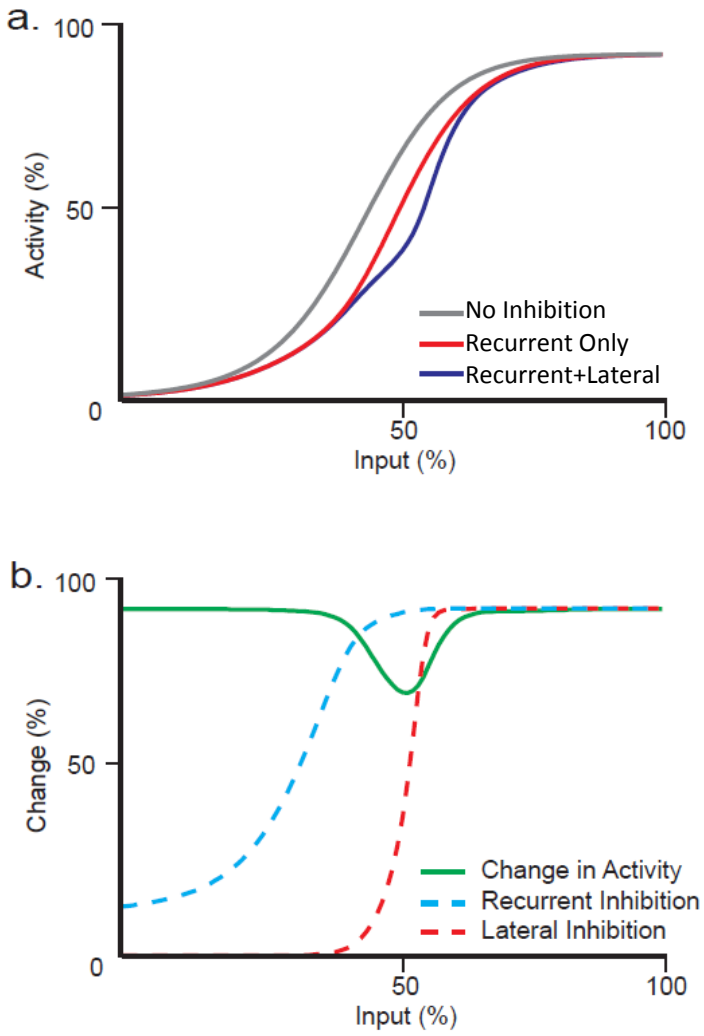

Figure 3.2. Activity-dependent inhibition resulting from integration in granule cells. a) Difference in mitral cell F-I curves as a result of inhibition. Absence of inhibition (grey) compared to recurrent inhibition only (red) and recurrent plus lateral inhibition (blue). **b)** Relationship of the percentage change in firing rate of recurrent vs. recurrent plus lateral inhibition (green) to the activation of both recurrent (blue) as well as lateral (red) inhibition.

to physiological results showing short term depression of granule cell output (Dietz and Murthy, 2005). This can be seen in **Fig. 3.3A** where the inhibitory capacity of the granule cell is reduced at earlier time points as activity of the postsynaptic cell is increased. This decrease in inhibitory capacity then results in a reduction in mitral cell inhibition for these later time points, similar to our physiological results (compare **Fig 2.10** and **3.3B**).

Next, we investigated the role of presynaptic activity in determining the effectiveness of activity-dependent inhibition. In our experimental results, we showed that increased presynaptic activity resulted in a decrease in the lower and upper thresholds of the activity-dependent range of lateral inhibition (**Fig. 2.13**). We hypothesized that the shift in the lower threshold was due to the increased presynaptic input to the granule cell reducing the requirement of the postsynaptic neuron to fire to effectively recruit additional inhibition. Consistent with this hypothesis, increasing the activity of the presynaptic mitral cell in our model resulted in a progressive decrease in the lower threshold of activity-dependent inhibition (**Fig. 3.4A**). However, without the inclusion of granule cell short-term depression, the upper threshold of this range remained constant and did not shift to lower frequencies as in our experiments. By including short-term depression of granule cell activity, the upper threshold shifted down as in our experiments (**Fig. 3.4B**). This indicates that short-term depression of granule cells (Dietz and Murthy, 2005) could have important implications in tuning the frequency dependence of this activity-dependent inhibition, especially during robust network activity.

3.4.3 Contrast Enhancement via Activity-Dependent Lateral Inhibition

The physiological results described in **chapter 2** suggest a mechanism for specifying lateral inhibition in which the number of activated granule cells and thus the strength of inhibition is regulated dynamically by correlated mitral cell activity. Such a mechanism will allow lateral inhibition to be rapidly remapped across populations of activated mitral cells. The fractured

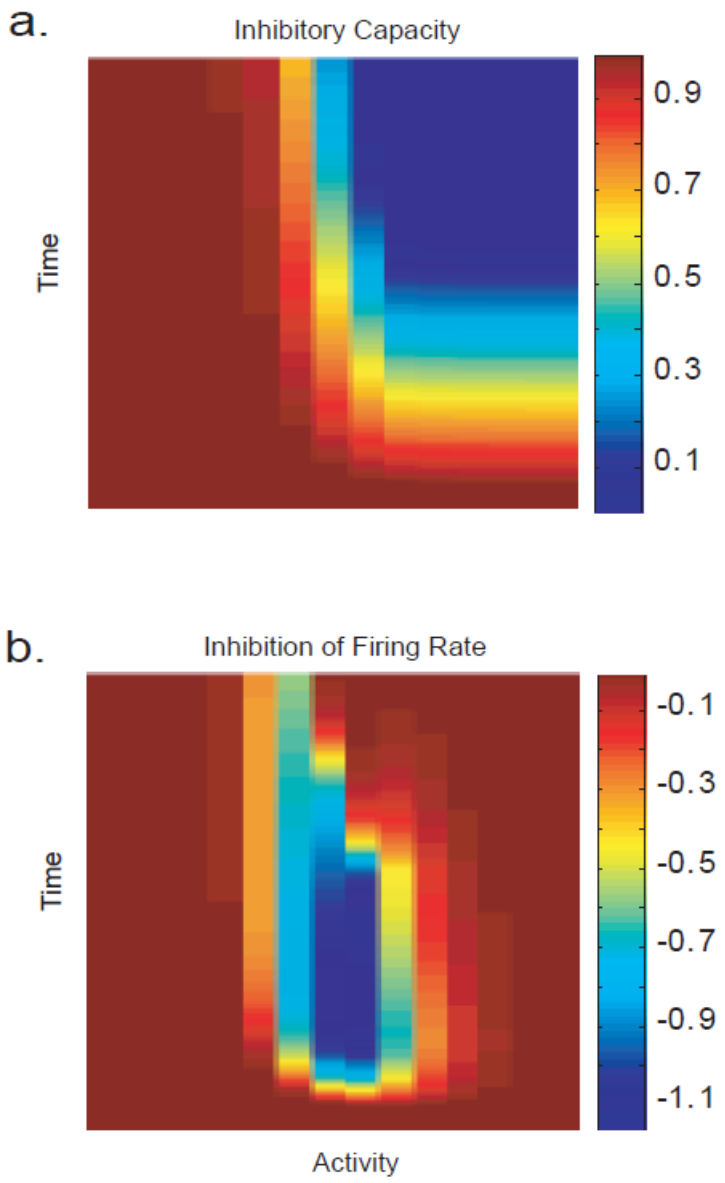

Figure 3.3. Short-term depression and the effect on activity-dependent inhibition. a) Inhibitory capacity of granule cells plotted as a function of postsynaptic mitral cell activity and time. **b)** Evolution of lateral inhibition as a function of postsynaptic mitral cell activity and time as in **Fig. 2.9**.

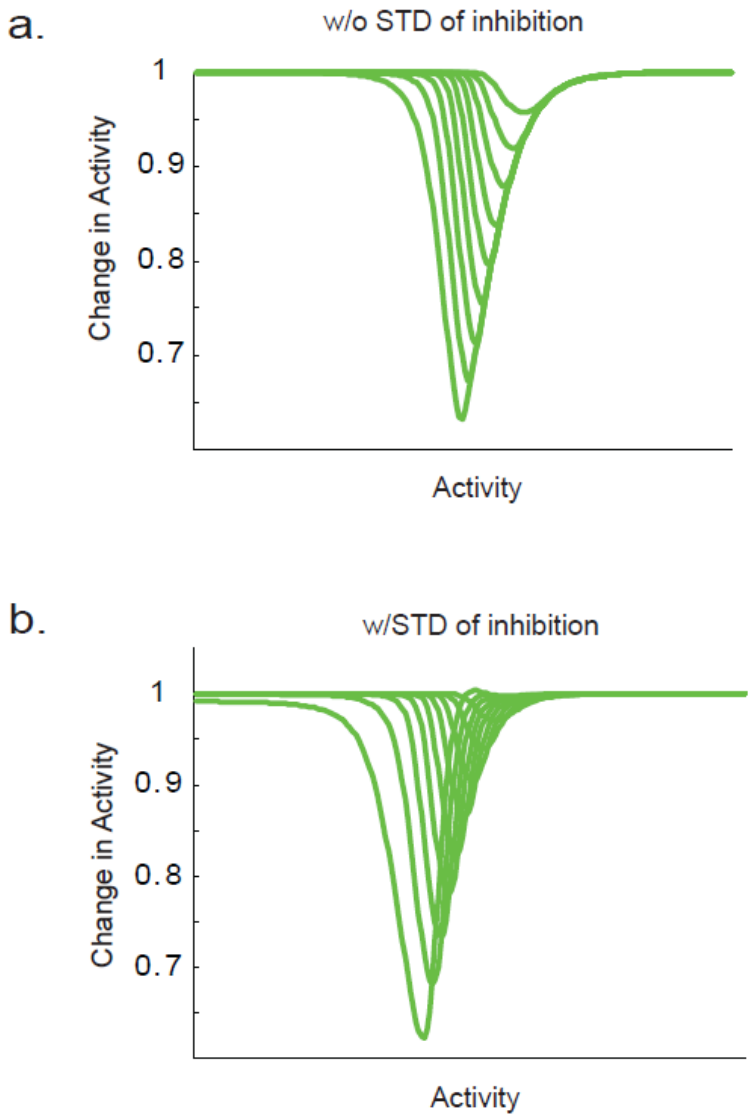

Figure 3.4. Modulation of the activity-dependent range. a) Increasing activation of the presynaptic mitral cell results in a progressive shift of the lower threshold of activity-dependent inhibition to lower frequencies of postsynaptic activity but no change in the upper threshold. **b)** Addition of short-term depression of granule cell output results in a shift in a progressive reduction in the upper threshold of activity-dependent inhibition as well.

manner in which odor-evoked patterns of activity are mapped onto the bulb (Wilson et al., 2004), suggests that such a dynamic activity-dependent regulation of lateral inhibition may enhance contrast and facilitate discrimination between patterns of odor-evoked mitral cell activity (Linster et al., 2005). We used a model to investigate whether this mechanism can effectively enhance contrast between mitral cells with similar response profiles (**Fig. 3.5**). The key features of this model were that the strength of lateral inhibition was maximal at intermediate levels of postsynaptic activity, as we observed in our experiments (compare **Figs. 2.6b** and **3.5b**) and that the connectivity in the model was all-to-all. The all-to-all connectivity is important for several reasons. First, it removes all spatial structure of the input stimulus. This allows us to isolate the functional effect of activity-dependent lateral inhibition without any potential confounding influence resulting from the spatial structure of activity within the network. Furthermore, the connectivity within the olfactory bulb is widespread with an individual mitral cell connecting with up to half to two-thirds of the other cells in the bulb (Mori et al., 1981). Therefore, a model exhibiting widespread connectivity would be more physiological than one in which connectivity is spatially restricted to only nearby neurons.

Using this model we tested whether such circuits would be sufficient to enhance contrast between similar stimuli and to decorrelate activity across populations of mitral cells responding to similar odors, similar to what has been observed *in vivo* (Friedrich and Laurent, 2001). The firing rate at which the strength of lateral inhibition was maximal was chosen to be approximately the mean activity within the network.

The first measure of functional importance we decided to use was an application to two-point discrimination. The accuracy of discrimination of two points is based on how close the points can get to one another before they are indistinguishable. In this classic view, lateral inhibition functions to sharpen two points which increases the peak difference between the two, increasing the ability to distinguish between them. This is achieved in other systems by

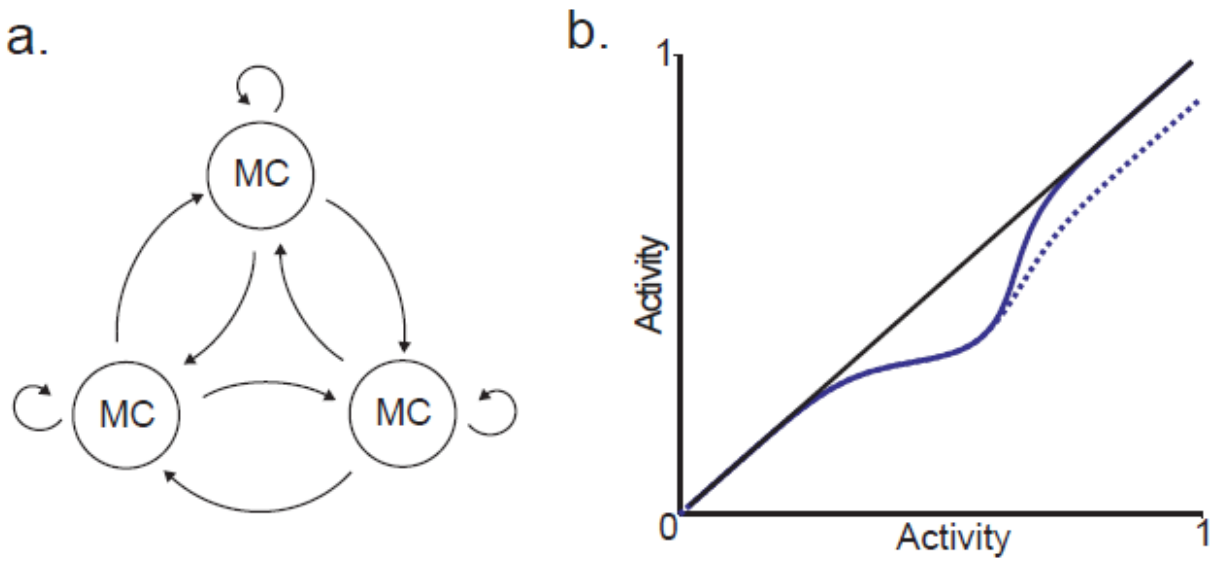

Figure 3.5. Network implementation of activity-dependent inhibition. a) Schematic of network connectivity of the computational model indicating all-to-all connectivity. **b)** Each neuron exhibited the same type of activity-dependent gating of lateral inhibition as observed in our results (compare **Fig. 2.6b and Fig. 3.5b**). Two types of activity-dependent inhibition were compared (full return to baseline activity, solid line, and 50% return to baseline activity, dotted line).

center-surround inhibition based on a fixed topographic arrangement of neurons where neurons located near one another in space inhibit one another to a greater degree than do neurons located farther away (Hartline et al., 1956). In our model, the spatial arrangement of neurons is removed due to the all-all connectivity. We then tested whether activity-dependent lateral inhibition alone was sufficient to increase contrast and improve two-point discrimination as measured by an increase in the maximum difference in intensity between the peaks of the two blurred images. As predicted, the model resulted in a sharpening in the blurred images (**Fig. 3.6A**). This change was quantified by plotting the intensity pixels along a line drawn horizontally through the peaks of the blurred images (**Fig. 3.6B**). When the pixel intensities were compared before (blue line) to after (red line) processing via activity-dependent lateral inhibition, there is a clear increase in the maximum difference between the peak of the images and the trough indicating an increase in two-point discrimination. To demonstrate that the spatial structure of the image is not required, the image was pseudo-randomized before processing by the model and then un-randomized after processing (**Fig. 3.6A**, middle panel). This randomization did not affect the results of the model.

Next we tested the model using simulated olfactory receptor neuron input to the network (Friedrich and Korsching, 1998). Olfactory receptor neuron activity was simulated by randomly assigning activity values to 60 points in a 25x25 array and convolving the map with a circular Gaussian function (standard deviation of 2 pixels). After processing by activity-dependent lateral inhibition the output of the network (analogous to mitral cell activity) showed increased contrast as compared to the initial input (**Fig. 3.7**). In some examples, we tested whether spatial patterning was important by randomizing the positions of all pixels before running the simulation and then unrandomizing after the network had reached steady state. This randomization had no effect on the processing of the model, as expected given the all-to-all connectivity in the model.

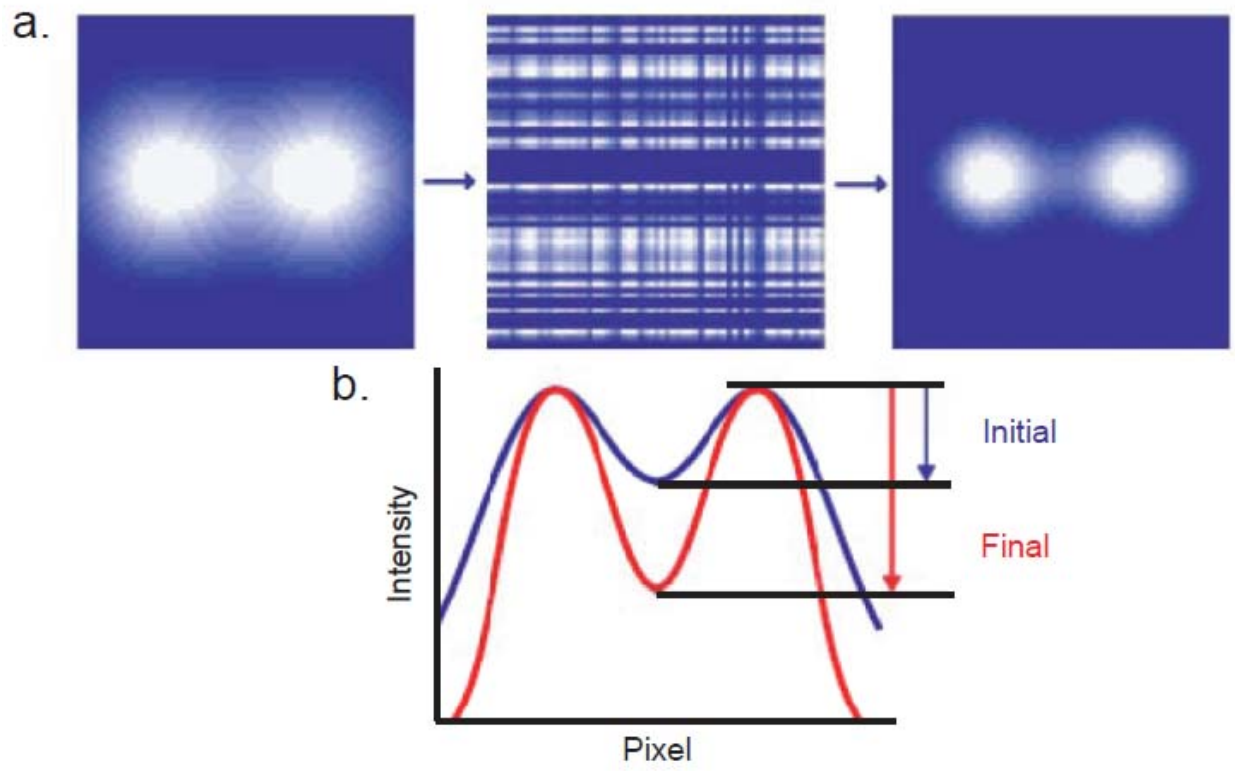

Figure 3.6. Enhanced two-point discrimination. Effectiveness of activity-dependent inhibition investigated using two-point discrimination. **a)** Two overlapping stimuli are shown before (left panel) and after (right panel) activity-dependent inhibition. To confirm that spatial structure was not required, input image was randomized (center panel) before processing with inhibition. b) Pixel intensities from a horizontal line drawn through the center of the network showing an increase in the maximal difference between the two input stimuli.

3.4.4 Decorrelation of Similar Olfactory Input Patterns

A particular odorant activates a range of olfactory sensory neurons that then project to the olfactory bulb, activating a specific pattern of glomeruli, with similar odors producing similar patterns of glomerular activation (Sharp et al., 1975;Rubin and Katz, 1999;Spors and Grinvald, 2002). Now, imagine if you were an animal trying to differentiate between similar odors. These similar odors would result in similar patterns of activated mitral cells in the olfactory bulb. This would then make discrimination between these odors based on the pattern of mitral cell activity relatively more difficult then more dissimilar odors that result in more distinct patterns of mitral cell activity. Therefore, it would be advantageous to an animal to have a method to make initially similar odor-evoked patterns of activity more dissimilar and consequently easier to differentiate. Given these benefits to odor discrimination, we next examined the effect of activity-dependent inhibition on simulated patterns of olfactory receptor neuron inputs with varying degrees of similarity.

Work by Friedrich and Laurent (2001) in zebrafish olfactory bulb showed that mitral cell activity patterns show a progressive decorrelation (i.e. the patterns become more dissimilar) in time via processing within the olfactory bulb. To test if activity-dependent lateral inhibition alone was sufficient to result in the same kind of decorrelation, we generated sixteen input maps having varying degrees of correlation (**Fig. 3.8**, see methods). If activity-dependent lateral inhibition functions to increase the ability to discriminate similar odors, we should observe a decrease in correlation between initially similar responses, like that observed *in vivo* (Friedrich and Laurent, 2001;Yaksi et al., 2007). As predicted, applying this activity-dependent lateral inhibition to each map decreased the correlation between initially similar patterns of simulated odor-evoked activity. This change was evident in the cross correlation matrices (compare left and right panels in **Fig. 3.8**) and by computing the average level of pairwise correlations of input and output (**Fig. 3.9A,B**). Models in which the strength of inhibition was independent of postsynaptic activity (i.e. inhibition resulted in either a constant subtractive or divisive change in activity, see **section 4.2.1**) did not generate substantial levels of decorrelation, even when the overall level of inhibition reduced activity to a greater degree (**Fig. 3.9A, B**). This

observation held whether the inhibition was modeled as subtractive or divisive, indicating that the activity-dependence of lateral inhibition is critical for mediating decorrelation in networks without spatial structure to their connections (**Fig. 3.9A,B** average pairwise correlation across all maps of 0.33, closed arrow, reduced to 0.11, open arrow, by activity-dependent lateral inhibition).

To determine if the residual inhibition at higher firing rates that we sometimes observed in our experiments (**Fig. 2.2A, B**) affects the computational functions of the model, we tested the model with a substantial amount of residual inhibition (50% residual inhibition relative to peak inhibition, **Fig 3.5B**, dotted line). Even with this substantial amount of residual inhibition, the model still exhibited robust decorrelation (**Fig 3.9B**). One difference between our simulations and the data on time-dependent decorrelation is that we did not see examples of patterns of activity evoked by two different odors becoming increasingly decorrelated across time, as is seen in a subset of cells recorded experimentally (Friedrich and Laurent, 2001). This may be due to the simplicity of our model which does not include features such as excitatory coupling between mitral cells (Margrie et al., 2001;Carlson et al., 2000;Schoppa et al., 1998) or short term plasticity of lateral inhibition (Dietz and Murthy, 2005) that may be important for these aspects of the described results.

3.4.5 Parallel Processing with Activity-Dependent Lateral Inhibition Applied to Image Processing

One interesting aspect in olfactory processing is that of parallel processing. A potential mechanism employed in the olfactory bulb to mediate parallel processing is that of neuronal microcircuits (Shepherd and Greer, 2004). An example of this is the parallel pathways of mitral and tufted cells. While both mitral and tufted cells send their apical dendrites to the same glomerulus they exhibit different physiological properties and project to different locations (Macrides et al., 1985; Nagayama et al., 2004). In addition to mitral and tufted cells, it has been

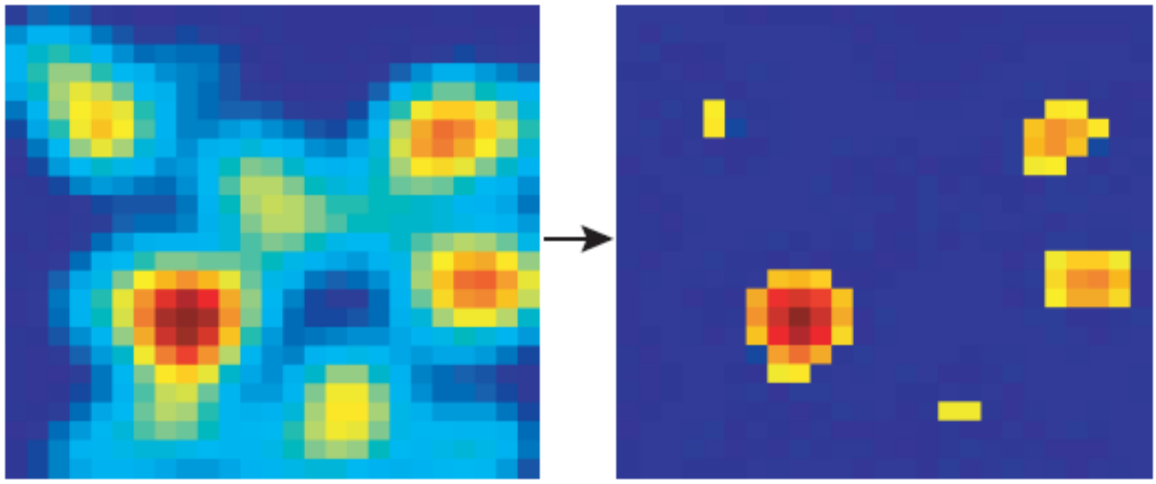

Figure 3.7. Simulated olfactory response patterns exhibit contrast enhancement. Example of a simulated olfactory response pattern before (left panel) and after (right panel, colormap rescaled) processing by activity-dependent lateral inhibition.

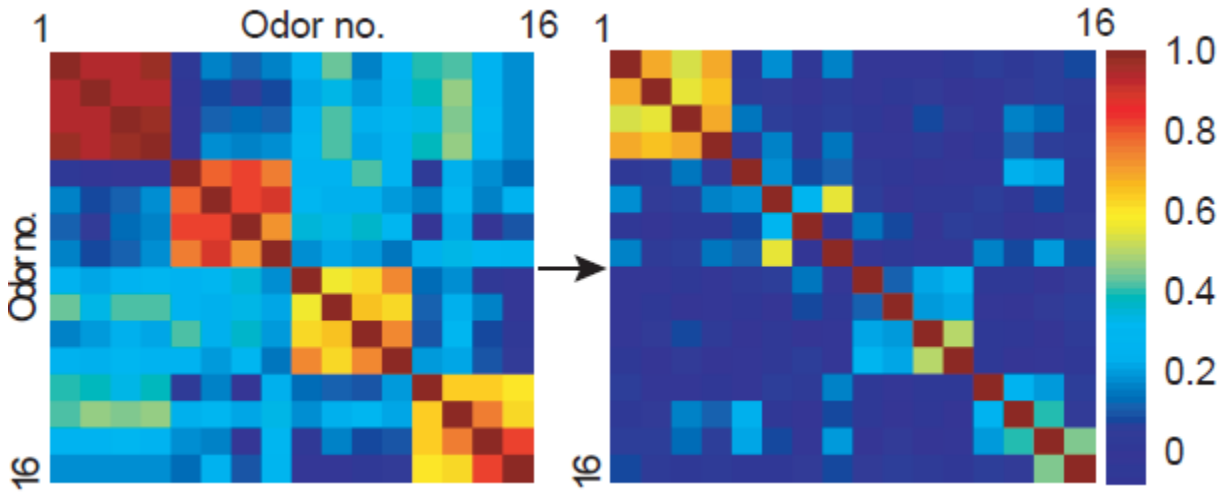

Figure 3.8. Contrast enhancement and decorrelation of similar input patterns. Correlation matrix of 16 different olfactory response patterns (example shown in **Fig. 3.7**) of simulated mitral cell activity before (left panel) and after (right panel) activity-dependent lateral inhibition. Four families of simulated olfactory responses were created with high correlation within families and low correlation between maps in different families.

hypothesized that different subsets of mitral and granule cells make specific connections with one another to form microcircuits (Shepherd and Greer, 2004). Could these microcircuits transform the same olfactory receptor neuron input in a given glomerulus in different ways? If this were the case, what could be the functional implications of this and how could the activity-dependent lateral inhibition observed in our physiological studies impact this?

To explore the potential utility of activity-dependent lateral inhibition in the context of parallel processing, we applied this model of inhibition to image processing. When an image was given as the stimulus to a larger but otherwise identical network model, activity-dependent lateral inhibition resulted in substantial contrast enhancement even when applied to a version of the image in which pixel position was randomized (**Fig. 3.10**). This independence of the operation on the spatial structure contained within the image represents a novel method of enhancing contrast within images and emphasizes the general utility of this form of inhibition.

In the model, the peak of activity-dependent inhibition is set at a specific value relative to the overall network activity. If the peak of this inhibition is shifted to other values as was observed to occur physiologically (**Fig. 2.12**) and computationally (**Fig. 3.4**), different aspects of the image can be emphasized. In the first case, the top left image shows increased contrast enhancement of primarily the foreground aspect of the image including the buildings and trees (**Fig. 3.10**, top right panel). However, by shifting the peak of inhibition to lower values, lower pixel values are preferentially enhanced which resulted in an enhancement of contrast in the background clouds (**Fig. 3.10**, bottom right panel).

Therefore, activity-dependent lateral inhibition, in addition to mediating useful lateral interactions between neurons without requiring spatial arrangement of input, can effectively process different aspects of the input based on the specific frequency-tuning of this activity dependence, allowing for parallel processing of this input.

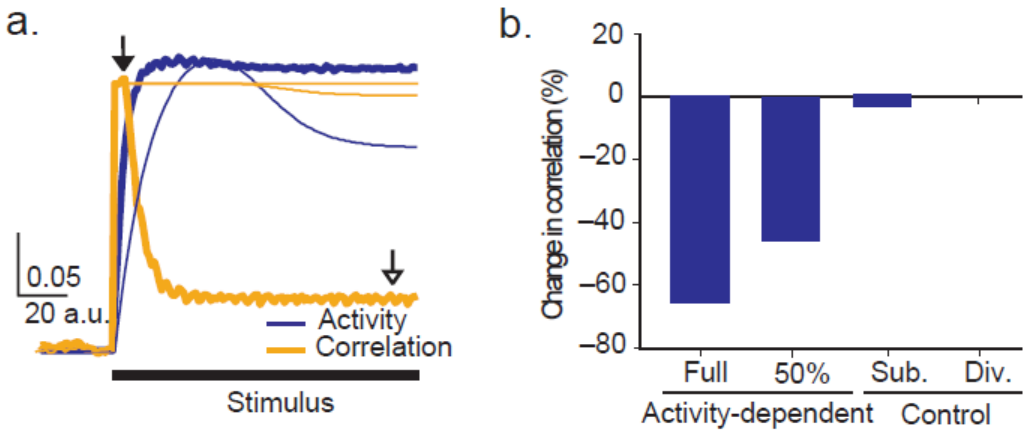

Figure 3.9. Decorrelation and comparison to other forms of lateral inhibition. a,b) Average activity and correlation across all maps for activity dependent lateral inhibition and other models of inhibition. Initially high correlation (0.33, thick line, closed arrow) was substantially decreased by activity dependent lateral inhibition (0.11, thick line, open arrow, scale bar: 0.025 correlation units/arbitrary time units) but not for networks with subtractive or divisive inhibition (thin lines).

3.5 DISCUSSION

Inhibition in neuronal circuits is widespread and a potentially powerful functional tool in processing information in the brain. Our modeling work shows that integration of activity within a simple network of neurons is sufficient to generate the activity-dependence of lateral inhibition observed in our physiological results. Furthermore, we show that activity-dependent lateral inhibition can mediate contrast enhancement and decorrelation of similar inputs. We also go on to show that this processing can be achieved in parallel and use an application to image processing to highlight how the same network of neurons can process different aspects of the same input, potentially increasing the computational power of the network as well as increasing the information retrieved from a given stimulus.

3.5.1 Significance in Olfactory Processing

Since their early descriptions by Ramon y Cajal (1995), granule cells in the olfactory bulb have presented an intriguing question as to their function. They are a unique neuronal class in many ways from their lack of an axon to their reciprocal dendrodendritic synapses (Jahr and Nicoll, 1982). While they mediate recurrent as well as lateral inhibition within the bulb, the nature of how this inhibition is specified and allocated to various neurons in the bulb is still not clear.

One of the central issues in understanding what functional role inhibition has in the olfactory bulb revolves around how information is represented within the bulb. Initially, it was thought that olfactory information was mapped topographically onto the two-dimensional sheet of neurons in the olfactory bulb such that neurons responding to similar odors are

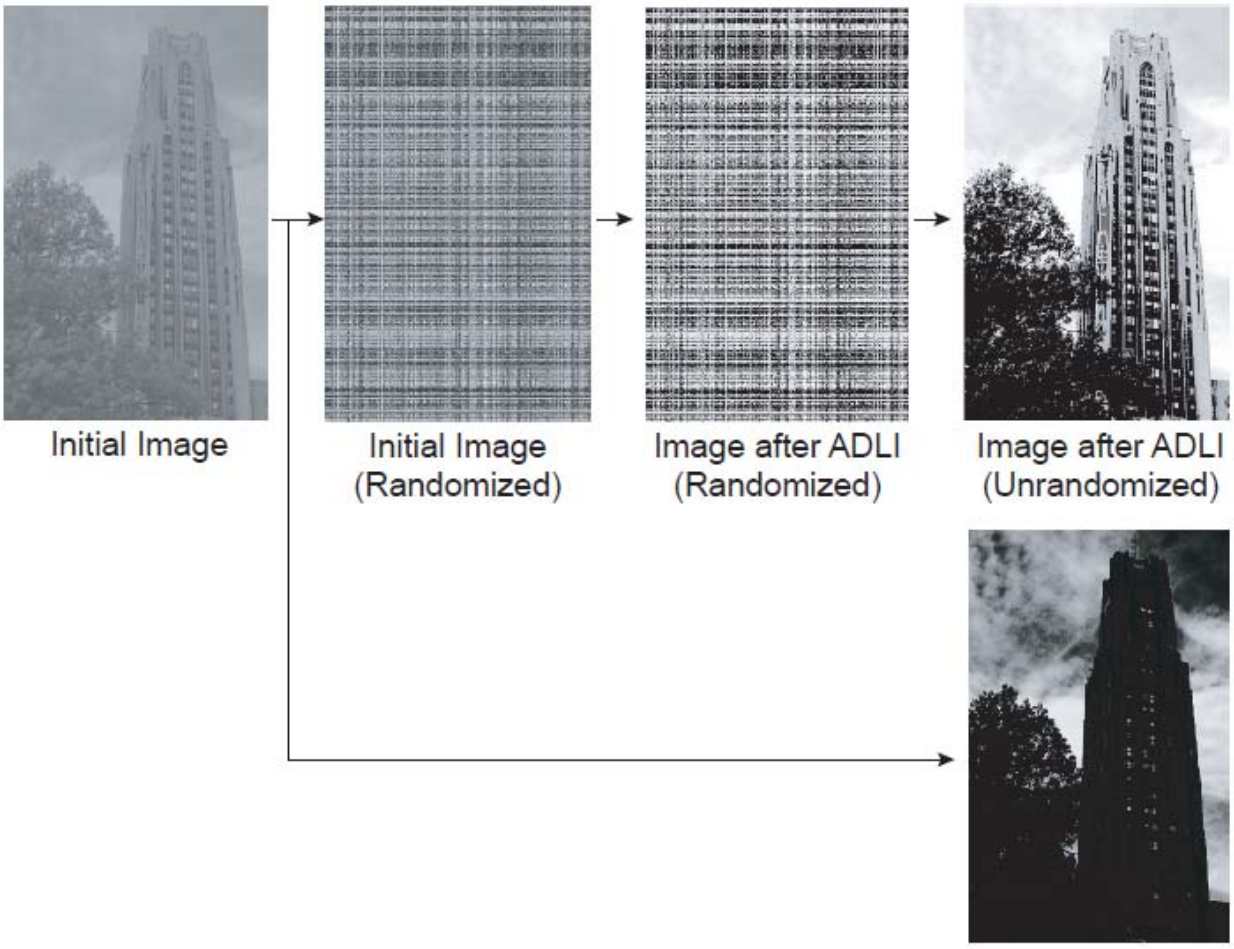

Figure 3.10. Parallel processing applied to image processing. Activity-dependent lateral inhibition was applied to image processing. An image was used as input to the network (left panel) and randomized before processing with the model (center panels). Different aspects of the image are enhanced as a result of different ranges of activity-dependent inhibition relative to pixel intensity.

located near one another in the olfactory bulb (Meister and Bonhoeffer, 2001;Belluscio and Katz, 2001;Uchida et al., 2000;Yokoi et al., 1995). However, it appears that at most, odorants are represented in broad regions of the bulb (Rubin and Katz, 1999;Johnson and Leon, 2000a;Uchida et al., 2000;Wachowiak and Cohen, 2001). Through the physiological results presented in **chapter 2**, we show that inhibition is specified in an activity-dependent manner resulting in a dynamic remapping of effective inhibition based on the activity of mitral cells.

We explored the functional implications of this dynamic specification of lateral inhibition and through our simulations we show that this activity-dependence is sufficient to not only improve two-point discrimination but also to qualitatively enhance contrast in simulated olfactory input. Furthermore, activity-dependent inhibition is able to decorrelate similar input patterns in a spatially independent manner similar to that observed *in vivo* (Friedrich and Laurent, 2001;Yaksi et al., 2007). Considering that similar odors tend to result in similar patterns of activity within the olfactory bulb, then decreasing the similarity between initially similar patterns would make them easier to differentiate. In this way, activity-dependent lateral inhibition would allow the animal to tell the difference between more similar odors then it would be able to otherwise.

Another interesting implication of this dynamic connectivity is its potential usefulness in processing different aspects of olfactory information in parallel. This could be achieved by selectively tuning different mitral cells connected to the same glomerulus for different postsynaptic frequencies. This could result in an enhancement of information in different aspects of the olfactory signal that could, for example, enhance the general category of a smell (i.e. flower) in addition to the specific identity of the odor (i.e. jasmine) or it could be employed to extract different components of a complex odor mixture.

3.5.2 Implications throughout the Brain

One of the most exciting results of this research is its potential for neuronal computation outside of the olfactory bulb. There are many brain areas where inhibition plays a prominent role in neuronal computation but where neuronal representations are discontinuous.

One such area is the inferotemporal cortex where neurons respond to complex object features and neurons near one another can respond to qualitatively different features (Tanaka, 1996;Logothetis and Sheinberg, 1996). GABA-mediated inhibition has also been shown to augment the responses of neurons in this area such that blocking inhibition changes their responses (Wang et al., 2000). Another area where dynamic connectivity could be useful is in the hippocampus where the representation of neurons called 'place cells' have strong and reliable behavioral correlates to their activity (O'Keefe and Dostrovsky, 1971;Ranck, Jr., 1973). While sometimes representations are highly correlated with spatial location (Best et al., 2001), in other instances activity is related to non-spatial factors (Young et al., 1994;Wood et al., 1999) and can alternate between different representations in the same location (Markus et al., 1995) or as a result of the orientation of the landmarks (Knierim et al., 1998). Given this dynamic representation in hippocampal neurons, a method of specifying lateral interactions based on the activity of the neurons similar to what we report in **chapter 2** could be especially useful.

4.0 GENERAL DISCUSSION

4.1 SUMMARY OF FINDINGS

Research presented in this dissertation focused on the lateral interaction between MCs in the olfactory bulb. In **chapter 2**, I present results from my investigation of how the activity of MCs influences the amount of inhibition that they receive from other MCs in the network. Furthermore, we investigated the role of the inhibitory granule cells in the interaction between MCs. I concluded that the activity of a given MC acted as an effective gate to lateral inhibition from other MCs. The activity-dependence of inhibition showed a specific range of postsynaptic activity where lateral inhibition was effective. I also concluded that granule cells integrate activity between the MCs that connect to it and show supralinear recruitment when multiple MCs are activated. These results indicate a novel method of specifying neuronal interactions that we term dynamic connectivity. I go on to explore the functional implications of this novel form of inhibition in **chapter 3** and show that it not only is able to effectively enhance contrast of simulated olfactory input, but is also able to substantially decorrelate similar input patterns when other previously described forms of inhibition are not able to. In the following section, I will discuss these results and their functional implications in olfaction as well as in other brain areas.

4.2 PHYSIOLOGICAL RELEVANCE OF ACTIVITY-DEPENDENT LATERAL INHIBITION

4.2.1 Activity-Dependent Lateral Inhibition as a Novel Method of Neuronal Interaction

From the early experiments by Hartline (1938) in the eye of the *Limulus*, it was clear that interactions between sensory neurons had important implications in modulating their sensory representations. These early experiments gave insight into one of the most fundamental types of interactions between neurons, that of lateral inhibition. While inhibitory granule cells are abundant in the olfactory bulb and MCs receive large amounts of lateral inhibition, it has been unclear how this modulates MC activity. Because the type of modulation is integral to the functional implications of inhibition, we directly investigated this by conducting whole-cell recordings of MCs. We found that the effectiveness of lateral inhibition (quantified as a reduction in firing rate) was dependent not only on the activity of presynaptic MCs but also on the activity of the MC receiving the lateral inhibition (postsynaptic MC). This resulted in lateral inhibition reducing the firing rate of a MC only in a defined range of postsynaptic firing rates and we call this activity-dependent lateral inhibition. But how is this different from how lateral inhibition has been characterized previously?

Initially, it was believed that inhibition had a divisive effect on firing rate (Blomfield, 1974;Koch et al., 1983;Nelson et al., 1994). This hypothesis was based on Ohm's law where the membrane potential is determined by the current divided by membrane conductance (Koch and Segev, 1998). Increasing inhibition, increases membrane conductance and therefore reduces membrane potential in a divisive manner. It was assumed that the divisive effect on membrane potential also resulted in a division of firing rate (**Fig. 1.3**). A divisive reduction is a reduction resulting in a constant fractional change in firing rate. For example, if inhibition produced a 20% reduction in firing rate, this would result in a 20 Hz reduction in firing rate if

the cell was firing initially at 100 Hz. As the firing rate of the neuron increases, the absolute reduction in firing rate also increases but the fractional change in firing rate remains constant. This concept of division of firing rate was originally suggested to be important in neural computations by Reichardt (1961), and has been used in many models of neural processing (Salinas and Sejnowski, 2001) including those characterizing the response of neurons in the visual cortex (Carandini and Heeger, 1994). However, theoretical (Gabbiani et al., 1994;Holt and Koch, 1997) as well as physiological (Connors et al., 1988;Ulrich, 2003) results indicated that this type of inhibition was unable to result in divisive effects on firing rate, but rather had a subtractive effect. This would result in a constant absolute reduction in firing rate. For example, if inhibition resulted in a 20 Hz reduction in firing rate when the cell was firing at 100 Hz, it would also result in a 20 Hz reduction in firing rate when the cell was firing at 50 Hz. In this way, the absolute reduction in firing rate remains constant, while the fractional change in firing rate changes. However, the introduction of synaptic noise (Prescott and De, 2003;Doiron et al., 2001) has been shown in modeling studies to result in divisive effects on firing rate. Furthermore, the location of synaptic input along the dendritic tree has been proposed to be important (Koch et al., 1983) and recent physiological studies have indicated that both subtractive as well as divisive effects on firing rate can occur from inhibition depending on the location of synaptic input along the dendritic tree (Mehaffey et al., 2005), highlighting the multiple factors involved in determining the functional transformation mediated by inhibitory connectivity.

Whether subtractive or divisive, the key distinction between these previous results and the results presented in this study is that both subtractive and divisive inhibition have a constant effect on the firing rate of a neuron and the activity of the postsynaptic neuron is not able to modulate the effectiveness of the inhibition that it receives. This contrasts with our physiological results where the effectiveness of lateral inhibition in reducing spike rate is determined by the activity of the postsynaptic neuron (**section 2.4.1**) as well as the presynaptic neuron (**section 2.4.3**).

4.2.2 Frequency Dependence and Odor-Evoked Firing Rates

Our results from recording from pairs of MCs show that lateral inhibition is effective at reducing firing rate only when a MC is firing between 30-100 Hz on average (**section 2.4.1**). Because of this activity-dependence, MCs firing at elevated rates are immune to the effect of lateral inhibition and therefore their spike rates are unchanged by the activity of presynaptic MCs. This could have important implications if lateral inhibition functions in a manner to enhance contrast (**section 3.4.3**). However, is the range of 30-100 Hz physiologically relevant to MCs?

Oscillations in the olfactory bulb are preserved across species and appear to have important functional implications to olfactory processing. Specifically, studies have indicated that the beta (20-40 Hz) and gamma (40-80 Hz) frequency bands are important in many physiologic functions (Adrian, 1942; Eeckman and Freeman, 1990;Laurent and Naraghi, 1994; Hopfield, 1995;Perez-Orive et al., 2002; Wilson and Mainen, 2006). The physiological relevance of the activity-dependent inhibition that we observed is highlighted by the fact that it spans these two important frequency bands. Furthermore, individual MCs have been shown to fire up to approximately 200 Hz in response to odorants *in vivo* (Egana et al., 2005) and so the upper boundary of 100 Hz is well within the physiological firing rates of these neurons.

Furthermore, several results from our experiments also highlight the dynamic nature of this activity-dependent gating of inhibition. For example, in **section 2.4.1** we showed that activating a larger subset of granule cells by extracellular stimulation in the glomerular layer resulted in an effective range of inhibition between 20-65 Hz which is clearly within the physiological range of MC firing rates. Also, in **section 2.4.3** we showed that increasing presynaptic MC activity from 50 to 100 Hz resulted in a decrease in the upper threshold of this range of 30 Hz. These two results highlight both the dynamic nature of this effect and the importance that overall network activity will play in determining the specific aspects of activity-dependent inhibition *in vivo*.

4.2.3 Lateral Inhibition and the Speed of Odor Discrimination

Timing of activity within the olfactory bulb continues to present an intriguing question with respect to odor discrimination. Brief activation of individual MCs results in granule cell-mediated inhibition lasting for several hundred milliseconds (Isaacson and Strowbridge, 1998;Urban and Sakmann, 2002). Latencies of activation of glomeruli (Spors et al., 2006) as well as granule cells (Kapoor and Urban, 2006) provide further indications that olfactory representations evolve over several hundred milliseconds. Odor-evoked activity also has been shown to be decorrelated over several hundreds of milliseconds, potentially allowing improved discrimination between two similar odors (Friedrich and Laurent, 2001;Bhandawat et al., 2007;Yaksi et al., 2007). If inhibition has a role in improving discriminations, then how do these timescales relate to the timescale relevant for odor discrimination?

The time necessary for odor discrimination was recently addressed by three studies using the relationship between speed and accuracy in olfactory discrimination (Uchida and Mainen, 2003;Abraham et al., 2004;Rinberg et al., 2006). In many sensory systems, there exists a tradeoff between the speed of discrimination and accuracy such that accuracy decreases as discrimination time decreases (Luce, 1986). The first study to address this issue in olfaction showed that mice needed about 300 ms to perform both simple as well as difficult discriminations and therefore the authors concluded that temporal aspects of odor coding were not important in discrimination (Uchida and Mainen, 2003). However, accuracy also decreased for difficult discriminations, confounding interpretation of these results. Later studies using different behavioral paradigms that controlled for accuracy (Abraham et al., 2004) as well as odor discrimination time (Rinberg et al., 2006) showed that as discrimination time decreased, accuracy also decreased. Taking into account time for odor diffusion and processing of motor commands, it was estimated that simple odors could be discriminated in less than 100 ms in the olfactory bulb, while difficult discriminations take an additional 70-100 ms (Schaefer and Margrie, 2007). Therefore, the general conclusion from these studies is that odor discrimination in the olfactory bulb occurs very rapidly. How then does this relate to the onset of activity-dependent lateral inhibition?

While our studies only briefly addressed the temporal evolution of activity-dependent inhibition, differences in spike density functions as a result of inhibition between a pair of MCs (**Fig. 2.10**) suggests that integration of activity in time could have important implications for activity-dependent inhibition. These results show that the onset of inhibition shortens from a 300 ms delay to be nearly instantaneous as postsynaptic activity increases. This shortening of onset time of inhibition with increasing activity could be related to observations showing a decrease in latency times with increasing odorant concentration (Margrie et al., 2003;Spors et al., 2006). However, the onset of inhibition could vary significantly *in vivo* with increased network activity and therefore paired MC recordings i*n vivo* similar to those we conducted *in vitro* would be ideal to determine the onset latency of inhibition as a result of odorant-evoked activity.

4.3 MECHANISMS OF ACTIVITY-DEPENDENT INHIBITION

Given the unique dependence on postsynaptic activity for lateral inhibition that we observed in the olfactory bulb, an interesting question arises as to the mechanism behind this inhibition. We hypothesized that the basic effect of activity-dependence was due to integration of activity across both pre- and postsynaptic neurons. The olfactory bulb offers several ways to achieve this integration.

4.3.1 Integration of Activity within the Olfactory Bulb

How might the olfactory bulb achieve the integration of activity between pre- and postsynaptic MCs? While the interactions between mitral and granule cells have traditionally been thought of as the primary mediator of lateral inhibition in the bulb (Jahr and Nicoll, 1982), recent studies in both mice (Aungst et al., 2003) and *Drosophila* (Olsen and Wilson, 2008) have shown that

interglomerular inhibition can occur at the level of the glomerular layer. In mice, these interactions were mediated by excitatory SA cells synapsing on inhibitory PG cells in glomeruli up to 1mm away resulting in inhibition of MCs in those glomeruli (Aungst et al., 2003). The potential functional importance of these interactions were highlighted by showing that elimination of these interglomerular interactions resulted in broadening of tuning curves in *Drosophila* (Olsen and Wilson, 2008).

While it is possible that lateral inhibition at the level of the glomerular layer could play a role in interglomerular inhibition, it likely does not significantly contribute to the activity-dependent lateral inhibition observed in our experiments for several reasons. First, activity-dependent inhibition was observed between pairs of MCs even when the apical dendrite of one of the MCs was cut before reaching the glomerulus and therefore, interactions within the glomerular layer were not possible (**Fig 2.4**). It is also unclear how these glomerular layer interactions would allow for the cooperativity between pre- and postsynaptic MCs considering that these interglomerular interactions are mediated via axonal transmitter release (Aungst et al., 2003;Shepherd and Greer, 2004).

These considerations lead us to propose that the activity-dependent lateral inhibition we observed is likely primarily mediated by interactions between mitral and granule cells. Several aspects of our data are consistent with this hypothesis. First, we show that blocking glutamatergic transmission by application of APV and CNQX reduced the amount of inhibition received as a result of extracellular stimulation in the granule cell layer (**Fig 2.16**). This result indicates that postsynaptic MC activity modulates the inhibition that it receives as a result of granule cell stimulation, supporting the hypothesis that integration of activity within granule cells contributes to the activity-dependence observed. Furthermore, imaging granule cell activity as a result of glomerular layer stimulation resulted in a supralinear increase in the number of active granule cells when two glomeruli are stimulated simultaneously as compared to when they are stimulated alone (**Fig 2.17**). In **chapter 3**, we also show that integration of activity within granule cells is sufficient to reproduce the activity-dependent inhibition observed in our physiological experiments.

Granule cells are known to make contacts with up to 50-100 different MCs and are therefore in a prime position to integrate activity across these different cells (Egger and Urban, 2006). Furthermore, inhibition can be localized to a single synapse and reciprocal (Jahr and Nicoll, 1982) as well as lateral (Isaacson and Strowbridge, 1998) inhibition can occur independent of Na^+ spikes. In addition, widespread transmitter release can also occur as a result of action potentials since granule cells have been shown to fire spikes as a result from odor exposure *in vivo* (Wellis and Scott, 1990). Granule cells have several molecular as well as structural features, described below, that could have important roles in mediating the kind of integration across neurons that is likely to underlie activity-dependent inhibition.

4.3.2 Molecular Coincidence Detection in Granule Cells

There are several molecular components in the granule cell dendritic tree that could be involved in allowing for integration of activity across MCs. One of the most likely is the NMDAR which is critical for synaptic transmission in olfaction (Isaacson and Strowbridge, 1998;Schoppa et al., 1998) and is also present in extrasynaptic locations (Isaacson and Murphy, 2001). This receptor is well known to mediate coincidence detection in several areas and has a central role in many forms of long term potentiation (Malenka and Nicoll, 1999). The NMDAR has several unique features including Ca^{++} permeability 5-10 times that of Na^+ or K^+ as well as a voltage-dependence mediated by an Mg^{++} block (Nowak et al., 1984;Mayer and Westbrook, 1987;Ascher and Nowak, 1988). The coincidence detection of the channel is mediated by this Mg^{++} block since conductance due to glutamate binding increases as the postsynaptic cell is depolarized and thus removing the Mg^{++} block (Nowak et al., 1984;Mayer and Westbrook, 1987;Ascher and Nowak, 1988). This has also been demonstrated in the olfactory bulb where Mg^{++} washout results in increase in granule cell-mediated inhibition (Isaacson and Strowbridge, 1998). The NMDAR also has slow deactivation kinetics (Lester et al., 1990) resulting in prolonged action potential trains in many systems (Ismail et al., 1986;Dickenson and Sullivan, 1990;D'Angelo et al., 1995).

Another likely molecular mechanism for coincidence detection in granule cells could be mediated by inactivating K^+ channels (I_A). These channels are K^+ permeable and are inactivated as a result of deporalization, requiring a period of hyperpolarization for activation (Connor and Stevens, 1971;Rudy, 1988). In the olfactory bulb, I_A has been shown to specifically attenuate brief depolarization mediated by AMPARs whereas activation of longer lasting NMDARs are able to overcome its effects (Schoppa and Westbrook, 1999). Therefore, by specifically attenuated short duration depolarizations, I_A can act as a coincidence detector by enhancing longer duration input either from convergent depolarizations across the dendritic tree or through activation of the NDMAR (Schoppa and Westbrook, 1999).

4.3.3 Dendritic Integration in Granule Cells

Another interesting feature of granule cells is their dendritic tree. Granule cells have a primary ascending dendrite that extends into the external plexiform layer and ramifies in a tree approximately 30-200 microns in diameter (Orona et al., 1984). A given granule cell makes connections with up to 50-100 mitral cells that are connected to different glomeruli (Shepherd and Greer, 2004). Granule cells therefore have a unique perspective on the olfactory network, able to integrate information across different MCs and glomeruli to shape the inhibitory output of the olfactory bulb. How do their dendritic trees effect this integration? Previous compartmental modeling studies predicted that there should be regional responses where the dendritic response would be localized to a regional subset of the dendritic tree (Woolf et al., 1991a;Woolf and Greer, 1994). Are these functions present within granule cells? How local and/or global can granule cell responses be?

It has been shown that synaptically evoked Ca^{++} transients via NMDARs and voltage gated Ca^{++} channels can be localized to a single spine (Egger et al., 2005) and so GC responses can be highly localized in the dendritic tree. The closest evidence of activity confined to a subset of the dendritic tree comes from studies in turtle and frog where synaptically evoked dendritic Na^+ spikes have been reported (Zelles et al., 2006;Pinato and Midtgaard, 2005). While

these spikes invade the entire branch, they fail just before the soma and do not invade other primary branches of these multipolar dendritic trees. Global subthreshold responses have also been shown and are a result of subthreshold depolarizations and are dependent on LVA Ca^{++} channels (Egger et al., 2005;Egger et al., 2003;Pinato and Midtgaard, 2005). These dendritic spikes could have an important role in integrating activity within GCs as dendritic spikes have been shown to be an efficient coincidence detection mechanism in dendrites (Segev and Rall, 1988). Furthermore, integration within the dendritic tree has been shown to mediate important functions in other sensory systems such as mediating orientation tuning in complex cells in visual cortex (Mel et al., 1998).

Whether GCs exhibit responses that are confined to specific regions or that spread throughout the dendritic tree, it is clear that they are capable of sub- and suprathrehsold responses allowing for interaction between different subsets of MCs based on their overall activity. Therefore, because of their position at the center of a connection with 50-100 MCs, they are uniquely positioned to integrate activity among these cells and contribute to the activity-dependence of lateral inhibition.

4.4 FUNCTIONAL IMPLICATIONS IN OLFACTION

What types of transformations of olfactory information are the most appropriate in olfaction? What is the ultimate goal of processing in the olfactory bulb? These are challenging questions to address in olfaction. The nature of olfactory information is complex, possibly being described by thousands of dimensions. Therefore, unlike other senses such as vision and audition, it is unclear how a two-dimensional array of neurons in the olfactory bulb represents and transforms this complex space. We believe the dynamic connectivity enabled by the

activity-dependent lateral inhibition that we observed in our physiological experiments could have interesting implications for processing olfactory information which I review below.

4.4.1 Contrast Enhancement and Decorrelation

Contrast enhancement is one of the classic functions that lateral inhibition is thought to mediate and has been described in many sensory systems (Hartline, 1938;Kaas et al., 1984;Kyriazi et al., 1996). By inhibiting neighboring neurons with similar response profiles, the difference between their activities is enhanced and thus the difference between two similar stimuli is enhanced (von Bekesy, 1967). This effectively increases the ability to discriminate between two similar stimuli (**section 3.4.4**).

One of the key requirements for lateral inhibition to enhance contrast in this way is that the spatial location of neurons should vary with the similarity of their receptive fields such that neurons have increasingly similar receptive fields the closer they are to one another. Several studies have analyzed the spatial distribution of the odor-evoked response of ORNs (Friedrich and Korsching, 1997;Bozza et al., 2004;Spors and Grinvald, 2002) as well as mitral and granule cells (Motokizawa, 1996;Johnson and Leon, 2000a;Meister and Bonhoeffer, 2001;Friedrich and Laurent, 2001;Yaksi et al., 2007). While it is possible that the responses of similar odors are located in similar broad regions of the olfactory bulb, results of these studies suggest that a fine chemotopic organization where MRR varies smoothly with location in the olfactory bulb does not exist (Friedrich and Korsching, 1998;Rubin and Katz, 1999;Johnson and Leon, 2000a).

Due to this lack of a fine grained chemotopic map in the olfactory bulb, it is unclear what the functional role of lateral inhibition in the olfactory bulb is. It is possible that lateral inhibition mediates functions other than contrast enhancement. Studies have investigated its role in synchrony and oscillations (Teramae and Tanaka, 2004;Nakao et al., 2005;Galan et al., 2006;Lagier et al., 2007), as well as its role in latency coding (Hopfield, 1995;Friedrich et al., 2004;Kapoor and Urban, 2006) and possibly gain control (Olsen and Wilson, 2008). While one

or more of these functions can also be mediated by lateral inhibition, the results presented in **chapter 2** suggest that activity-dependent lateral inhibition could allow for contrast enhancement in the olfactory bulb.

Given the ability of GCs to integrate activity across both pre- and postsynaptic MCs, we hypothesized that there could be a novel method for specifying lateral inhibition which resulted from the cooperative activation of the GCs mediating inhibition. In the results presented in **chapter 2**, we show that lateral inhibition is only effective in a specific range of postsynaptic firing rates (**section 2.4.1**). This is contrary to how lateral inhibition was thought to transform postsynaptic activity, as it was previously thought to mediate either constant divisive (Blomfield, 1974;Koch et al., 1983;Nelson et al., 1994;Salinas and Sejnowski, 2001) or subtractive (Connors et al., 1988;Holt and Koch, 1997;Ulrich, 2003;Mehaffey et al., 2005) effects on postsynaptic activity. Because activity-dependent lateral inhibition instead mediates a dynamic remapping of inhibition based on current network activity, we hypothesized that this could allow for contrast enhancement in the absence of a chemotopic organization of olfactory bulb neurons.

We investigated this hypothesis by creating a computational model of MCs exhibiting activity-dependent inhibition and all-to-all connectivity (**section 3.4.3**). We showed that not only did this result in an increase in two-point discrimination (**Fig. 3.6**) but also qualitatively enhanced the contrast in simulated odorant input (**Fig. 3.8**). As a further measure of the functional implication of this dynamic connectivity, we investigated its ability to decorrelate similar olfactory input patterns. It has been shown that odor-evoked activity resulting in similar patterns of activity in the olfactory bulb are progressively decorrelated as a result of processing within the olfactory bulb (Friedrich and Laurent, 2001;Yaksi et al., 2007). As predicted, our model of MCs exhibiting activity-dependent lateral inhibition was able to significantly decorrelate similar input patterns as observed these *in vivo* results (**Fig. 3.8**).

4.4.2 Parallel Processing of Odor Information

One intriguing idea that has been raised by the results presented in this dissertation is the possibility for parallel processing in the olfactory bulb. Our physiological results show that lateral inhibition between two MCs is effective only in a specific range (approximately 30-40 Hz) of postsynaptic firing rates (**section 2.4.1**). However, the specific frequencies of postsynaptic firing rates of this range varied for different MCs (**Fig. 2.8**). When we investigated the dynamic nature of this range further, we found that by increasing presynaptic MC activity, both the upper and lower thresholds of this range were lowered (**section 2.4.4**). This result supported our hypothesis that the activity dependence of lateral inhibition is a result of integration of activity between MCs such that an increase in the activity of one MC (the presynaptic cell in this experiment) resulted in a decrease in the requirement for activity in the second MC (postsynaptic). However, this result also raises another interesting possibility. If the activity-dependent range is itself a dynamic property based not only on the connectivity between MCs but also on real-time network activity, how could this affect olfactory processing? One possibility is that it could allow for parallel processing of odorant information in the olfactory bulb. If MCs connected to the same glomerulus exhibit different frequency ranges of activity-dependent inhibition, they could possibly extract different aspects of the olfactory input by being selectively tuned to different frequencies.

To investigate this possibility, we applied this activity-dependent inhibition to image processing (**section 3.4.5**). By changing the range of activity-dependent inhibition relative to pixel intensity, we were able to enhance different aspects of the image (**Fig. 3.10**). In the first example, the foreground including the building and trees was enhanced while in the second example, the background including the clouds was enhanced. In this way, two different aspects of the same image were extracted by shifting the activity-dependent range of inhibition. It is possible that in the olfactory bulb, if different MCs connected to the same glomerulus are tuned to different frequency ranges, then they would be able to extract different features of the olfactory input. This would effectively mediate parallel processing that could greatly enhance the amount of information extracted from a single odorant presentation.

4.5 FUNCTIONAL IMPLICATIONS IN OTHER BRAIN AREAS

4.5.1 Requirements for Dynamic Connectivity

Given the unique dendrodendritic synapse that mediates inhibition between mitral and granule cells, one could ask if the dynamic connectivity resulting from activity-dependent inhibition is merely a result of the unique anatomy and physiology of the bulb? Could activity-dependent inhibition be employed in other areas of the brain, and if so, what are the physiological requirements?

The key requirement necessary for activity-dependence is that postsynaptic activity is able to be integrated along with presynaptic activity to determine the overall amount of inhibition. This integration of activity would result in the modulation of the amount of inhibition received by an individual neuron as a result of its own activity. Furthermore, if the inhibitory neurons exhibited a relatively high threshold of activation such that activity from both pre- and postsynaptic neurons were *required* to effectively activate these inhibitory cells, then the network would exhibit activity-dependent inhibition in specific, elevated frequency ranges of postsynaptic activity.

Is this type of cooperative activation of inhibitory neurons observed in other brain areas? A recent study by Scanziani's group investigated inhibition of layer 2/3 pyramidal neurons in the somatosensory cortex (Kapfer et al., 2007). By simultaneously recording from three different pyramidal neurons, they were able to show a supralinear increase in inhibition in a third cell as a result of combined activity in the first two cells. In fact, activation of either of the first two cells alone was not sufficient to result in inhibition of the third cell, similar to our results from paired MC recordings (**Fig. 2.5**, top panel). These results indicate that inhibitory cells in the somatosensory cortex integrate activity across multiple pyramidal neurons and therefore provide the basis for activity-dependent lateral inhibition similar to what we

observed in our experiments. However, this study did not analyze the effect of this integration of activity in inhibitory neurons with respect to the firing rate of the postsynaptic neuron and therefore a direct comparison to our data is not possible.

4.5.2 Areas Relevant to Activity-Dependent Processing

Are there brain areas outside of olfaction where this dynamic connectivity might be useful? The nonlinear recruitment of inhibitory cells in the somatosensory cortex described above suggests that dynamic connectivity could be important outside of olfaction, even in areas where there already exists a topographic arrangement of neurons. However, there are other areas in the brain where inhibitory interactions have an important role and yet there is a more discontinuous arrangement of neuronal representations. Activity-dependent inhibition could be especially applicable to these regions.

For example, while early visual representations in the retina and LGN maintain a topographic mapping of the visual world, higher order areas such as the infertemporal cortex, do not maintain this topographic mapping. Instead, neurons in this area respond to complex object features and neurons near one another can respond to qualitatively different features (Tanaka, 1996;Logothetis and Sheinberg, 1996). In many ways, this is similar to the olfactory bulb, where mitral cells located near one another can respond to very different odors. Despite this discontinuous representation of object features in the inferotemporal cortex, a recent study showed that GABA-mediated inhibition augments the responses of neurons in this area such that blocking inhibition changes their responses (Wang et al., 2000). These results indicating an important functional role for GABA-mediated inhibition in an area with a discontinuous representation suggest that activity-dependent inhibition could have important implications.

Another area where dynamic connectivity could be useful is in the hippocampus where the representation of neurons called ‘place cells’ have strong and reliable behavioral correlates

to their activity (O'Keefe and Dostrovsky, 1971;Ranck, Jr., 1973). In some circumstances their activity is highly correlated with an animal's location, and thus investigators have hypothesized the presence of a "cognitive map" (Best et al., 2001). However, in other cases place cell activity is tied to non-spatial factors (Young et al., 1994;Wood et al., 1999) and can alternate between different representations in the same location (Markus et al., 1995) or as a result of the orientation of the landmarks (Knierim et al., 1998). Therefore the representation of specific cells and the relationship between these representations across different cells in the hippocampus is very dynamic. Given this dynamic representation in hippocampal neurons, a method of specifying lateral interactions based on the activity of the neurons could be especially useful. In fact, the temporal fidelity of hippocampal principal neurons has been shown to be modulated by $GABA_A$Rs such that inhibition results in less jitter and shorter integration windows. This leads to a requirement of specific spike timings to activate the cell where blocking $GABA_A$Rs results in longer time constants suggesting a functional switch to integration rather then coincidence detection (Pouille and Scanziani, 2001). Later studies from this group also indicated that recurrent inhibition shifts along the somato-dendritic axis as a result of postsynaptic firing rate (Pouille and Scanziani, 2004). This frequency-dependent shift in the dynamics of inhibition is similar to the activity-dependent inhibition we observed in our experiments. Even though this result was shown for recurrent inhibition rather than lateral inhibition, it indicates that dynamic connectivity similar to that shown in our physiological results in **chapter 2** could be employed in this area as well.

4.6 GENERAL CONCLUSIONS

The research presented in this dissertation focused on the lateral interactions between mitral cells in the olfactory bulb and the functional implications of the dynamics of these interactions.

We provide evidence for a novel form of lateral interaction between neurons that we call activity-dependent lateral inhibition. Furthermore, through our computational studies we show that it can mediate useful computations within the olfactory bulb including enhancing contrast and decorrelating initially similar input patterns. Below I outline the major results of these studies:

- We initially investigated the lateral inhibition between mitral cells in the olfactory bulb and found the effectiveness of lateral inhibition (defined as a reduction in postsynaptic firing rate) was determined not only by the activity of the presynaptic mitral cell but also by the specific firing rate of the postsynaptic mitral cell. We call this novel form of interaction between neurons activity-dependent lateral inhibition

- Lateral inhibition is effective only within a defined band of frequencies such that there is a lower and upper threshold of postsynaptic firing rates where lateral inhibition is effective. This range was 20-65 Hz when evoking lateral inhibition via extracellular stimulation in the glomerular layer and 30-100 Hz in paired mitral cell experiments. Mitral cells firing below or above this range are immune to the effect of lateral inhibition.

- This activity-dependent range is also dynamically determined based on network activity. We found that increasing the activity of the presynaptic mitral cell resulted in a reduction of both the lower and upper thresholds of this range of approximately 30-40 Hz. This also supports our hypothesis that activity-dependent inhibition is a result of integration of pre- as well as postsynaptic activity within granule cells.

- To investigate the role of granule cells in mediating activity-dependent inhibition we imaged granule cell spiking activity as a result extracellular stimulation within individual glomeruli. Consistent with our hypothesis, we show that granule cells are recruited in a supralinear fashion when multiple glomeruli are stimulated.

- We also investigate the role of granule cells using computational techniques and show that a simple network of Wilson-Cowan style neurons is able to result in activity-dependent inhibition and therefore integration within granule cells is sufficient to reproduce our physiological results. These computational results also show that short-term depression of granule cells could play an important role in determining the upper threshold of the activity-dependent range of inhibition.

- Results from further computational studies show that activity-dependent lateral inhibition is able to improve two-point discrimination, enhance contrast, as well as decorrelate initially similar input patterns to the network. Activity-dependent lateral inhibition is also sufficient to mediate these functions such that spatial structure of the network or stimulus is not required.

- Our physiological results showed that the activity-dependent range was itself a dynamic property of network activity as well as the observation that different mitral cell pairs showed different activity-dependent ranges of inhibition. Given these results, we explored the potential for mediating parallel processing of different stimulus features in olfaction with an application to image processing. By adjusting the activity-dependent range of inhibition relative to pixel intensity, we were able to selectively enhance different aspects of an image, highlighting the potential usefulness in mediating parallel processing of odorant information in the bulb.

BIBLIOGRAPHY

Abraham NM, Spors H, Carleton A, Margrie TW, Kuner T, Schaefer AT (2004) Maintaining accuracy at the expense of speed: stimulus similarity defines odor discrimination time in mice. Neuron 44:865-876.

Adrian ED (1942) Olfactory reactions in the brain of the hedgehog. J Physiol 100:459-473.

Araneda RC, Kini AD, Firestein S (2000) The molecular receptive range of an odorant receptor. Nat Neurosci 3:1248-1255.

Arctander S (1969) *Perfume and Flavor Chemicals*. New Jersey: Montclair.

Aroniadou-Anderjaska V, Zhou FM, Priest CA, Ennis M, Shipley MT (2000) Tonic and synaptically evoked presynaptic inhibition of sensory input to the rat olfactory bulb via GABA(B) heteroreceptors. J Neurophysiol 84:1194-1203.

Ascher P, Nowak L (1988) The role of divalent cations in the N-methyl-D-aspartate responses of mouse central neurones in culture. J Physiol 399:247-266.

Aungst JL, Heyward PM, Puche AC, Karnup SV, Hayar A, Szabo G, Shipley MT (2003) Centre-surround inhibition among olfactory bulb glomeruli. Nature 426:623-629.

Axel R (1995) The molecular logic of smell. Sci Am 273:154-159.

Barnard EA, Skolnick P, Olsen RW, Mohler H, Sieghart W, Biggio G, Braestrup C, Bateson AN, Langer SZ (1998) International Union of Pharmacology. XV. Subtypes of gamma-aminobutyric acidA receptors: classification on the basis of subunit structure and receptor function. Pharmacol Rev 50:291-313.

Belluscio L, Katz LC (2001) Symmetry, stereotypy, and topography of odorant representations in mouse olfactory bulbs. J Neurosci 21:2113-2122.

Berkowicz DA, Trombley PQ (2000) Dopaminergic modulation at the olfactory nerve synapse. Brain Res 855:90-99.

Best PJ, White AM, Minai A (2001) Spatial processing in the brain: the activity of hippocampal place cells. Annu Rev Neurosci 24:459-486.

Bhandawat V, Olsen SR, Gouwens NW, Schlief ML, Wilson RI (2007) Sensory processing in the Drosophila antennal lobe increases reliability and separability of ensemble odor representations. Nat Neurosci 10:1474-1482.

Bhandawat V, Reisert J, Yau KW (2005) Elementary response of olfactory receptor neurons to odorants. Science 308:1931-1934.

Blomfield S (1974) Arithmetical operations performed by nerve cells. Brain Res 69:115-124.

Bosking WH, Zhang Y, Schofield B, Fitzpatrick D (1997) Orientation selectivity and the arrangement of horizontal connections in tree shrew striate cortex. J Neurosci 17:2112-2127.

Bozza T, McGann JP, Mombaerts P, Wachowiak M (2004) In vivo imaging of neuronal activity by targeted expression of a genetically encoded probe in the mouse. Neuron 42:9-21.

Bressler SL, Freeman WJ (1980) Frequency analysis of olfactory system EEG in cat, rabbit, and rat. Electroencephalogr Clin Neurophysiol 50:19-24.

Brody CD, Hopfield JJ (2003) Simple networks for spike-timing-based computation, with application to olfactory processing. Neuron 37:843-852.

Buck L, Axel R (1991) A novel multigene family may encode odorant receptors: a molecular basis for odor recognition. Cell 65:175-187.

Buck LB (1996) Information coding in the vertebrate olfactory system. Annu Rev Neurosci 19:517-44:517-544.

Buonviso N, Chaput MA (1990) Response similarity to odors in olfactory bulb output cells presumed to be connected to the same glomerulus: electrophysiological study using simultaneous single-unit recordings. J Neurophysiol 63:447-454.

Buonviso N, Chaput MA, Berthommier F (1992) Temporal pattern analyses in pairs of neighboring mitral cells. J Neurophysiol 68:417-424.

Buonviso N, Revial MF, Jourdan F (1991) The Projections of Mitral Cells from Small Local Regions of the Olfactory Bulb: An Anterograde Tracing Study Using PHA-L (Phaseolus vulgaris Leucoagglutinin). Eur J Neurosci 3:493-500.

Cajal S (1995) Histology of the Nervous System of Man and Vertebrates. Oxford: Oxford University Press.

Cang J, Isaacson JS (2003) In vivo whole-cell recording of odor-evoked synaptic transmission in the rat olfactory bulb. J Neurosci 23:4108-4116.

Carandini M, Heeger DJ (1994) Summation and division by neurons in primate visual cortex. Science 264:1333-1336.

Carlson GC, Shipley MT, Keller A (2000) Long-lasting depolarizations in mitral cells of the rat olfactory bulb. J Neurosci 20:2011-2021.

Carr CE, Konishi M (1988) Axonal delay lines for time measurement in the owl's brainstem. Proc Natl Acad Sci U S A 85:8311-8315.

Carr CE, Konishi M (1990) A circuit for detection of interaural time differences in the brain stem of the barn owl. J Neurosci 10:3227-3246.

Chen WR, Shepherd GM (1997) Membrane and synaptic properties of mitral cells in slices of rat olfactory bulb. Brain Res 745:189-196.

Chen WR, Xiong W, Shepherd GM (2000) Analysis of relations between NMDA receptors and GABA release at olfactory bulb reciprocal synapses. Neuron 25:625-633.

Christie JM, Schoppa NE, Westbrook GL (2001) Tufted cell dendrodendritic inhibition in the olfactory bulb is dependent on NMDA receptor activity. J Neurophysiol 85:169-173.

Christie JM, Westbrook GL (2003) Regulation of backpropagating action potentials in mitral cell lateral dendrites by A-type potassium currents. J Neurophysiol 89:2466-2472.

Connor JA, Stevens CF (1971) Inward and delayed outward membrane currents in isolated neural somata under voltage clamp. J Physiol (Lond) 213:1-19.

Connors BW, Malenka RC, Silva LR (1988) Two inhibitory postsynaptic potentials, and GABAA and GABAB receptor-mediated responses in neocortex of rat and cat. Journal of Physiology 406:443-468.

Coopersmith R, Leon M (1984) Enhanced neural response to familiar olfactory cues. Science 225:849-851.

D'Angelo E, De FG, Rossi P, Taglietti V (1995) Synaptic excitation of individual rat cerebellar granule cells in situ: evidence for the role of NMDA receptors. J Physiol 484 (Pt 2):397-413.

Davison IG, Boyd JD, Delaney KR (2004) Dopamine inhibits mitral/tufted--> granule cell synapses in the frog olfactory bulb. J Neurosci 24:8057-8067.

Dayan P, Abbott LF (2001) Theoretical Neuroscience. Cambridge, MA: MIT Press.

Dickenson AH, Sullivan AF (1990) Differential effects of excitatory amino acid antagonists on dorsal horn nociceptive neurones in the rat. Brain Res 506:31-39.

Didier A, Carleton A, Bjaalie JG, Vincent JD, Ottersen OP, Storm-Mathisen J, Lledo PM (2001) A dendrodendritic reciprocal synapse provides a recurrent excitatory connection in the olfactory bulb. Proc Natl Acad Sci U S A 98:6441-6446.

Dietz SB, Murthy VN (2005) Contrasting short-term plasticity at two sides of the mitral-granule reciprocal synapse in the mammalian olfactory bulb. J Physiol 569:475-488.

Doiron B, Longtin A, Berman N, Maler L (2001) Subtractive and divisive inhibition: effect of voltage-dependent inhibitory conductances and noise. Neural Comput 13:227-248.

Duchamp-Viret P, Duchamp A, Chaput M (1993) GABAergic control of odor-induced activity in the frog olfactory bulb: electrophysiological study with picrotoxin and bicuculline. Neuroscience 53:111-120.

Dulac C, Torello AT (2003) Molecular detection of pheromone signals in mammals: from genes to behaviour. Nat Rev Neurosci 4:551-562.

Eccles JC, FATT P, LANDGREN S, WINSBURY GJ (1954) Spinal cord potentials generated by volleys in the large muscle afferents. J Physiol 125:590-606.

Eeckman FH, Freeman WJ (1990) Correlations between unit firing and EEG in the rat olfactory system. Brain Res 528:238-244.

Egana JI, Aylwin ML, Maldonado PE (2005) Odor response properties of neighboring mitral/tufted cells in the rat olfactory bulb. Neuroscience 134:1069-1080.

Egger V, Svoboda K, Mainen ZF (2003) Mechanisms of lateral inhibition in the olfactory bulb: efficiency and modulation of spike-evoked calcium influx into granule cells. J Neurosci 23:7551-7558.

Egger V, Svoboda K, Mainen ZF (2005) Dendrodendritic synaptic signals in olfactory bulb granule cells: local spine boost and global low-threshold spike. J Neurosci 25:3521-3530.

Egger V, Urban NN (2006) Dynamic connectivity in the mitral cell-granule cell microcircuit. Seminars in Cell and Developmental Biology 17.

Engel AK, Konig P, Kreiter AK, Schillen TB, Singer W (1992) Temporal coding in the visual cortex: new vistas on integration in the nervous system. Trends Neurosci 15:218-226.

Ennis M, Zhou FM, Ciombor KJ, Aroniadou-Anderjaska V, Hayar A, Borrelli E, Zimmer LA, Margolis F, Shipley MT (2001) Dopamine D2 receptor-mediated presynaptic inhibition of olfactory nerve terminals. J Neurophysiol 86:2986-2997.

Ennis M, Zimmer LA, Shipley MT (1996) Olfactory nerve stimulation activates rat mitral cells via NMDA and non-NMDA receptors in vitro. Neuroreport 7:989-992.

Fantana AL, Soucy ER, Meister M (2002) The rat olfactory bulb lacks chemotopy at fine spatial scales.

Fletcher ML, Smith AM, Best AR, Wilson DA (2005) High-frequency oscillations are not necessary for simple olfactory discriminations in young rats. J Neurosci 25:792-798.

Freeman WJ (1979) Nonlinear gain mediating cortical stimulus-response relations. Biol Cybern 33:237-247.

Friedman D, Strowbridge BW (2000) Functional Role of NMDA Autoreceptors in Olfactory Mitral Cells. J Neurophysiol 84:39-50.

Friedrich RW, Habermann CJ, Laurent G (2004) Multiplexing using synchrony in the zebrafish olfactory bulb. Nat Neurosci 7:862-871.

Friedrich RW, Korsching SI (1997) Combinatorial and chemotopic odorant coding in the zebrafish olfactory bulb visualized by optical imaging. Neuron 18:737-752.

Friedrich RW, Korsching SI (1998) Chemotopic, combinatorial, and noncombinatorial odorant representations in the olfactory bulb revealed using a voltage-sensitive axon tracer. J Neurosci 18:9977-9988.

Friedrich RW, Laurent G (2001) Dynamic optimization of odor representations by slow temporal patterning of mitral cell activity. Science 291:889-894.

Fujita SC, Mori K, Imamura K, Obata K (1985) Subclasses of olfactory receptor cells and their segregated central projections demonstrated by a monoclonal antibody. Brain Res 326:192-196.

Gabbiani F, Midtgaard J, Knopfel T (1994) Synaptic integration in a model of cerebellar granule cells. J Neurophysiol 72:999-1009.

Galan RF, Fourcaud-Trocme N, Ermentrout GB, Urban NN (2006) Correlation-induced synchronization of oscillations in olfactory bulb neurons. J Neurosci 26:3646-3655.

Gall CM, Hendry SH, Seroogy KB, Jones EG, Haycock JW (1987) Evidence for coexistence of GABA and dopamine in neurons of the rat olfactory bulb. J comp Neurol 266:307-318.

Glusman G, Yanai I, Rubin I, Lancet D (2001) The complete human olfactory subgenome. Genome Res 11:685-702.

Godfrey PA, Malnic B, Buck LB (2004) The mouse olfactory receptor gene family. Proc Natl Acad Sci U S A 101:2156-2161.

Gross-Isseroff R, Lancet D (1988) Concentration-dependent changes of perceived odor quality. pp 191-204.

Guthrie KM, Anderson AJ, Leon M, Gall C (1993) Odor-induced increases in c-fos mRNA expression reveal an anatomical "unit" for odor processing in olfactory bulb. Proc Natl Acad Sci U S A 90:3329-3333.

Haberly LB, Price JL (1978) Association and commissural fiber systems of the olfactory cortex of the rat. J Comp Neurol 178:711-740.

Halabisky B, Friedman D, Radojicic M, Strowbridge BW (2000) Calcium influx through NMDA receptors directly evokes GABA release in olfactory bulb granule cells. J Neurosci 20:5124-5134.

Halasz N, Nowycky M, Hokfelt T, Shepherd GM, Markey K, Goldstein M (1982) Dopaminergic periglomerular cells in the turtle olfactory bulb. Brain Res Bull 9:383-389.

Hallem EA, Nicole FA, Zwiebel LJ, Carlson JR (2004) Olfaction: mosquito receptor for human-sweat odorant. Nature 427:212-213.

Hartline HK (1938) The response of single optic nerve fibers of the vertebrate eye to illumination of the retina. pp 400-415.

Hartline HK, Wagner HG, Ratliff F (1956) Inhibition in the eye of Limulus. pp 651-673.

Hirsch JA, Gilbert CD (1991) Synaptic physiology of horizontal connections in the cat's visual cortex. J Neurosci 11:1800-1809.

Holt GR, Koch C (1997) Shunting inhibition does not have a divisive effect on firing rates. Neural Comput 9:1001-1013.

Hopfield JJ (1995) Pattern recognition computation using action potential timing for stimulus representation. Nature 376:33-36.

Hornung DE, Mozell MM (1977) Factors influencing the differential sorption of odorant molecules across the olfactory mucosa. J Gen Physiol 69:343-361.

Hornung DE, Youngentob SL, Mozell MM (1987) Olfactory mucosa/air partitioning of odorants. Brain Res 413:147-154.

Hubel DH, Wiesel TN (1963) RECEPTIVE FIELDS OF CELLS IN STRIATE CORTEX OF VERY YOUNG, VISUALLY INEXPERIENCED KITTENS. J Neurophysiol 26:994-1002.

Isaacson JS (1999) Glutamate spillover mediates excitatory transmission in the rat olfactory bulb. Neuron 23:377-384.

Isaacson JS (2001) Mechanisms governing dendritic gamma-aminobutyric acid (GABA) release in the rat olfactory bulb. Proc Natl Acad Sci U S A 98:337-342.

Isaacson JS, Murphy GJ (2001) Glutamate-mediated extrasynaptic inhibition. direct coupling of nmda receptors to ca(2+)-activated k(+) channels. Neuron 31:1027-1034.

Isaacson JS, Strowbridge BW (1998) Olfactory reciprocal synapses: dendritic signaling in the CNS. Neuron 20:749-761.

Ismail R, Pardede N, Darwin S, Nazir M, Mukti S (1986) Home-made rice water salt solution for oral rehydration therapy--a field trial. J Diarrhoeal Dis Res 4:20-25.

Jahr CE, Nicoll RA (1982) An intracellular analysis of dendrodendritic inhibition in the turtle in vitro olfactory bulb. J Physiol (Lond) 326:213-34:213-234.

Johnson BA, Farahbod H, Xu Z, Saber S, Leon M (2004) Local and global chemotopic organization: general features of the glomerular representations of aliphatic odorants differing in carbon number. J Comp Neurol 480:234-249.

Johnson BA, Leon M (2000a) Modular representations of odorants in the glomerular layer of the rat olfactory bulb and the effects of stimulus concentration. J Comp Neurol 422:496-509.

Johnson BA, Leon M (2000b) Odorant molecular length: one aspect of the olfactory code. J Comp Neurol 426:330-338.

Johnson DM, Illig KR, Behan M, Haberly LB (2000) New features of connectivity in piriform cortex visualized by intracellular injection of pyramidal cells suggest that "primary" olfactory cortex functions like "association" cortex in other sensory systems. J Neurosci 20:6974-6982.

Jourdan F, Duveau A, Astic L, Holley A (1980) Spatial distribution of [14C]2-deoxyglucose uptake in the olfactory bulbs of rats stimulated with two different odours. Brain Res 188:139-154.

Kaas JH, Nelson RJ, Sur M, Dykes RW, Merzenich MM (1984) The somatotopic organization of the ventroposterior thalamus of the squirrel monkey, Saimiri sciureus. J Comp Neurol 226:111-140.

Kadunce DC, Vaughan JW, Wallace MT, Benedek G, Stein BE (1997) Mechanisms of within- and cross-modality suppression in the superior colliculus. J Neurophysiol 78:2834-2847.

Kaiser KM, Zilberter Y, Sakmann B (2001) Back-propagating action potentials mediate calcium signalling in dendrites of bitufted interneurons in layer 2/3 of rat somatosensory cortex. J Physiol 535:17-31.

Kandel ER, Schwartz JH, Jessell TM (2000) Principles of neural science. New York: McGraw-Hill, Health Professions Division.

Kapfer C, Glickfeld LL, Atallah BV, Scanziani M (2007) Supralinear increase of recurrent inhibition during sparse activity in the somatosensory cortex. Nat Neurosci 10:743-753.

Kapoor V, Urban NN (2006) Glomerulus-specific, long-latency activity in the olfactory bulb granule cell network. J Neurosci 26:11709-11719.

Kasowski HJ, Kim H, Greer CA (1999) Compartmental organization of the olfactory bulb glomerulus. J comp Neurol 407:261-274.

Katada S, Hirokawa T, Oka Y, Suwa M, Touhara K (2005) Structural basis for a broad but selective ligand spectrum of a mouse olfactory receptor: mapping the odorant-binding site. J Neurosci 25:1806-1815.

Kato T, Yokouchi K, Li Z, Fukushima N, Kawagishi K, Moriizumi T (1999) Calretinin-immunoreactive neurons in rostral migratory stream: neuronal differentiation. Neuroreport 10:2769-2772.

Katoh K, Koshimoto H, Tani A, Mori K (1993) Coding of odor molecules by mitral/tufted cells in rabbit olfactory bulb. II. Aromatic compounds. J Neurophysiol 70:2161-2175.

Kay LM (2005) Theta oscillations and sensorimotor performance. Proc Natl Acad Sci U S A.

Kida I, Xu F, Shulman RG, Hyder F (2002) Mapping at glomerular resolution: fMRI of rat olfactory bulb. Magn Reson Med 48:570-576.

King AJ, Palmer AR (1983) Cells responsive to free-field auditory stimuli in guinea-pig superior colliculus: distribution and response properties. J Physiol 342:361-381.

Knaus HG, Schwarzer C, Koch RO, Eberhart A, Kaczorowski GJ, Glossmann H, Wunder F, Pongs O, Garcia ML, Sperk G (1996) Distribution of high-conductance Ca(2+)-activated K+ channels in rat brain: targeting to axons and nerve terminals. J Neurosci 16:955-963.

Knierim JJ, Kudrimoti HS, McNaughton BL (1998) Interactions between idiothetic cues and external landmarks in the control of place cells and head direction cells. J Neurophysiol 80:425-446.

Knudsen EI (1982) Auditory and visual maps of space in the optic tectum of the owl. J Neurosci 2:1177-1194.

Knudsen EI, du LS, Esterly SD (1987) Computational maps in the brain. Annu Rev Neurosci 10:41-65.

Knudsen EI, Konishi M (1978) Space and frequency are represented separately in auditory midbrain of the owl. J Neurophysiol 41:870-884.

Koch C, Poggio T, Torre V (1983) Nonlinear interactions in a dendritic tree: localization, timing, and role in information processing. Proc Natl Acad Sci U S A 80:2799-2802.

Koch C, Segev I (1998) Methods in neuronal modeling
from ions to networks. Cambridge, Mass: MIT Press.

Komisaruk BR (1970) Synchrony between limbic system theta activity and rhythmical behavior in rats. J Comp Physiol Psychol 70:482-492.

Kosaka K, Hama K, Nagatsu I, Wu JY, Kosaka T (1988) Possible coexistence of amino acid (gamma-aminobutyric acid), amine (dopamine) and peptide (substance P); neurons containing immunoreactivities for glutamic acid decarboxylase, tyrosine hydroxylase and substance P in the hamster main olfactory bulb. Exp Brain Res 71:633-642.

Kuffler SW (1953) Discharge patterns and functional organization of mammalian retina. J Neurophysiol 16:37-68.

Kyriazi HT, Carvell GE, Brumberg JC, Simons DJ (1996) Effects of baclofen and phaclofen on receptive field properties of rat whisker barrel neurons. Brain Res 712:325-328.

Lagier S, Carleton A, Lledo PM (2004) Interplay between local GABAergic interneurons and relay neurons generates gamma oscillations in the rat olfactory bulb. J Neurosci 24:4382-4392.

Lagier S, Panzanelli P, Russo RE, Nissant A, Bathellier B, Sassoe-Pognetto M, Fritschy JM, Lledo PM (2007) GABAergic inhibition at dendrodendritic synapses tunes gamma oscillations in the olfactory bulb. Proc Natl Acad Sci U S A 104:7259-7264.

Lancet D, Lazard D, Heldman J, Khen M, Nef P (1988) Molecular transduction in smell and taste. Cold Spring Harb Symp Quant Biol 53 Pt 1:343-348.

Laurent G (1997) Olfactory processing: maps, time and codes. Curr Opin Neurobiol 7:547-553.

Laurent G (1999) A systems perspective on early olfactory coding. Science 286:723-728.

Laurent G, Naraghi M (1994) Odorant-induced oscillations in the mushroom bodies of the locust. J Neurosci 14:2993-3004.

Laurent G, Wehr M, Davidowitz H (1996) Temporal representations of odors in an olfactory network. J Neurosci 16:3837-3847.

Lei H, Christensen TA, Hildebrand JG (2002) Local inhibition modulates odor-evoked synchronization of glomerulus-specific output neurons. Nat Neurosci 5:557-565.

Lester RA, Clements JD, Westbrook GL, Jahr CE (1990) Channel kinetics determine the time course of NMDA receptor-mediated synaptic currents. Nature 346:565-567.

Leutgeb S, Leutgeb JK, Moser MB, Moser EI (2005) Place cells, spatial maps and the population code for memory. Curr Opin Neurobiol 15:738-746.

Li YX, Rinzel J (1994) Equations for InsP3 receptor-mediated [Ca2+]i oscillations derived from a detailed kinetic model: a Hodgkin-Huxley like formalism. J Theor Biol 166:461-473.

Lin DY, Zhang SZ, Block E, Katz LC (2005) Encoding social signals in the mouse main olfactory bulb. Nature 434:470-477.

Linster C, Gervais R (1996) Investigation of the role of interneurons and their modulation by centrifugal fibers in a neural model of the olfactory bulb. J Comput Neurosci 3:225-246.

Linster C, Johnson BA, Morse A, Yue E, Leon M (2002) Spontaneous versus reinforced olfactory discriminations. J Neurosci 22:6842-6845.

Linster C, Johnson BA, Yue E, Morse A, Xu Z, Hingco EE, Choi Y, Choi M, Messiha A, Leon M (2001) Perceptual correlates of neural representations evoked by odorant enantiomers. J Neurosci 21:9837-9843.

Linster C, Sachse S, Galizia CG (2005) Computational modeling suggests that response properties rather than spatial position determine connectivity between olfactory glomeruli. J Neurophysiol 93:3410-3417.

Logothetis NK, Sheinberg DL (1996) Visual object recognition. Annu Rev Neurosci 19:577-621.

Lowe G (2002) Inhibition of backpropagating action potentials in mitral cell secondary dendrites. J Neurophysiol 88:64-85.

Lowe G, Gold GH (1993) Nonlinear amplification by calcium-dependent chloride channels in olfactory receptor cells. Nature 366:283-286.

Luce RD (1986) Response times
their role in inferring elementary mental organization.

Luo M, Katz LC (2001) Response correlation maps of neurons in the Mammalian olfactory bulb. Neuron 32:1165-1179.

Ma J, Lowe G (2007) Calcium permeable AMPA receptors and autoreceptors in external tufted cells of rat olfactory bulb. Neuroscience 144:1094-1108.

Macrides F, Schneider SP (1982) Laminar organization of mitral and tufted cells in the main olfactory bulb of the adult hamster. J comp Neurol 208:419-430.

Maher BJ, Westbrook GL (2005) SK channel regulation of dendritic excitability and dendrodendritic inhibition in the olfactory bulb. J Neurophysiol 94:3743-3750.

Maher BJ, Westbrook GL (2008) Co-Transmission of Dopamine and GABA in Periglomerular Cells. J Neurophysiol 99:1559-1564.

Malenka RC, Nicoll RA (1999) Long-term potentiation--a decade of progress? Science 285:1870-1874.

Malnic B, Godfrey PA, Buck LB (2004) The human olfactory receptor gene family. Proc Natl Acad Sci U S A 101:2584-2589.

Malnic B, Hirono J, Sato T, Buck LB (1999) Combinatorial receptor codes for odors. Cell 96:713-723.

Margrie TW, Meyer AH, Caputi A, Monyer H, Hasan MT, Schaefer AT, Denk W, Brecht M (2003) Targeted whole-cell recordings in the mammalian brain in vivo. Neuron 39:911-918.

Margrie TW, Sakmann B, Urban NN (2001) Action potential propagation in mitral cell lateral dendrites is decremental and controls recurrent and lateral inhibition in the mammalian olfactory bulb. Proc Natl Acad Sci U S A 98:319-324.

Markus EJ, Qin YL, Leonard B, Skaggs WE, McNaughton BL, Barnes CA (1995) Interactions between location and task affect the spatial and directional firing of hippocampal neurons. J Neurosci 15:7079-7094.

Martin C, Beshel J, Kay LM (2007) An olfacto-hippocampal network is dynamically involved in odor-discrimination learning. J Neurophysiol 98:2196-2205.

Mayer ML, Westbrook GL (1987) Permeation and block of N-methyl-D-aspartic acid receptor channels by divalent cations in mouse cultured central neurones. J Physiol 394:501-527.

Mehaffey WH, Doiron B, Maler L, Turner RW (2005) Deterministic multiplicative gain control with active dendrites. J Neurosci 25:9968-9977.

Meister M, Bonhoeffer T (2001) Tuning and topography in an odor map on the rat olfactory bulb. J Neurosci 21:1351-1360.

Mel BW, Ruderman DL, Archie KA (1998) Translation-invariant orientation tuning in visual "complex" cells could derive from intradendritic computations. J Neurosci 18:4325-4334.

Miyamichi K, Serizawa S, Kimura HM, Sakano H (2005) Continuous and overlapping expression domains of odorant receptor genes in the olfactory epithelium determine the dorsal/ventral positioning of glomeruli in the olfactory bulb. J Neurosci 25:3586-3592.

Mombaerts P, Wang F, Dulac C, Chao SK, Nemes A, Mendelsohn M, Edmondson J, Axel R (1996) Visualizing an olfactory sensory map. Cell 87:675-686.

Montague AA, Greer CA (1999) Differential distribution of ionotropic glutamate receptor subunits in the rat olfactory bulb. J comp Neurol 405:233-246.

Mori K, Kishi K, Ojima H (1983) Distribution of dendrites of mitral, displaced mitral, tufted, and granule cells in the rabbit olfactory bulb. J comp Neurol 219:339-355.

Mori K, Nowycky MC, Shepherd GM (1981) Electrophysiological analysis of mitral cells in the isolated turtle olfactory bulb. J Physiol (Lond) 314:281-94:281-294.

Mori K, Takahashi YK, Igarashi K, Nagayama S (2005) Odor maps in the dorsal and lateral surfaces of the rat olfactory bulb. Chem Senses 30 Suppl 1:i103-i104.

Mori K, Takahashi YK, Igarashi KM, Yamaguchi M (2006) Maps of odorant molecular features in the Mammalian olfactory bulb. Physiol Rev 86:409-433.

Motokizawa F (1996) Odor representation and discrimination in mitral/tufted cells of the rat olfactory bulb. Exp Brain Res 112:24-34.

Mountcastle V (1957) Modality and topographic properties of single neurons of cat's somatic sensory cortex. J Neurophysiol 20:408-434.

Mozell MM (1964) EVIDENCE FOR SORPTION AS A MECHANISM OF THE OLFACTORY ANALYSIS OF VAPOURS. Nature 203:1181-1182.

Murphy GJ, Glickfeld LL, Balsen Z, Isaacson JS (2004) Sensory neuron signaling to the brain: properties of transmitter release from olfactory nerve terminals. J Neurosci 24:3023-3030.

Nakao H, Arai K-S, Nagai K, Tsubo Y, Kuramoto Y (2005) Synchrony of limit-cycle oscillators induced by random external impulses. Phys Rev E 72.

Nelson S, Toth L, Sheth B, Sur M (1994) Orientation selectivity of cortical neurons during intracellular blockade of inhibition. Science 265:774-777.

Nowak L, Bregestovski P, Ascher P, Herbet A, Prochiantz A (1984) Magnesium gates glutamate-activated channels in mouse central neurones. Nature 307:462-465.

Nowycky MC, Mori K, Shepherd GM (1981) GABAergic mechanisms of dendrodendritic synapses in isolated turtle olfactory bulb. J Neurophysiol 46:639-648.

Nusser Z, Kay LM, Laurent G, Homanics GE, Mody I (2001) Disruption of GABA(A) receptors on GABAergic interneurons leads to increased oscillatory power in the olfactory bulb network. J Neurophysiol 86:2823-2833.

O'Keefe J, Dostrovsky J (1971) The hippocampus as a spatial map. Preliminary evidence from unit activity in the freely-moving rat. Brain Res 34:171-175.

Olsen SR, Wilson RI (2008) Lateral presynaptic inhibition mediates gain control in an olfactory circuit. Nature.

Onoda N, Mori K (1980) Depth distribution of temporal firing patterns in olfactory bulb related to air-intake cycles. J Neurophysiol 44:29-39.

Orona E, Rainer EC, Scott JW (1984) Dendritic and axonal organization of mitral and tufted cells in the rat olfactory bulb. J comp Neurol 226:346-356.

Pelosi P (1996) Perireceptor events in olfaction. J Neurobiol 30:3-19.

Perez-Orive J, Mazor O, Turner GC, Cassenaer S, Wilson RI, Laurent G (2002) Oscillations and sparsening of odor representations in the mushroom body. Science 297:359-365.

Petralia RS, Yokotani N, Wenthold RJ (1994) Light and electron microscope distribution of the NMDA receptor subunit NMDAR1 in the rat nervous system using a selective anti-peptide antibody. J Neurosci 14:667-696.

PHILLIPS CG, Powell TP, Shepherd GM (1963) RESPONSES OF MITRAL CELLS TO STIMULATION OF THE LATERAL OLFACTORY TRACT IN THE RABBIT. J Physiol 168:65-88.

Pimentel DO, Margrie TW (2008) Glutamatergic transmission and plasticity between olfactory bulb mitral cells. J Physiol.

Pinato G, Midtgaard J (2005) Dendritic sodium spikelets and low-threshold calcium spikes in turtle olfactory bulb granule cells. J Neurophysiol 93:1285-1294.

Pinching AJ, Powell TP (1971a) The neuron types of the glomerular layer of the olfactory bulb. J Cell Sci 9:305-345.

Pinching AJ, Powell TP (1971b) The neuropil of the glomeruli of the olfactory bulb. J Cell Sci 9:347-377.

Pinching AJ, Powell TP (1971c) The neuropil of the periglomerular region of the olfactory bulb. J Cell Sci 9:379-409.

Pouget A, Dayan P, Zemel R (2000) Information processing with population codes. Nat Rev Neurosci 1:125-132.

Pouille F, Scanziani M (2001) Enforcement of temporal fidelity in pyramidal cells by somatic feed-forward inhibition. Science 293:1159-1163.

Pouille F, Scanziani M (2004) Routing of spike series by dynamic circuits in the hippocampus. Nature 429:717-723.

Prescott SA, De KY (2003) Gain control of firing rate by shunting inhibition: roles of synaptic noise and dendritic saturation. Proc Natl Acad Sci U S A 100:2076-2081.

Price JL (1973) An autoradiographic study of complementary laminar patterns of termination of afferent fibers to the olfactory cortex. J Comp Neurol 150:87-108.

Price JL, Powell TP (1970) The synaptology of the granule cells of the olfactory bulb. J Cell Sci 7:125-155.

Rall W, Shepherd GM (1968) Theoretical reconstruction of field potentials and dendrodendritic synaptic interactions in olfactory bulb. J Neurophys 31:884-915.

Rall W, Shepherd GM, Reese TS, Brightman MW (1966) Dendrodendritic synaptic pathway for inhibition in the olfactory bulb. Experimental Neurology 14:44-56.

Ranck JB, Jr. (1973) Studies on single neurons in dorsal hippocampal formation and septum in unrestrained rats. I. Behavioral correlates and firing repertoires. Exp Neurol 41:461-531.

Ravel N, Chabaud P, Martin C, Gaveau V, Hugues E, Tallon-Baudry C, Bertrand O, Gervais R (2003) Olfactory learning modifies the expression of odour-induced oscillatory responses in the gamma (60-90 Hz) and beta (15-40 Hz) bands in the rat olfactory bulb. Eur J Neurosci 17:350-358.

Rennaker RL, Chen CF, Ruyle AM, Sloan AM, Wilson DA (2007) Spatial and temporal distribution of odorant-evoked activity in the piriform cortex. J Neurosci 27:1534-1542.

Renshaw B (1946) Central effects of centripetal impulses in axons of spinal ventral roots. pp 191-204.

Ressler KJ, Sullivan SL, Buck LB (1993) A zonal organization of odorant receptor gene expression in the olfactory epithelium. Cell 73:597-609.

Restrepo D, Arellano J, Oliva AM, Schaefer ML, Lin W (2004) Emerging views on the distinct but related roles of the main and accessory olfactory systems in responsiveness to chemosensory signals in mice. Horm Behav 46:247-256.

Revesz G (1934) System der optischen und haptischen Raumtäuschungen. pp 296-375.

Reyher CK, Lubke J, Larsen WJ, Hendrix GM, Shipley MT, Baumgarten HG (1991) Olfactory bulb granule cell aggregates: morphological evidence for interperikaryal electrotonic coupling via gap junctions. J Neurosci 11:1485-1495.

Rinberg D, Koulakov A, Gelperin A (2006) Speed-accuracy tradeoff in olfaction. Neuron 51:351-358.

Ring G, Mezza RC, Schwob JE (1997) Immunohistochemical identification of discrete subsets of rat olfactory neurons and the glomeruli that they innervate. J comp Neurol 388:415-434.

Ronnett GV, Cho H, Hester LD, Wood SF, Snyder SH (1993) Odorants differentially enhance phosphoinositide turnover and adenylyl cyclase in olfactory receptor neuronal cultures. J Neurosci 13:1751-1758.

Royet JP, Sicard G, Souchier C, Jourdan F (1987) Specificity of spatial patterns of glomerular activation in the mouse olfactory bulb: computer-assisted image analysis of 2-deoxyglucose autoradiograms. Brain Res 417:1-11.

Rubin BD, Katz LC (1999) Optical imaging of odorant representations in the mammalian olfactory bulb. Neuron 23:499-511.

Rubin BD, Katz LC (2001) Spatial coding of enantiomers in the rat olfactory bulb. Nat Neurosci 4:355-356.

Rudy B (1988) Diversity and ubiquity of K channels. Neuroscience 25:729-749.

Sachse S, Galizia CG (2002) Role of inhibition for temporal and spatial odor representation in olfactory output neurons: a calcium imaging study. J Neurophysiol 87:1106-1117.

Salinas E, Sejnowski TJ (2001) Gain modulation in the central nervous system: where behavior, neurophysiology, and computation meet. Neuroscientist 7:430-440.

Sam M, Vora S, Malnic B, Ma W, Novotny MV, Buck LB (2001) Neuropharmacology. Odorants may arouse instinctive behaviours. Nature 412:142.

Schaefer AT, Margrie TW (2007) Spatiotemporal representations in the olfactory system. Trends Neurosci 30:92-100.

Schaefer ML, Wong ST, Wozniak DF, Muglia LM, Liauw JA, Zhuo M, Nardi A, Hartman RE, Vogt SK, Luedke CE, Storm DR, Muglia LJ (2000) Altered stress-induced anxiety in adenylyl cyclase type VIII-deficient mice. J Neurosci 20:4809-4820.

Schafer JR, Kida I, Xu F, Rothman DL, Hyder F (2006) Reproducibility of odor maps by fMRI in rodents. Neuroimage 31:1238-1246.

Schoppa NE, Kinzie JM, Sahara Y, Segerson TP, Westbrook GL (1998) Dendrodendritic inhibition in the olfactory bulb is driven by NMDA receptors. J Neurosci 18:6790-6802.

Schoppa NE, Urban NN (2003) Dendritic processing within olfactory bulb circuits. Trends Neurosci 26:501-506.

Schoppa NE, Westbrook GL (1999) Regulation of synaptic timing in the olfactory bulb by an A-type potassium current. Nat Neurosci 2:1106-1113.

Schoppa NE, Westbrook GL (2002) AMPA autoreceptors drive correlated spiking in olfactory bulb glomeruli. Nat Neurosci 5:1194-1202.

Schwob JE, Gottlieb DI (1988) Purification and characterization of an antigen that is spatially segregated in the primary olfactory projection. J Neurosci 8:3470-3480.

Segev I (1999) Taming time in the olfactory bulb. Nat Neurosci 2:1041-1043.

Segev I, Rall W (1988) Computational study of an excitable dendritic spine. J Neurophys 60:499-523.

Sharp FR, Kauer JS, Shepherd GM (1975) Local sites of activity-related glucose metabolism in rat olfactory bulb during olfactory stimulation. Brain Res 98:596-600.

Shepherd GM (1963) NEURONAL SYSTEMS CONTROLLING MITRAL CELL EXCITABILITY. J Physiol 168:101-117.

Shepherd GM, Chen WR, Willhite D, Migliore M, Greer CA (2007) The olfactory granule cell: From classical enigma to central role in olfactory processing. Brain Res Rev.

Shepherd GM, Greer CA (2004) Olfactory bulb. In: The Synaptic Organization of the Brain (Shepherd GM, ed), New York: Oxford University Press.

Shinoda K, Shiotani Y, Osawa Y (1989) "Necklace olfactory glomeruli" form unique components of the rat primary olfactory system. J Comp Neurol 284:362-373.

Singer W, Gray CM (1995) Visual feature integration and the temporal correlation hypothesis. Annu Rev Neurosci 18:555-586.

Spors H, Grinvald A (2002) Spatio-temporal dynamics of odor representations in the mammalian olfactory bulb. Neuron 34:301-315.

Spors H, Wachowiak M, Cohen LB, Friedrich RW (2006) Temporal dynamics and latency patterns of receptor neuron input to the olfactory bulb. J Neurosci 26:1247-1259.

Spruston N, Schiller Y, Stuart G, Sakmann B (1995) Activity-dependent action potential invasion and calcium influx into hippocampal CA1 dendrites. Science 268:297-300.

Stewart WB, Kauer JS, Shepherd GM (1979) Functional organization of rat olfactory bulb analysed by the 2-deoxyglucose method. J comp Neurol 185:715-734.

Stopfer M, Bhagavan S, Smith BH, Laurent G (1997) Impaired odour discrimination on desynchronization of odour-encoding neural assemblies. Nature 390:70-74.

Stopfer M, Jayaraman V, Laurent G (2003) Intensity versus identity coding in an olfactory system. Neuron 39:991-1004.

Strotmann J, Conzelmann S, Beck A, Feinstein P, Breer H, Mombaerts P (2000) Local permutations in the glomerular array of the mouse olfactory bulb. J Neurosci 20:6927-6938.

Svoboda K, Helmchen F, Denk W, Tank DW (1999) Spread of dendritic excitation in layer 2/3 pyramidal neurons in rat barrel cortex in vivo. Nat Neurosci 2:65-73.

Tanaka K (1996) Representation of Visual Features of Objects in the Inferotemporal Cortex. Neural Netw 9:1459-1475.

Teicher MH, Stewart WB, Kauer JS, Shepherd GM (1980) Suckling pheromone stimulation of a modified glomerular region in the developing rat olfactory bulb revealed by the 2-deoxyglucose method. Brain Res 194:530-535.

Teramae JN, Tanaka D (2004) Robustness of the noise-induced phase synchronization in a general class of limit cycle oscillators. Phys Rev Lett 93:204103.

Teyke T, Gelperin A (1999) Olfactory oscillations augment odor discrimination not odor identification by Limax CNS. Neuroreport 10:1061-1068.

Treloar HB, Feinstein P, Mombaerts P, Greer CA (2002) Specificity of glomerular targeting by olfactory sensory axons. J Neurosci 22:2469-2477.

Tseng GF, Haberly LB (1989) Deep neurons in piriform cortex. II. Membrane properties that underlie unusual synaptic responses. J Neurophysiol 62:386-400.

Uchida N, Kepecs A, Mainen ZF (2006) Seeing at a glance, smelling in a whiff: rapid forms of perceptual decision making. Nat Rev Neurosci 7:485-491.

Uchida N, Mainen ZF (2003) Speed and accuracy of olfactory discrimination in the rat. Nat Neurosci 6:1224-1229.

Uchida N, Takahashi YK, Tanifuji M, Mori K (2000) Odor maps in the mammalian olfactory bulb: domain organization and odorant structural features. Nat Neurosci 3:1035-1043.

Ulrich D (2003) Differential arithmetic of shunting inhibition for voltage and spike rate in neocortical pyramidal cells. Eur J Neurosci 18:2159-2165.

Urban NN (2002) Lateral inhibition in the olfactory bulb and in olfaction. Physiol Behav 77:607-612.

Urban NN, Sakmann B (2002) Reciprocal intraglomerular excitation and intra- and interglomerular lateral inhibition between mouse olfactory bulb mitral cells. J Physiol 542:355-367.

Usrey WM, Reid RC (1999) Synchronous activity in the visual system. Annu Rev Physiol 61:435-456.

Vassar R, Ngai J, Axel R (1993) Spatial segregation of odorant receptor expression in the mammalian olfactory epithelium. Cell 74:309-318.

von Bekesy G (1967) Sensory Inhibition. New Jersey: Princeton University Press.

Wachowiak M, Cohen LB (1999) Presynaptic inhibition of primary olfactory afferents mediated by different mechanisms in lobster and turtle. J Neurosci 19:8808-8817.

Wachowiak M, Cohen LB (2001) Representation of odorants by receptor neuron input to the mouse olfactory bulb. Neuron 32:723-735.

Wachowiak M, Cohen LB, Zochowski MR (2002) Distributed and concentration-invariant spatial representations of odorants by receptor neuron input to the turtle olfactory bulb. J Neurophysiol 87:1035-1045.

Wachowiak M, Denk W, Friedrich RW (2004) Functional organization of sensory input to the olfactory bulb glomerulus analyzed by two-photon calcium imaging. Proc Natl Acad Sci U S A 101:9097-9102.

Wachowiak M, McGann JP, Heyward PM, Shao Z, Puche AC, Shipley MT (2005) Inhibition [corrected] of olfactory receptor neuron input to olfactory bulb glomeruli mediated by suppression of presynaptic calcium influx. J Neurophysiol 94:2700-2712.

Wang XJ, Buzsaki G (1996) Gamma oscillation by synaptic inhibition in a hippocampal interneuronal network model. Journal of Neuroscience 16:6402-6413.

Wang Y, Fujita I, Murayama Y (2000) Neuronal mechanisms of selectivity for object features revealed by blocking inhibition in inferotemporal cortex. Nat Neurosci 3:807-813.

Wehr M, Zador AM (2003) Balanced inhibition underlies tuning and sharpens spike timing in auditory cortex. Nature 426:442-446.

Wehr M, Zador AM (2005) Synaptic mechanisms of forward suppression in rat auditory cortex. Neuron 47:437-445.

Wellis DP, Scott JW (1990) Intracellular responses of identified rat olfactory bulb interneurons to electrical and odor stimulation. J Neurophysiol 64:932-947.

Wenstrup JJ, Ross LS, Pollak GD (1986) Binaural response organization within a frequency-band representation of the inferior colliculus: implications for sound localization. J Neurosci 6:962-973.

Werblin FS (1972) Lateral interactions at inner plexiform layer of vertebrate retina: antagonistic responses to change. Science 175:1008-1010.

Willhite DC, Nguyen KT, Masurkar AV, Greer CA, Shepherd GM, Chen WR (2006) Viral tracing identifies distributed columnar organization in the olfactory bulb. Proc Natl Acad Sci U S A.

Williamson AM, Ohara PT, Ralston HJ, III (1993) Electron microscopic evidence that cortical terminals make direct contact onto cells of the thalamic reticular nucleus in the monkey. Brain Res 631:175-179.

Wilson HR, Cowan JD (1972) Excitatory and inhibitory interactions in localized populations of model neurons. Biophys J 12:1-24.

Wilson RI, Laurent G (2005) Role of GABAergic inhibition in shaping odor-evoked spatiotemporal patterns in the Drosophila antennal lobe. J Neurosci 25:9069-9079.

Wilson RI, Mainen ZF (2006) Early events in olfactory processing. Annu Rev Neurosci 29:163-201.

Wilson RI, Turner GC, Laurent G (2004) Transformation of olfactory representations in the Drosophila antennal lobe. Science 303:366-370.

Wood ER, Dudchenko PA, Eichenbaum H (1999) The global record of memory in hippocampal neuronal activity [see comments]. Nature 397:613-616.

Woolf TB, Greer CA (1994) Local communication within dendritic spines: models of second messenger diffusion in granule cell spines of the mammalian olfactory bulb. Synapse 17:247-267.

Woolf TB, Shepherd GM, Greer CA (1991a) Local information processing in dendritic trees: subsets of spines in granule cells of the mammalian olfactory bulb. J Neurosci 11:1837-1854.

Woolf TB, Shepherd GM, Greer CA (1991b) Serial reconstructions of granule cell spines in the mammalian olfactory bulb. Synapse 7:181-192.

Xiong W, Chen WR (2002) Dynamic gating of spike propagation in the mitral cell lateral dendrites. Neuron 34:115-126.

Xu F, Kida I, Hyder F, Shulman RG (2000) Assessment and discrimination of odor stimuli in rat olfactory bulb by dynamic functional MRI. Proc Natl Acad Sci U S A 97:10601-10606.

Yaksi E, Judkewitz B, Friedrich RW (2007) Topological Reorganization of Odor Representations in the Olfactory Bulb. PLoS Biol 5:e178.

Yang X, Renken R, Hyder F, Siddeek M, Greer CA, Shepherd GM, Shulman RG (1998) Dynamic mapping at the laminar level of odor-elicited responses in rat olfactory bulb by functional MRI. Proc Natl Acad Sci U S A 95:7715-7720.

Yokoi M, Mori K, Nakanishi S (1995) Refinement of odor molecule tuning by dendrodendritic synaptic inhibition in the olfactory bulb. Proc Natl Acad Sci U S A 92:3371-3375.

Young BJ, Fox GD, Eichenbaum H (1994) Correlates of hippocampal complex-spike cell activity in rats performing a nonspatial radial maze task. J Neurosci 14:6553-6563.

Youngentob SL, Markert LM, Mozell MM, Hornung DE (1990) A method for establishing a five odorant identification confusion matrix task in rats. Physiol Behav 47:1053-1059.

Zelles T, Boyd JD, Hardy AB, Delaney KR (2006) Branch-specific Ca2+ influx from Na+-dependent dendritic spikes in olfactory granule cells. J Neurosci 26:30-40.

Zhang X, Firestein S (2002) The olfactory receptor gene superfamily of the mouse. Nat Neurosci 5:124-133.

Zozulya S, Echeverri F, Nguyen T (2001) The human olfactory receptor repertoire. Genome Biol 2:RESEARCH0018.

Zufall F, Leinders-Zufall T, Greer CA (2000) Amplification of odor-induced Ca(2+) transients by store-operated Ca(2+) release and its role in olfactory signal transduction. J Neurophysiol 83:501-512.